



Jets in heavy-ion collisions

Guang-You Qin

Central China Normal University

University of Science and Technology of China

Hefei, November 21, 2024

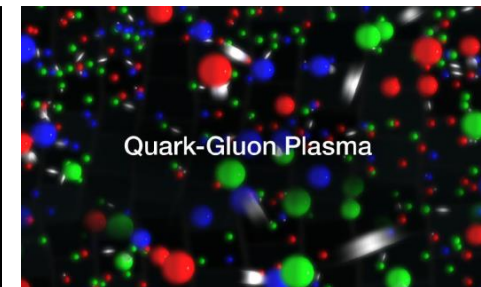
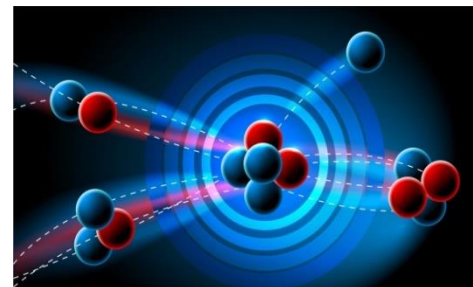
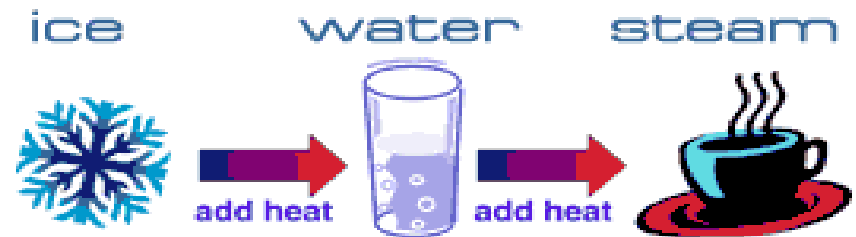
Outline

- Introduction to QGP & HiC
- High p_T hadrons
 - Flavor hierarchy of quenching and energy loss
- Full jets & medium response
 - Jet shape, hadron chemistry, EEC
- Summary

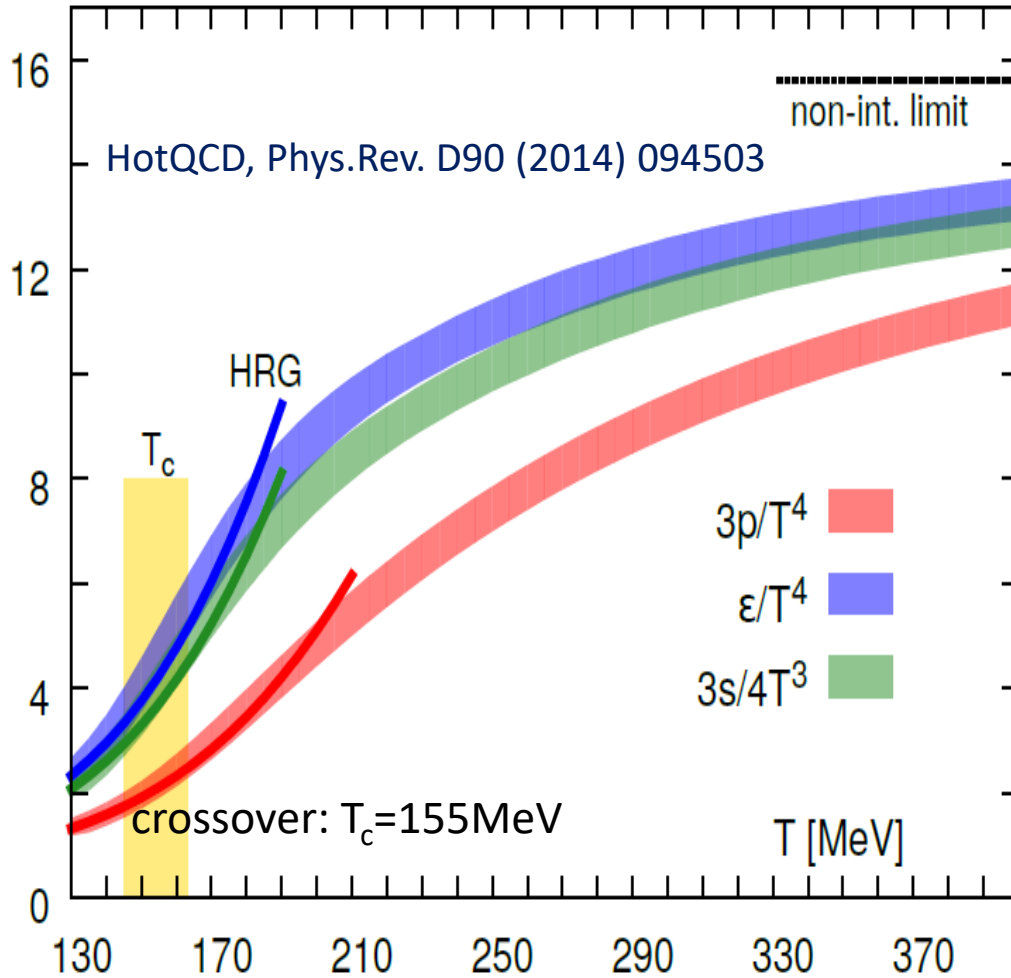
Heating up the matter

- How does the matter change when heated?
- Increasing temperature increases the kinetic energies of DOFs.
- High enough temperature can break the larger structures (DOFs) by activating more fundamental DOFs.
- Breaking molecules and chemical bonds: 10^3K , burning, flame, torch
- Breaking atoms (to get QED plasma): 10^5K , ionization
- Breaking nuclei: $10^8\text{-}10^9\text{K}$, nuclear reactions
- Breaking nucleons (to get QGP): 10^{12}K , relativistic nuclear collisions

$$k_B = 8.62 \times 10^{-5} \frac{\text{eV}}{\text{K}}, 1\text{eV} = 1.16 \times 10^4 \text{K}$$



Heating up the matter (via lattice QCD)



A transition (crossover) between hadronic matter and quark-gluon matter at $T_c = 155\text{MeV}$

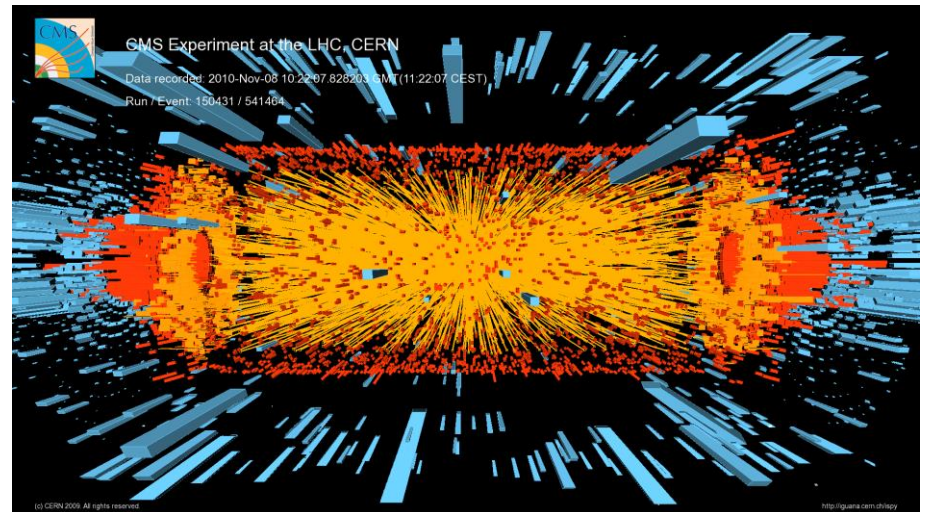
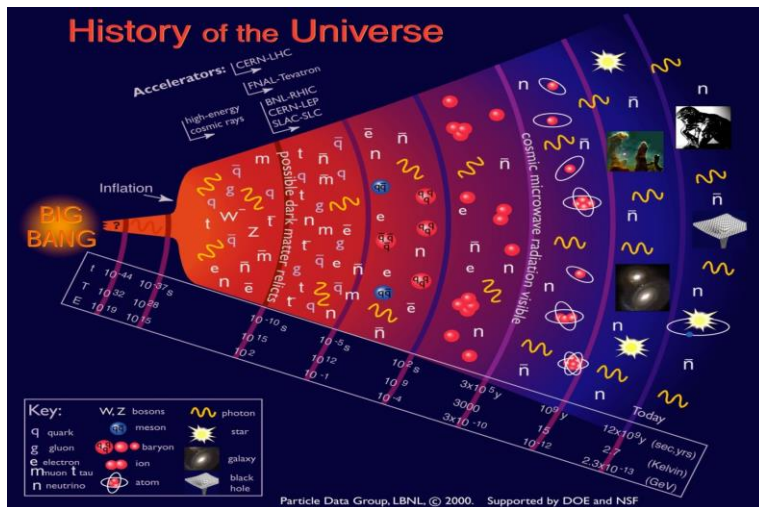
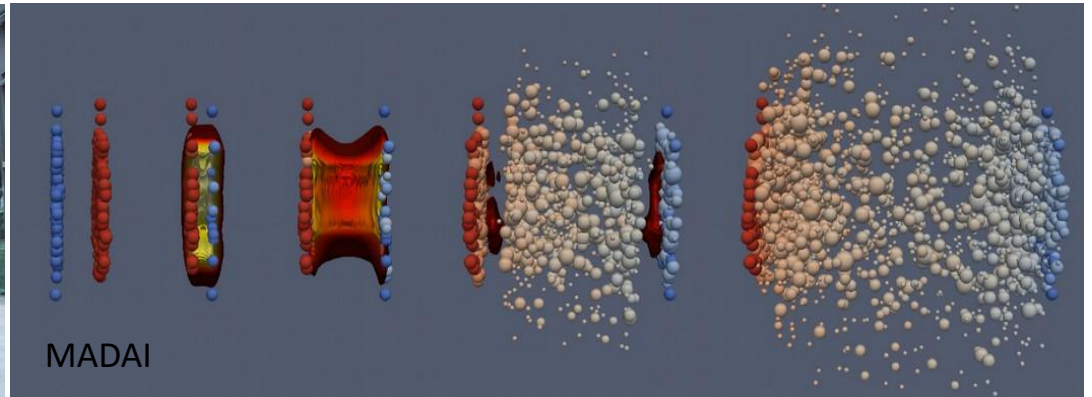
$T < T_c$, the thermodynamics of the system is described by HRG

$T \sim 400\text{MeV}$, not a non-interacting quark-gluon gas, but a strongly-interacting fluid

For non-interacting massless particles, $P = d \frac{\pi^2}{90} T^4$

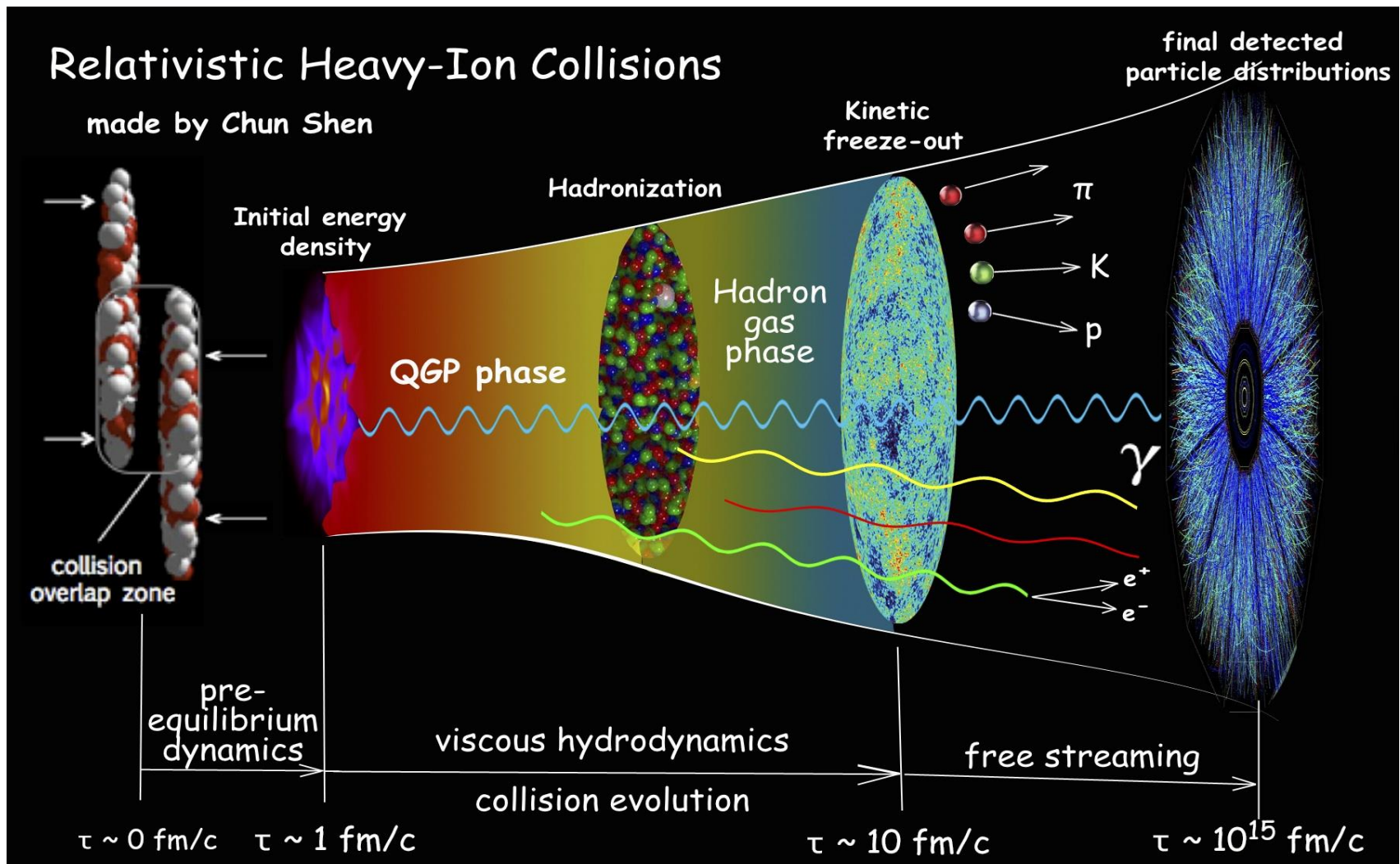
$$T_c = 155\text{MeV}/k_B = (155 * 10^6\text{eV})(1.6 * 10^{-19}\text{J/eV})/(1.38 * 10^{-23}\text{J/K}) = 1.8 * 10^{12}\text{K}$$

Heating up the matter via relativistic heavy-ion collisions

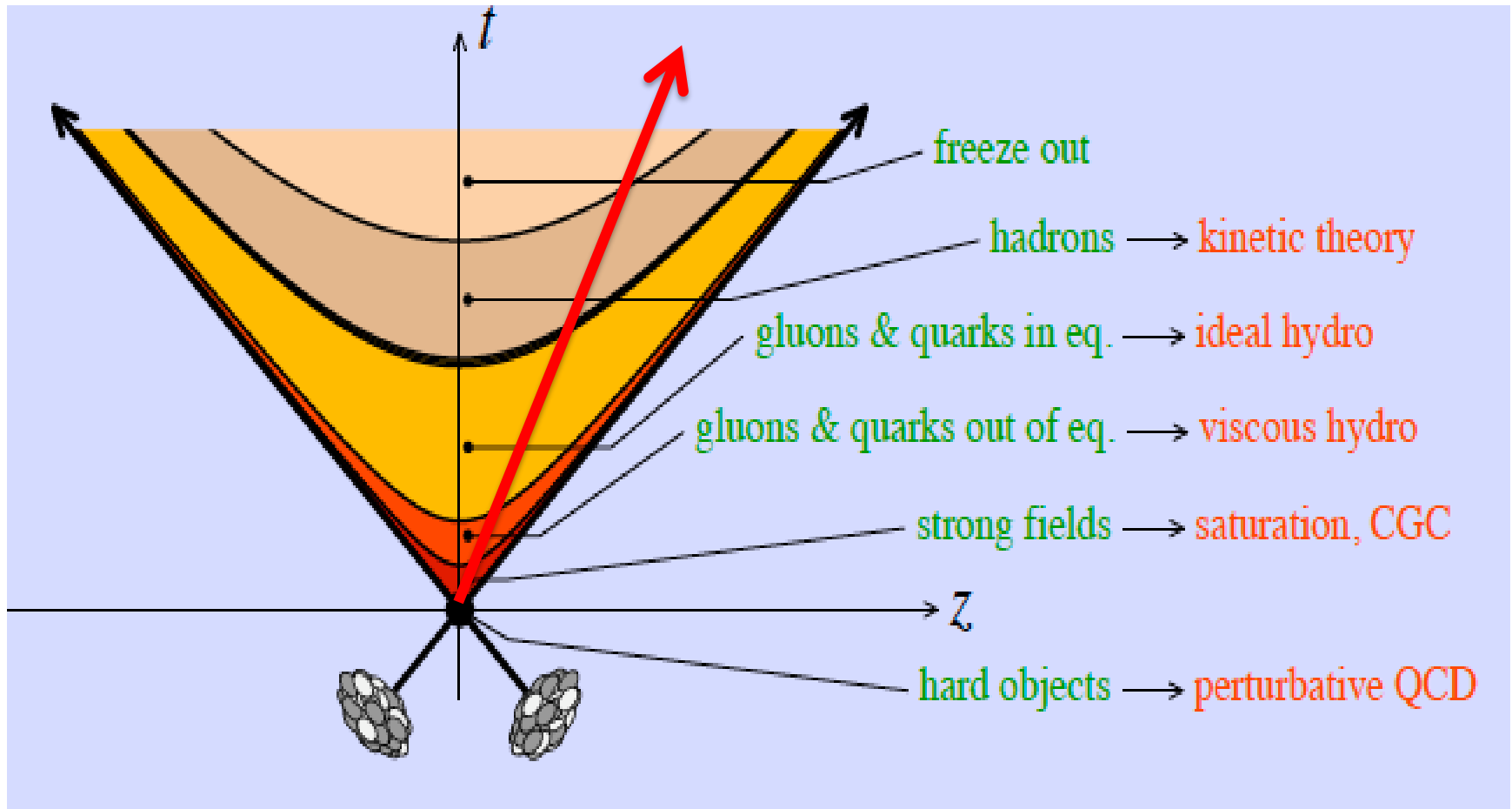


T. D. Lee, "A possible new form of matter", AIP Conf.Proc. 28 (1976) 65-81

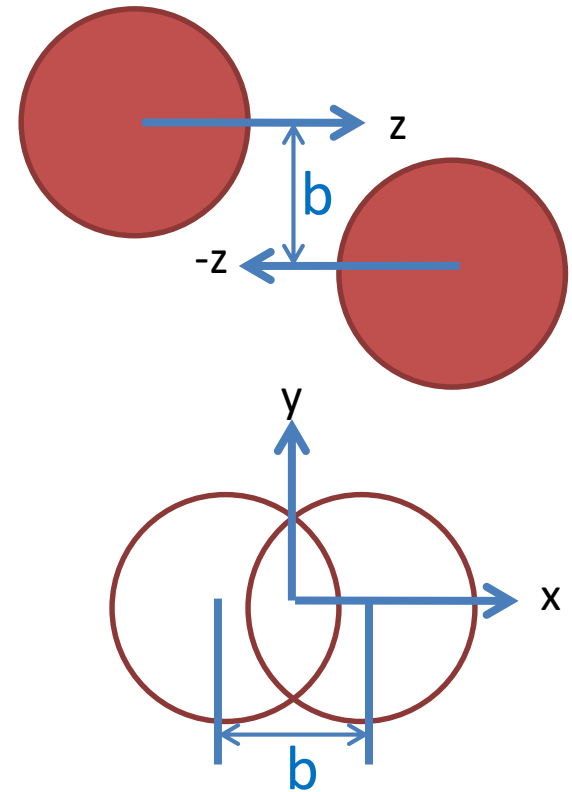
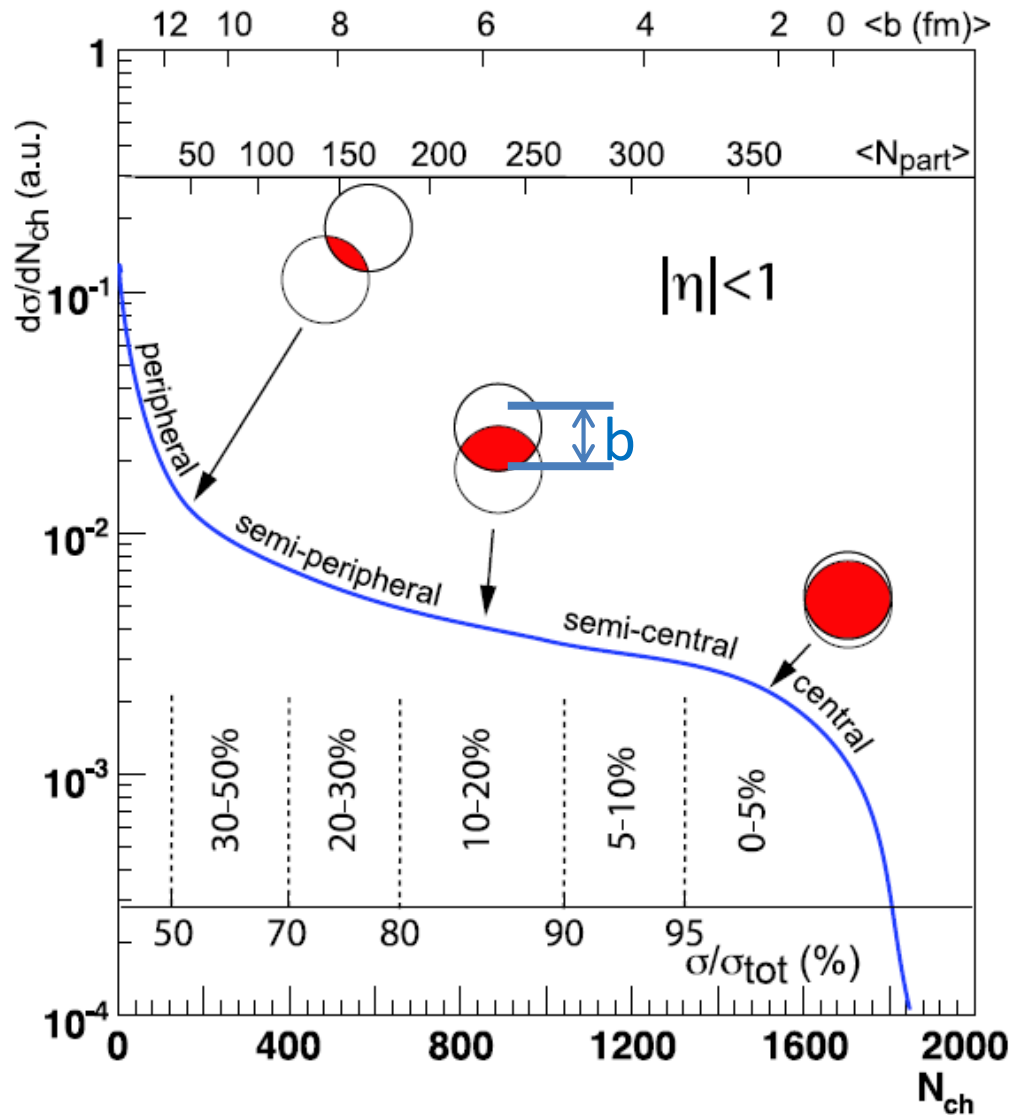
“Standard Model” of RHIC & LHC heavy-ion collisions



An interdisciplinary research field

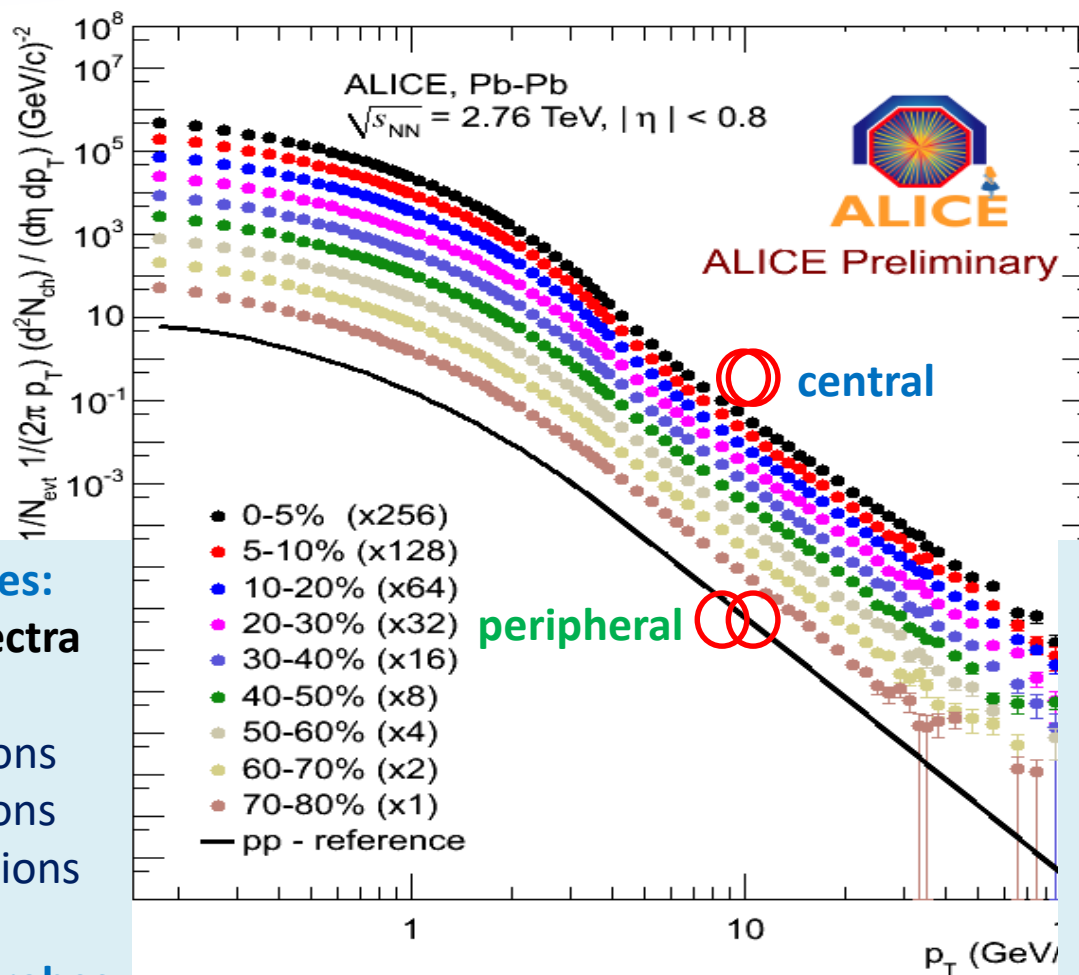


Collision centrality



Miller, Reygers, Sanders,
 Steinberg, Ann. Rev. Nucl.
 Part. Sci. 57 (2007) 205-243

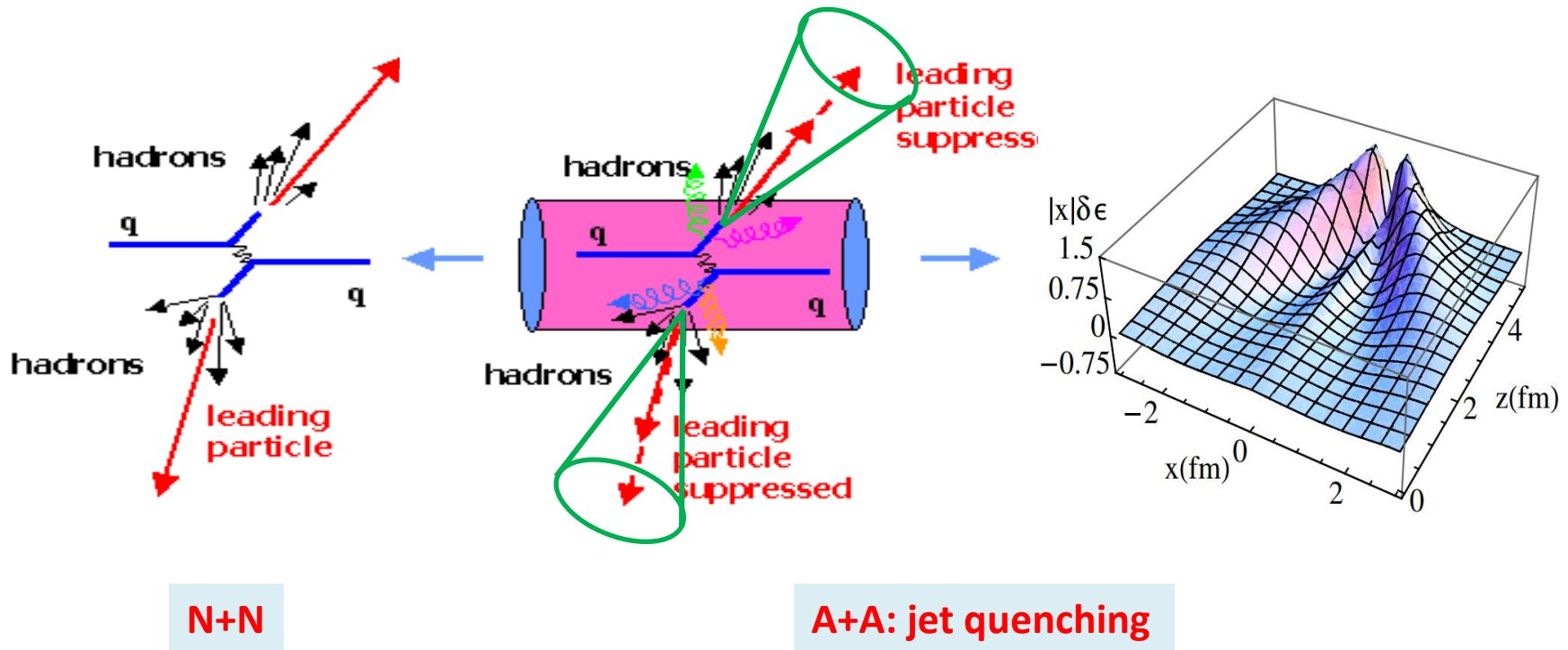
Probes of QGP in heavy-ion collisions



Soft Probes:
 Yields/Spectra
 Flows
 Fluctuations
 Correlations
 Decorrelations
 ...
 "Internal" probes

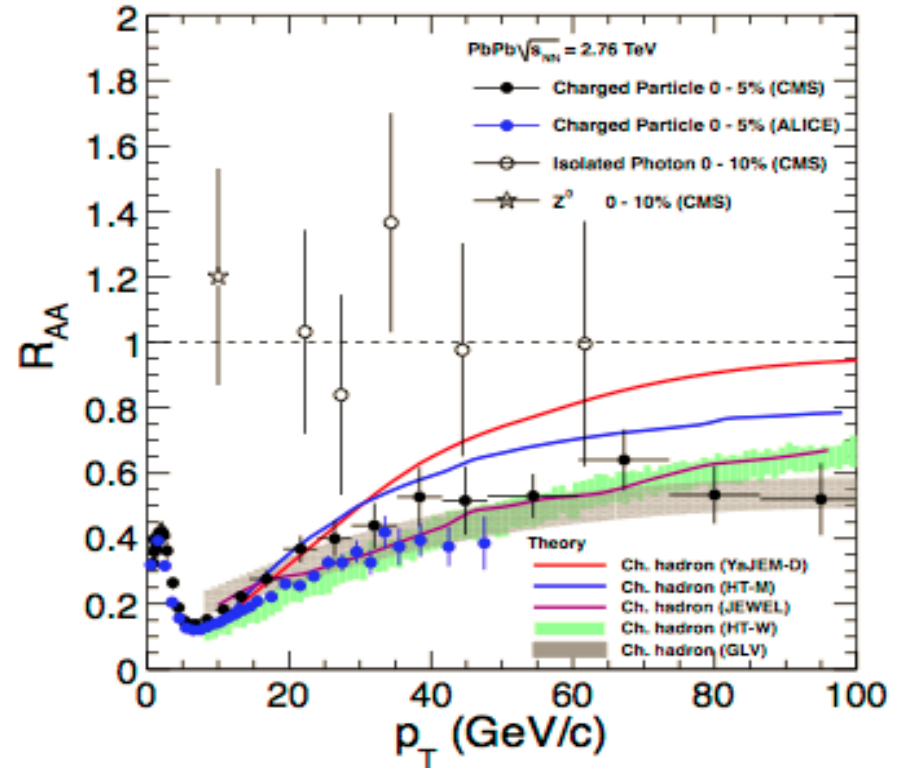
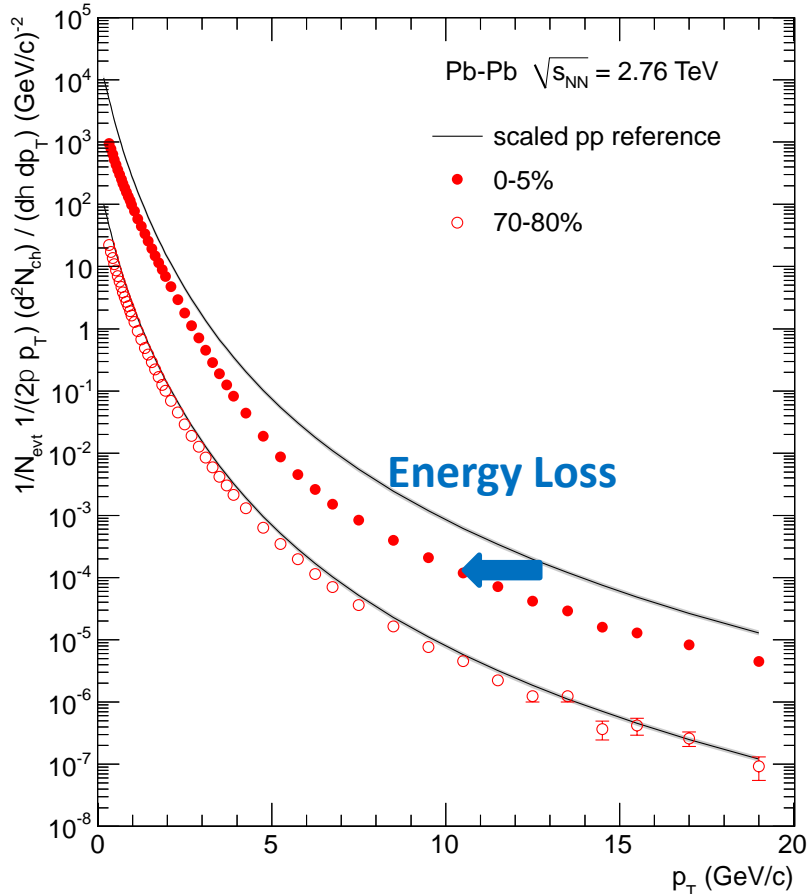
Hard Probes:
 Jets
 Large p_T hadrons
 Heavy quark/hadrons
 Quarkonia
 EM probes
 ...
 "External" probes

Jets in heavy-ion collisions



- 1) jet energy loss
- 2) jet deflection and broadening
- 3) modification of jet substructure
- 4) jet-induced medium excitation (medium response)

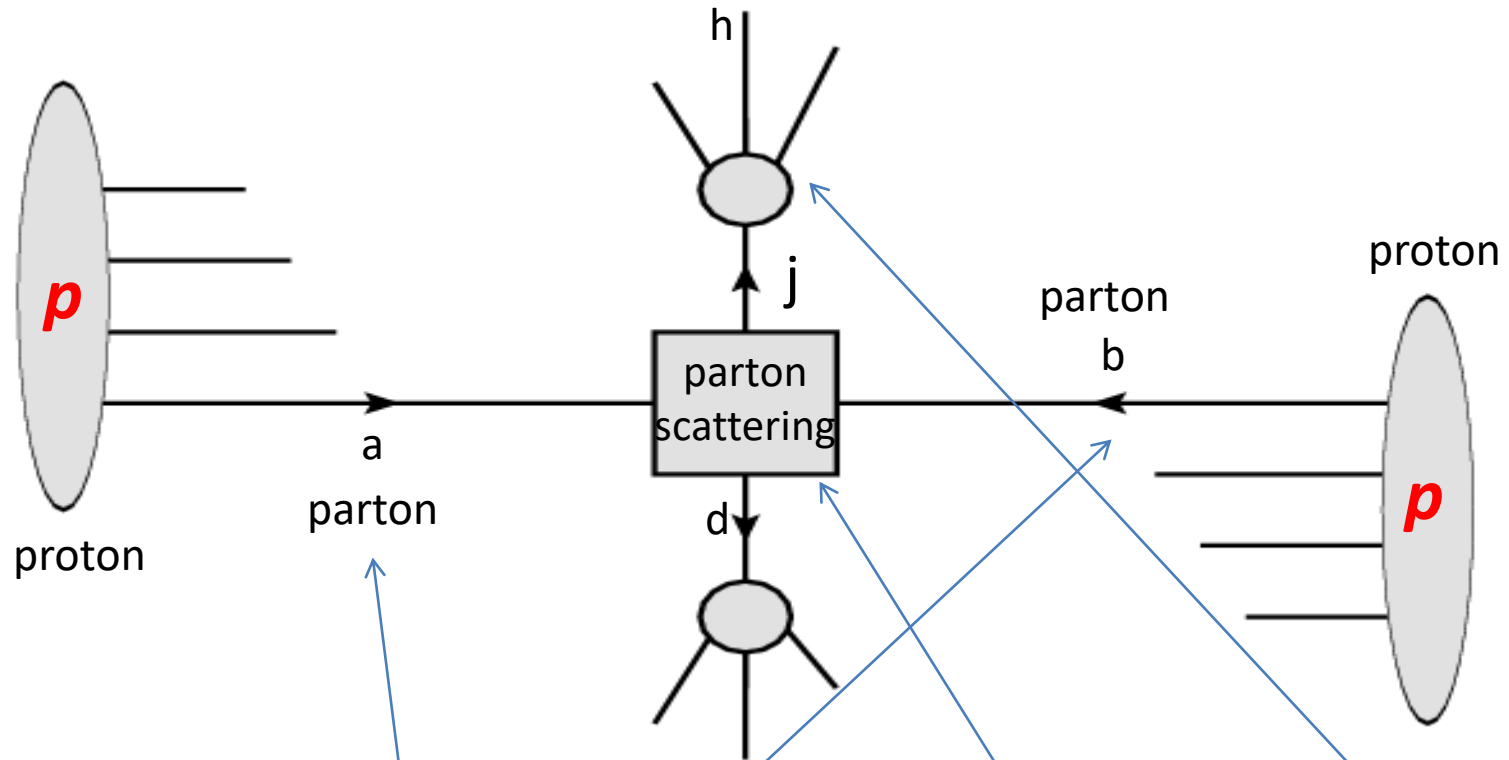
Evidence for jet quenching



Nuclear modification factor:

$$R_{AA}(p_T) = \frac{dN_{AA}/dp_T}{N_{coll}dN_{pp}/dp_T} = \frac{dN_{pp}(p_T+\Delta p_T)/dp_T}{dN_{pp}(p_T)/dp_T}$$

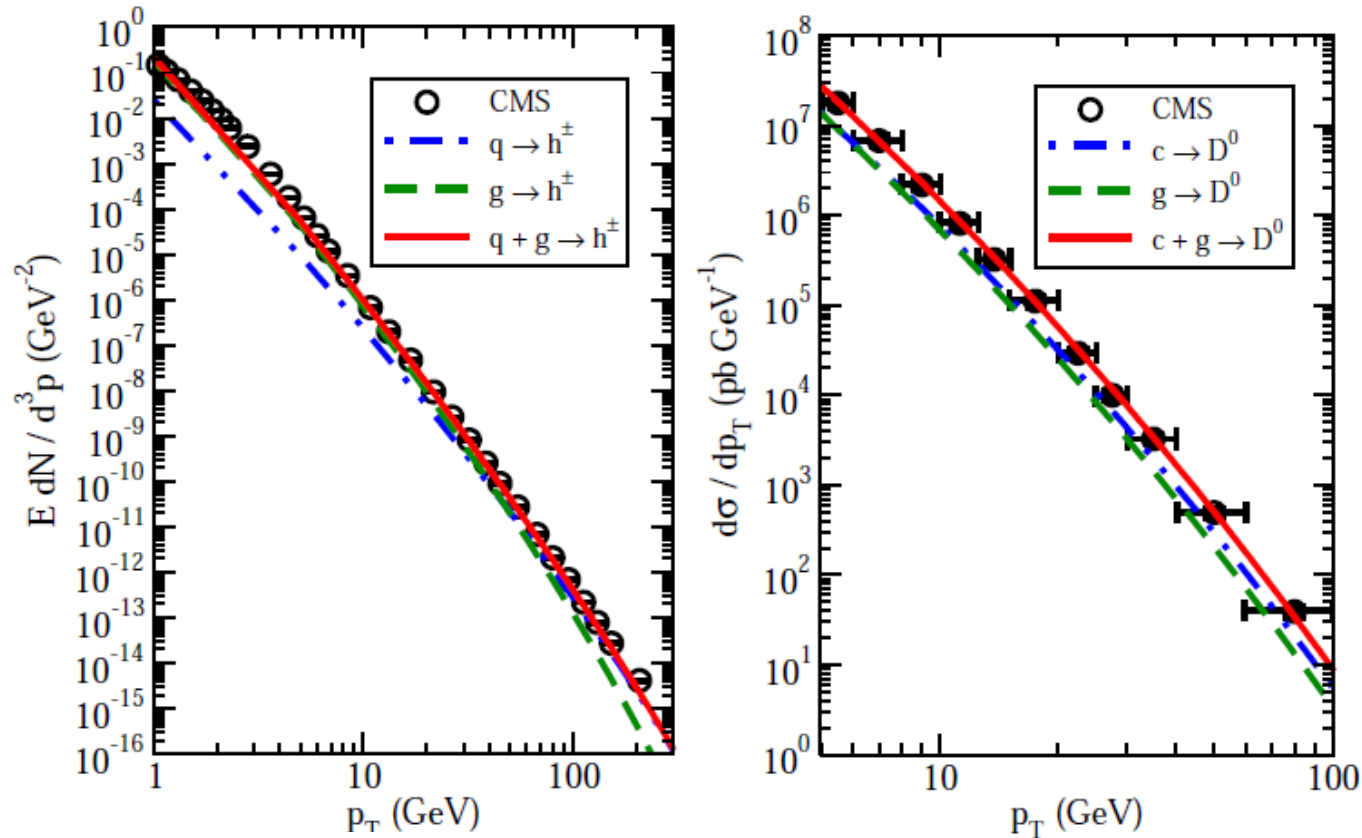
Leading hadron production in pp collisions



$$d\sigma_h = \sum_{abj} f_{a/A} \otimes f_{b/B} \otimes d\sigma_{ab \rightarrow jX} \otimes D_{h/j}$$

pQCD factorization: Large- p_T processes may be factorized into long-distance pieces in terms of PDF & FF, and short-distance parts describing hard interactions of partons.

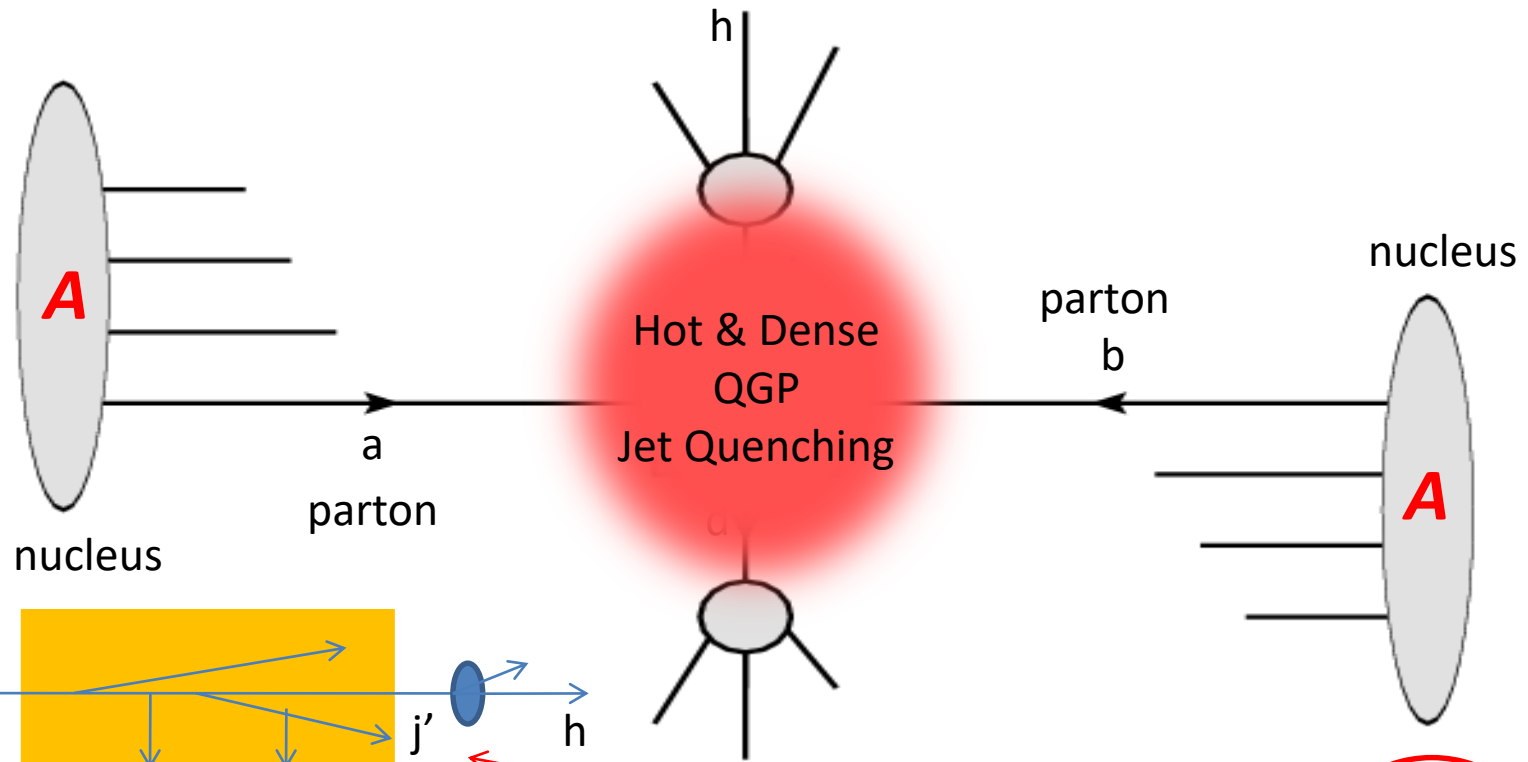
Hadron productions in pp collisions @ NLO



$$d\sigma_{pp \rightarrow hX} = \sum_{abc} \int dx_a \int dx_b \int dz_c f_a(x_a) f_b(x_b) d\hat{\sigma}_{ab \rightarrow c} D_{h/c}(z_c)$$

Based on B. Jager, A. Schafer, M. Stratmann, and W. Vogelsang, Phys. Rev. D67, 054005 (2003)
 F. Aversa, P. Chiappetta, M. Greco, and J. P. Guillet, Nucl. Phys. B327, 105 (1989).

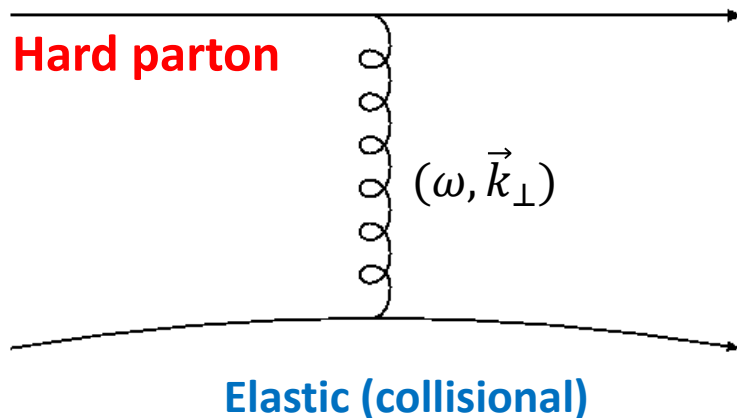
Leading hadron production in AA collisions



$$d\tilde{\sigma}_h = \sum_{abjX} f_{a/A} \otimes f_{b/B} \otimes d\sigma_{ab \rightarrow jX} \otimes \tilde{D}_{h/j}$$

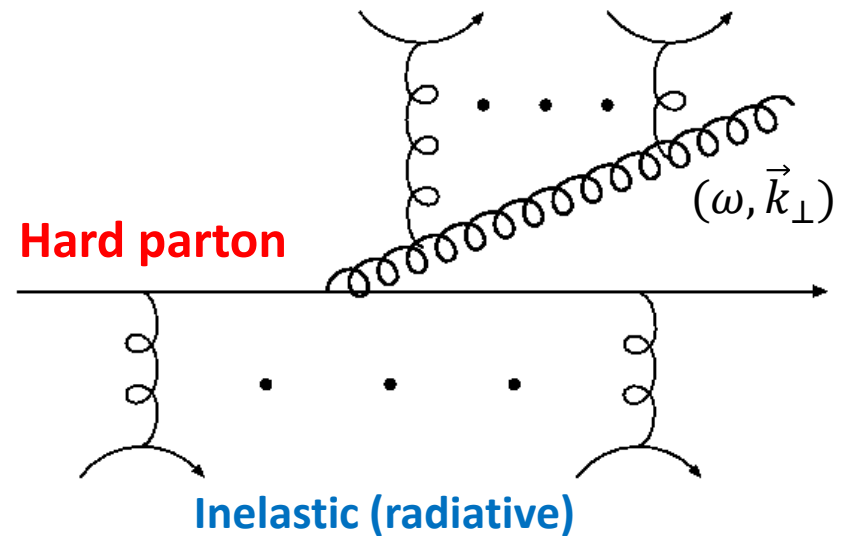
$$d\tilde{\sigma}_h = \sum_{abjj'} f_a \otimes f_b \otimes d\sigma_{ab \rightarrow jX} \otimes P_{j \rightarrow j'} \otimes D_{h/j'}$$

Jet-medium interaction



$$\frac{d\Gamma_{coll}}{d\omega dk_\perp^2 dt} (T, E, \dots) = ?$$

Bjorken 1982; Bratten, Thoma 1991; Thoma, Gyulassy, 1991; Mustafa, Thoma 2005; Peigne, Peshier, 2006; Djordjevic, 2006; Wicks et al (DGLV), 2007; GYQ et al (AMY), 2008; ...



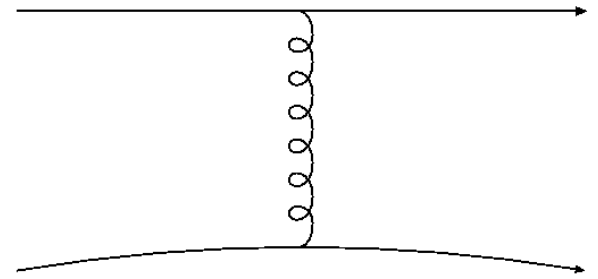
$$\frac{d\Gamma_{rad}}{d\omega dk_\perp^2 dt} (T, E, \dots) = ?$$

BDMPS-Z: Baier-Dokshitzer-Mueller-Peigne-Schiff-Zakharov
ASW: Amesto-Salgado-Wiedemann
AMY: Arnold-Moore-Yaffe (& Caron-Huot, Gale)
GLV: Gyulassy-Levai-Vitev (& Djordjevic, Heinz)
HT: Wang-Guo (& Zhang, Wang, Majumder)

Collisional energy loss

- From kinetic theory, the elastic scattering rate:

$$\Gamma_{ab \rightarrow cd}(\vec{p}_a, T) = \frac{\gamma_2}{2E_a} \int \frac{d^3 p_b}{(2\pi)^3 2E_b} \frac{d^3 p_c}{(2\pi)^3 2E_c} \frac{d^3 p_d}{(2\pi)^3 2E_d} \\ \times f_b(\vec{p}_b, T) [1 \pm f_c(\vec{p}_c, T)] [1 \pm f_d(\vec{p}_d, T)] \\ \times (2\pi)^4 \delta^{(4)}(p_a + p_b - p_c - p_d) |\mathcal{M}_{ab \rightarrow cd}|^2$$



- The collisional energy loss rate:

$$\frac{dE}{dt} = \frac{g_k}{2E} \int \frac{d^3 k}{(2\pi)^3 2k} \int \frac{d^3 p'}{(2\pi)^3 2E'} \int \frac{d^3 k'}{(2\pi)^3 2k'} \\ (2\pi)^4 \delta^4(P + K - P' - K') (E - E') |\bar{M}|^2 f(k) [1 \pm f(k')]$$

$$\left. \frac{dE}{dt} \right|_{qq} = \frac{2}{9} n_f \pi \alpha_s^2 T^2 \left[\ln \frac{ET}{m_g^2} + c_f + \frac{23}{12} + c_s \right]$$

$$\left. \frac{dE}{dt} \right|_{gg} = \frac{4}{3} \pi \alpha_s^2 T^2 \left[\ln \frac{ET}{m_g^2} + c_b + \frac{13}{6} + c_s \right]$$

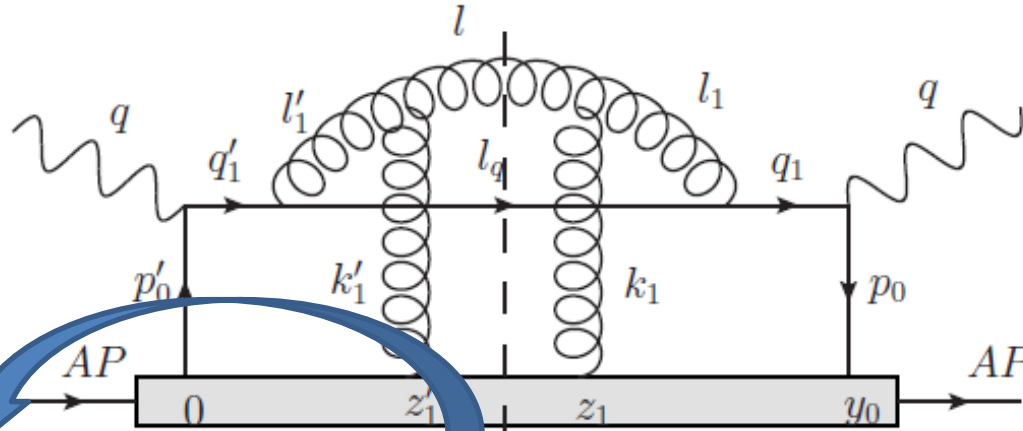
$$\left. \frac{dE}{dt} \right|_{qq} = \frac{1}{2} n_f \pi \alpha_s^2 T^2 \left[\ln \frac{ET}{m_g^2} + c_f + \frac{13}{6} + c_s \right]$$

$$\left. \frac{dE}{dt} \right|_{gg} = 3 \pi \alpha_s^2 T^2 \left[\ln \frac{ET}{m_g^2} + c_b + \frac{131}{48} + c_s \right]$$

- It is infrared logarithmic divergent, screened by plasma effects which are incorporated by including hard thermal loop corrections for soft momenta of order gT

Bjorken 1982; Bratten, Thoma 1991; Thoma, Gyulassy, 1991; Mustafa, Thoma 2005; Peigne, Peshier, 2006; Djordjevic (GLV), 2006; Wicks et al (DGLV), 2007; GYQ et al (AMY), 2008

Medium-induced radiation



Zhang, Hou, GYQ, PRC 2018 & PRC 2019; Zhang, GYQ, Wang, PRD 2019.

+ other 20 diagrams

$$\frac{dN_g^{med}}{dy d^2\mathbf{1}_\perp} = \frac{\alpha_s}{2\pi^2} P(y) \int dZ_1^- \int \frac{dk_1^- d^2\mathbf{k}_{1\perp}}{(2\pi)^3} \mathcal{D}(k_1^-, \mathbf{k}_{1\perp})$$

$$\times \left\{ \left[2 - 2 \cos \left(\frac{y(1-y)}{(y-\lambda_1^-)(1+\lambda_1^- - y)} \frac{(1_\perp - \mathbf{k}_{1\perp})^2 + (y-\lambda_1^-)^2 M^2}{l_\perp^2 + y^2 M^2} \frac{Z_1^-}{\tilde{\tau}_{form}^-} \right) \right] \right.$$

$$C_A \left[\frac{1 + (1 + \lambda_1^- - y)^2}{1 + (1 - y)^2} \left(\frac{y - \frac{\lambda_1^-}{2}}{y - \lambda_1^-} \right)^2 \frac{(1_\perp - \mathbf{k}_{1\perp})^2 + \frac{(y-\lambda_1^-)^4 M^2}{1+(1+\lambda_1^- - y)^2}}{[(1_\perp - \mathbf{k}_{1\perp})^2 + (y - \lambda_1^-)^2 M^2]^2} \right.$$

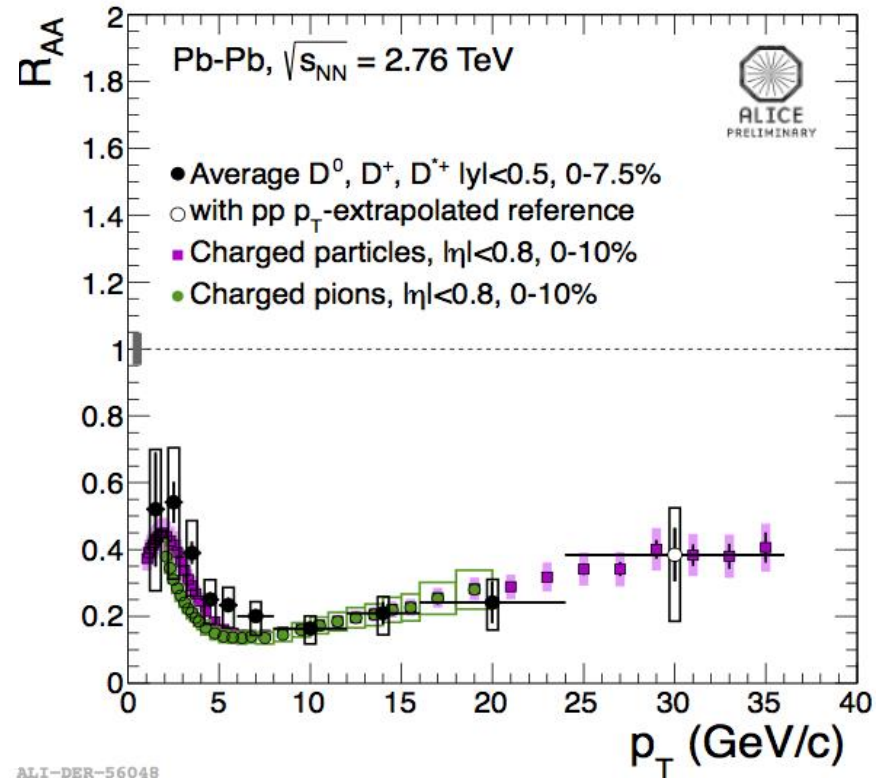
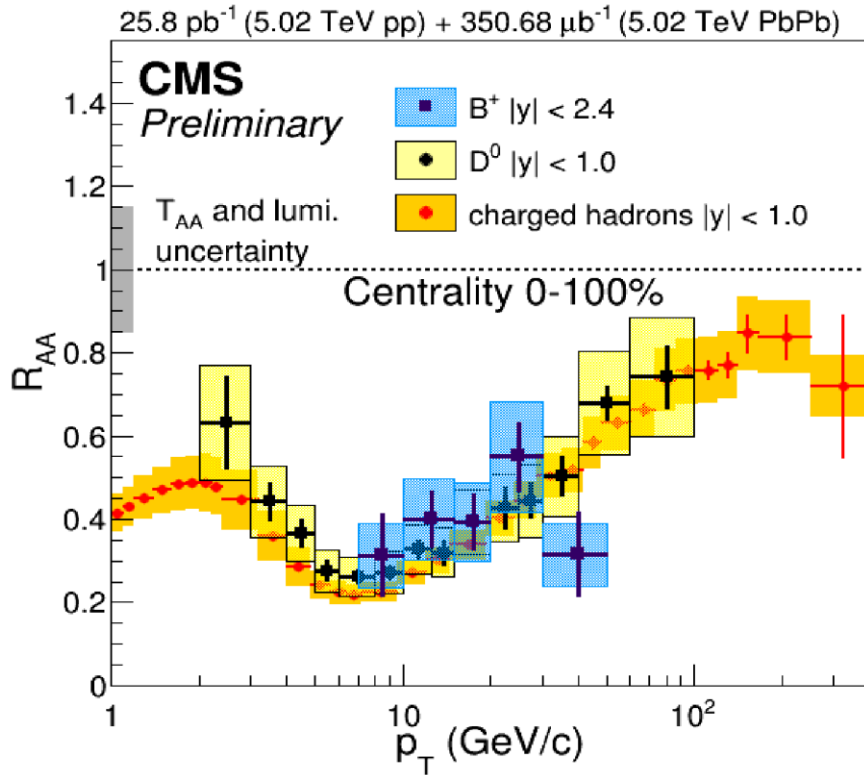
$$- \frac{1 + (1 + \lambda_1^- - y)(1 - y)}{2[1 + (1 - y)^2]} \left(\frac{y - \frac{\lambda_1^-}{2}}{y - \lambda_1^-} \right) \frac{1_\perp \cdot (1_\perp - \mathbf{k}_{1\perp}) + \frac{y^2 (y - \lambda_1^-)^2}{1 + (1 + \lambda_1^- - y)(1 - y)} M^2}{[l_\perp^2 + y^2 M^2] [(1_\perp - \mathbf{k}_{1\perp})^2 + (y - \lambda_1^-)^2 M^2]} \mathcal{D}(k_1^-, \mathbf{k}_{1\perp}) = (2\pi)^3 \frac{dP_{el}}{dk_1^- d^2\mathbf{k}_{1\perp} dZ_1^-}$$

$$\left. - \frac{1 + (1 + \lambda_1^- - y)(1 - \frac{y}{1+\lambda_1^-})}{2[1 + (1 - y)^2]} \left(\frac{y - \frac{\lambda_1^-}{2}}{y - \lambda_1^-} \right) \frac{(1_\perp - \mathbf{k}_{1\perp}) \cdot \left(1_\perp - \frac{y}{1+\lambda_1^-} \mathbf{k}_{1\perp} \right) + \frac{\left(\frac{y}{1+\lambda_1^-} \right)^2 (y - \lambda_1^-)^2}{1 + (1 + \lambda_1^- - y)(1 - \frac{y}{1+\lambda_1^-})} M^2}{\left[\left(1_\perp - \frac{y}{1+\lambda_1^-} \mathbf{k}_{1\perp} \right)^2 + \left(\frac{y}{1+\lambda_1^-} \right)^2 M^2 \right] [(1_\perp - \mathbf{k}_{1\perp})^2 + (y - \lambda_1^-)^2 M^2]} \right\} + \dots$$

Medium-induced gluon radiation spectrum is directly controlled by differential scattering rate (or generalized \hat{q})

Medium-induced gluon emission beyond collinear expansion & soft gluon emission limit with transverse & longitudinal scatterings for massive/massless quarks

Flavor hierarchy of jet quenching



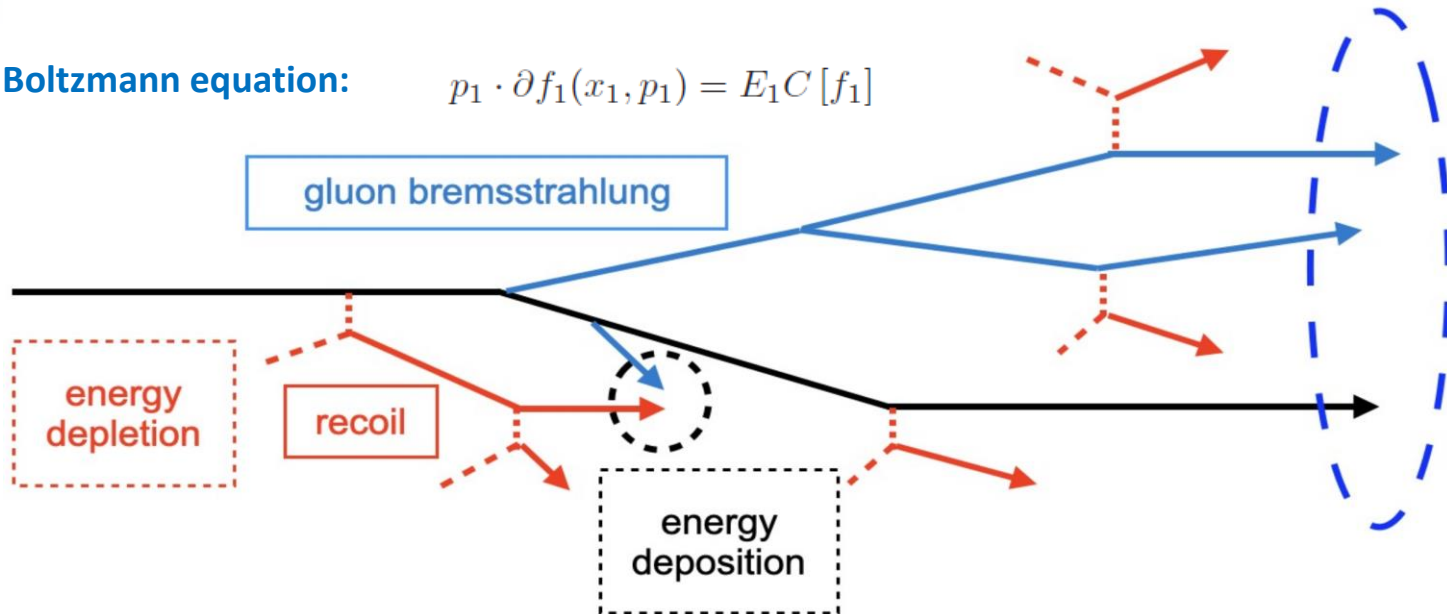
ALI-DER-56048

$$R_{AA} = \frac{1}{N_{coll}} \frac{dN^{AA} / d^2 p_T dy}{dN^{pp} / d^2 p_T dy}$$

Flavor hierarchy of parton energy loss:
 $\Delta E_g > \Delta E_q > \Delta E_c > \Delta E_b$.
 However, $R_{AA}(h) \approx R_{AA}(D)$. Why?

Linear Boltzmann Transport (LBT) Model

- Boltzmann equation:** $p_1 \cdot \partial f_1(x_1, p_1) = E_1 C [f_1]$



- Elastic collisions:**

$$\Gamma_{12 \rightarrow 34} = \frac{\gamma_2}{2E_1} \int \frac{d^3 p_2}{(2\pi)^3 2E_2} \int \frac{d^3 p_3}{(2\pi)^3 2E_3} \int \frac{d^3 p_4}{(2\pi)^3 2E_4} \times f_2(\vec{p}_2) \left[1 \pm f_3(\vec{p}_1 - \vec{k}) \right] \left[1 \pm f_4(\vec{p}_2 + \vec{k}) \right] \times (2\pi)^4 \delta^{(4)}(p_1 + p_2 - p_3 - p_4) |\mathcal{M}_{12 \rightarrow 34}|^2$$

Matrix elements taken from LO pQCD

$$P_{el} = 1 - e^{-\Gamma_{el} \Delta t}$$

- Inelastic collisions:**

$$\langle N_g \rangle = \Gamma_g \Delta t = \Delta t \int dx dk_{\perp}^2 \frac{dN_g}{dx dk_{\perp}^2 dt}$$

$$P_{inel} = 1 - e^{-\langle N_g \rangle}$$

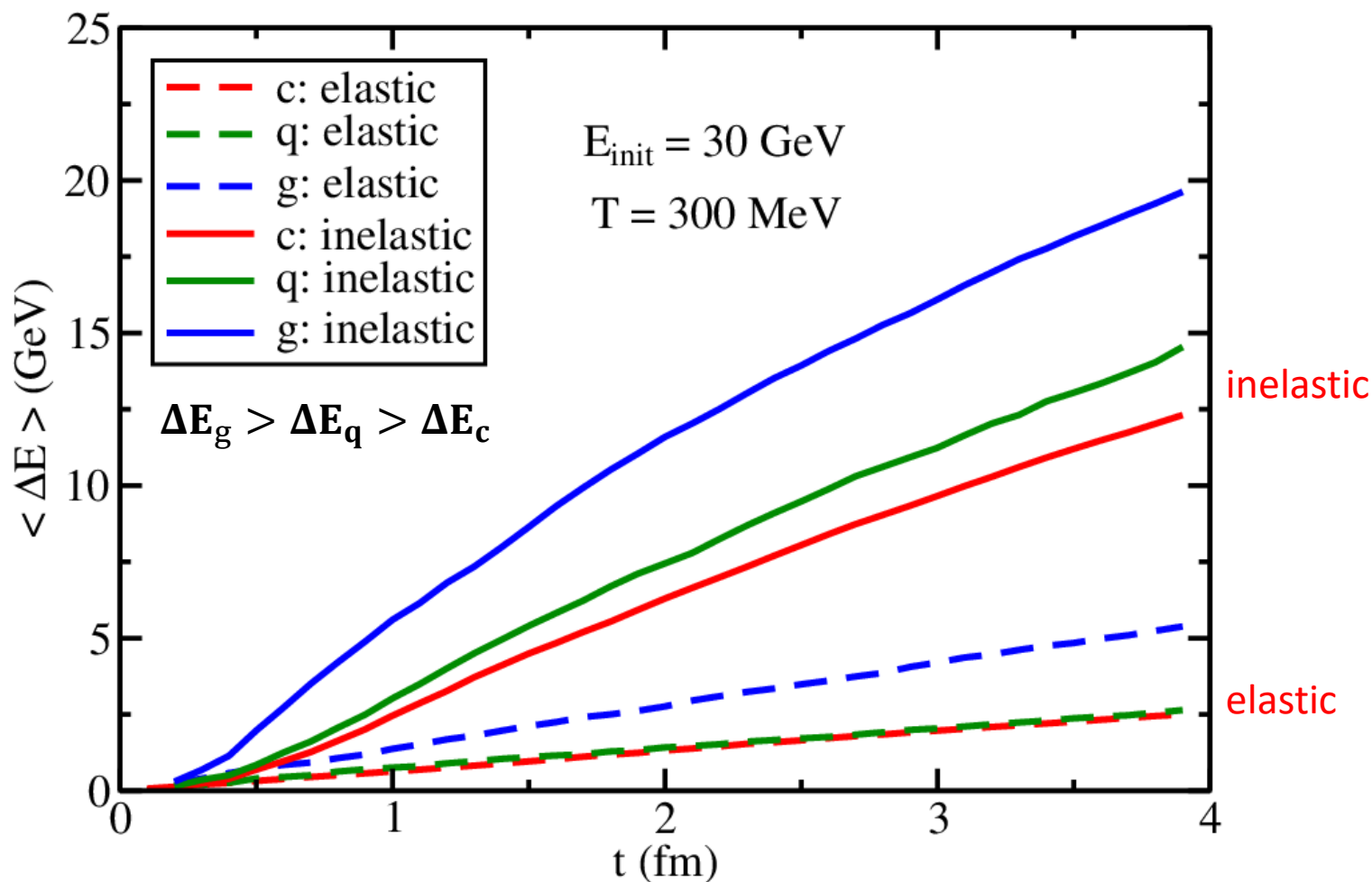
Medium-induced radiation spectra taken from HT: Guo, Wang PRL 2000; Zhang, Wang, Wang, PRL 2004; Zhang, Hou, GYQ, PRC 2019.

- Elastic + Inelastic:**

$$P_{tot} = 1 - e^{-\Gamma_{tot} \Delta t} = P_{el} + P_{inel} - P_{el} P_{inel}$$

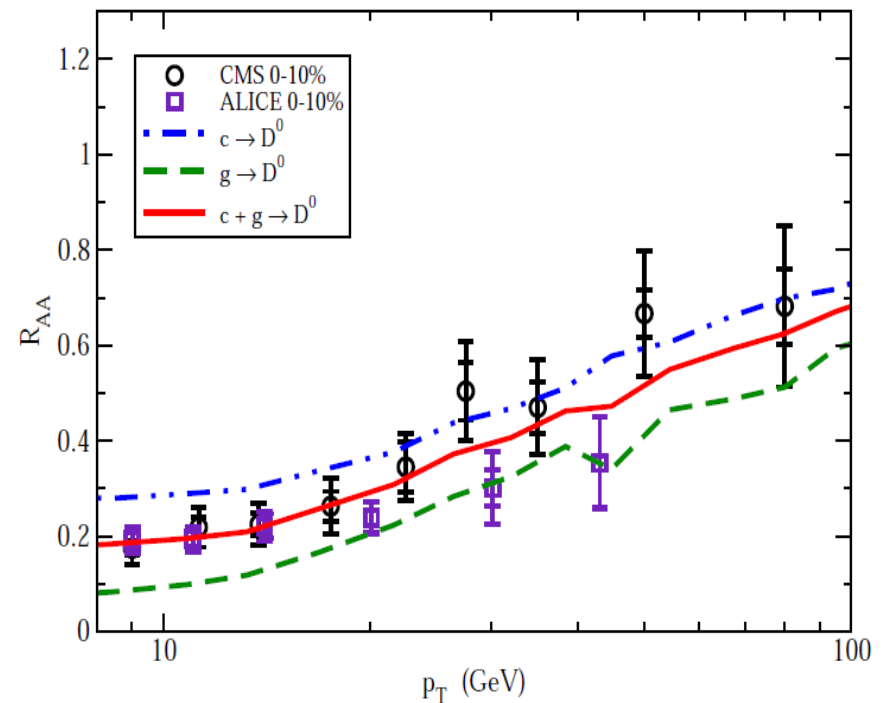
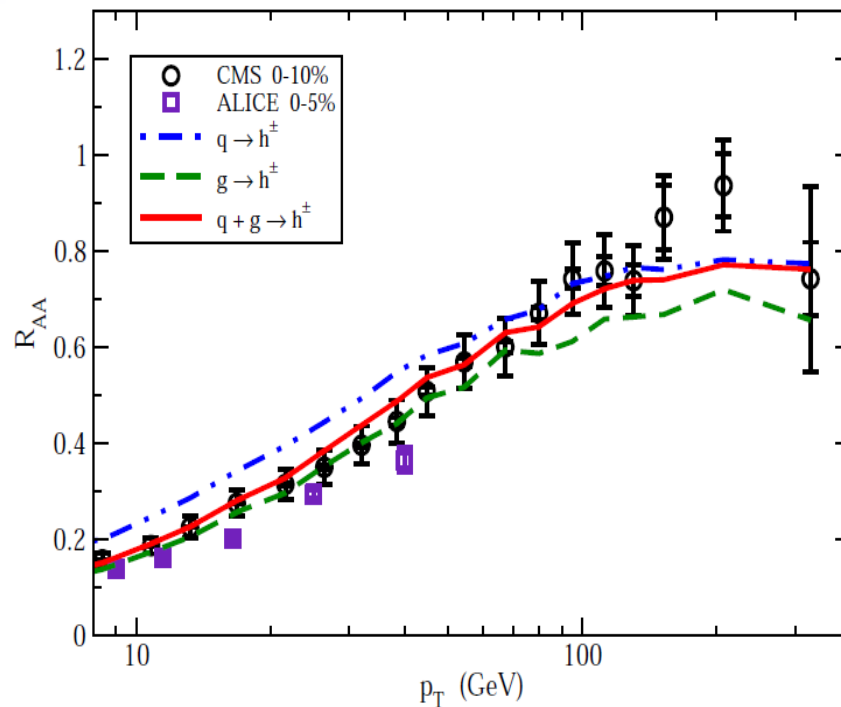
He, Luo, Wang, Zhu, PRC 2015; Cao, Luo, GYQ, Wang, PRC 2016, PLB 2018; etc.

Flavor hierarchy of parton energy loss



He, Luo, Wang, Zhu, PRC 2015; Cao, Luo, GYQ, Wang, PRC 2016 ; PLB 2018; etc.

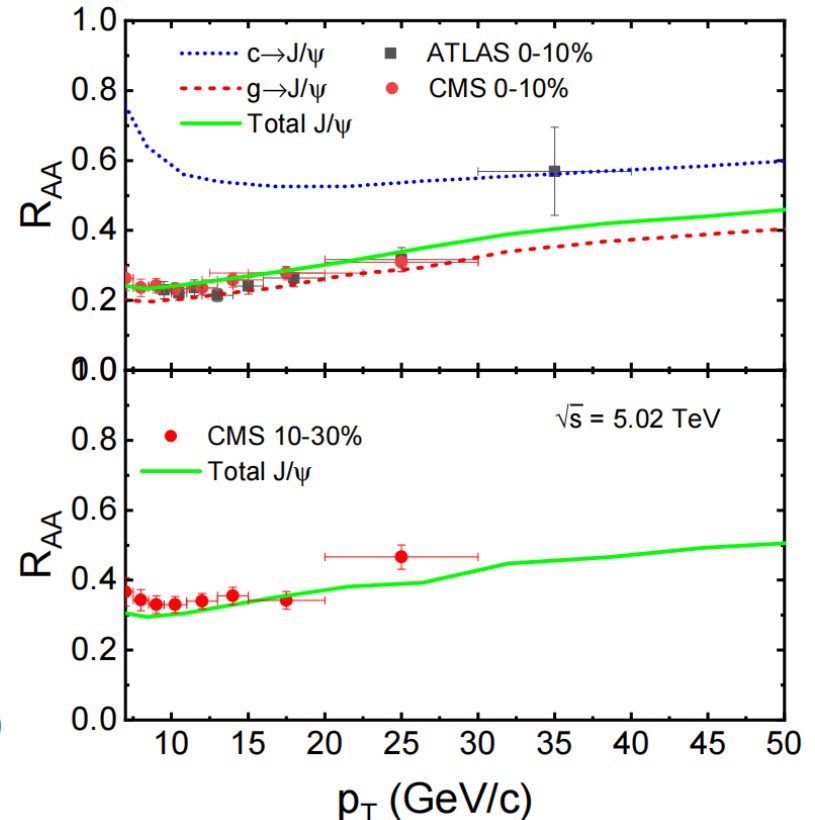
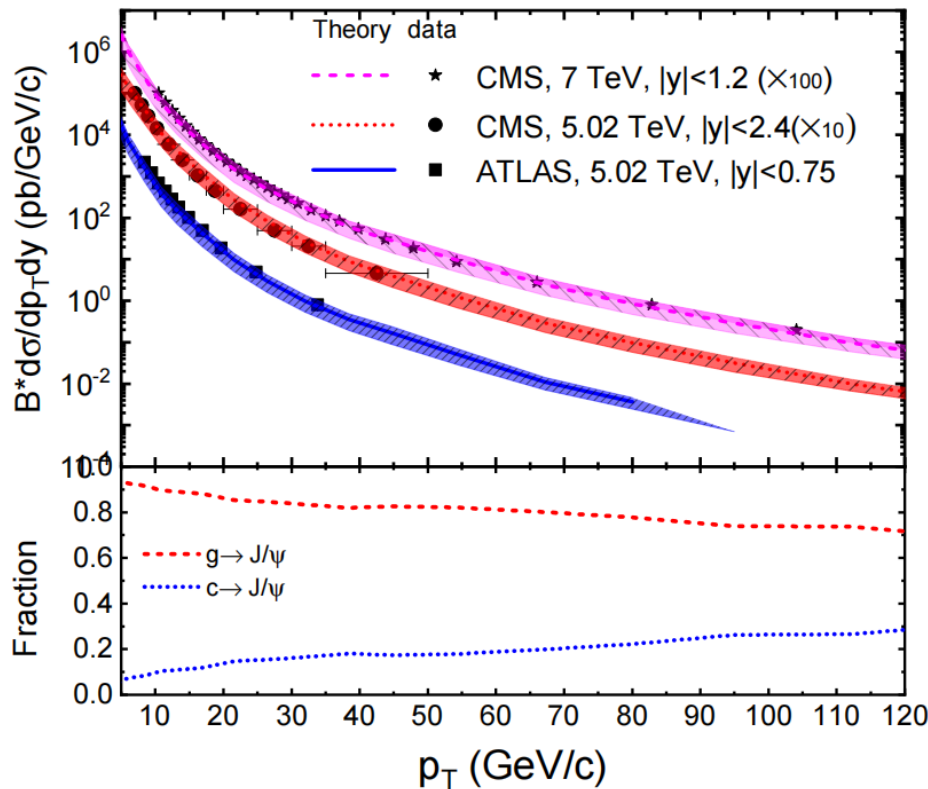
Flavor hierarchy of jet quenching



Build a state-of-art jet quenching framework (NLO-pQCD + LBT + Hydrodynamics)
Quark-initiated hadrons have less quenching effects than gluon-initiated hadrons.
Combining both quark and gluon contributions, we obtain a nice description of charged hadron & D meson R_{AA} over a wide range of p_T .

Xing, Cao, GYQ, Xing, PLB 2020

Glucons dominate high p_T J/Ψ suppression



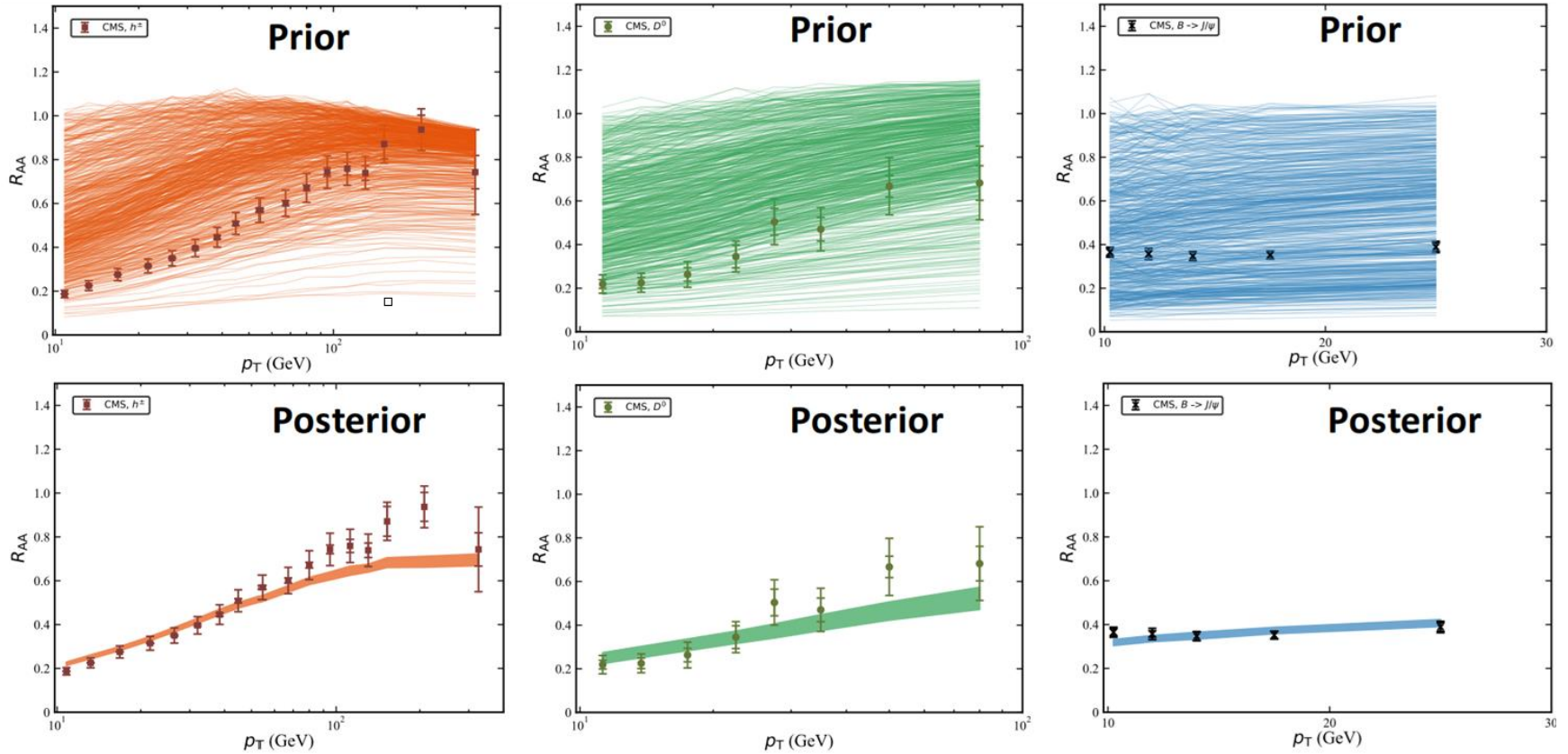
$$d\sigma[AB \rightarrow J/\psi + X] = \sum_i d\hat{\sigma}_{AB \rightarrow i+X} \otimes D_{i \rightarrow J/\psi} \quad D_{i \rightarrow J/\psi}(z, \mu) = \sum_n \hat{d}_{i \rightarrow [Q\bar{Q}(n)]}(z, \mu) \langle \mathcal{O}_{[Q\bar{Q}(n)]}^{J/\psi} \rangle$$

The gluon jet quenching is the driving force for high p_T J/Ψ suppression.

S.-L. Zhang, J. Liao, GYQ, E. Wang, H. Xing, Sci.Bull. 68 (2023) 2003-2009

Ma, Qiu, Zhang, PRD, 2014; Bodwin, Kim, Lee, JHEP 2012; Bodwin, Chung, Kim, Lee, PRL 2014

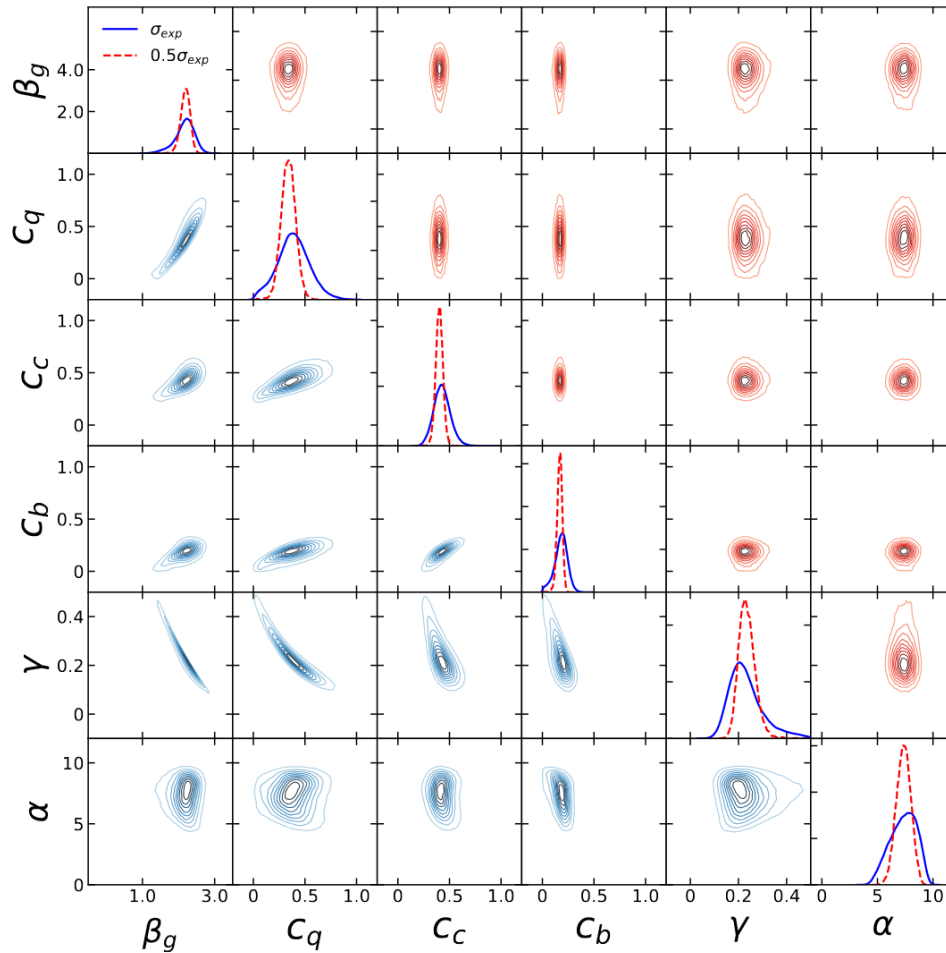
Bayesian analysis of high p_T hadron R_{AA}



$$\frac{1}{\langle N_{\text{coll}} \rangle} \frac{d\sigma_{AA \rightarrow hX}}{dp_T^h} = \sum_j \int dp_T^j dx dz \frac{d\hat{\sigma}_{p'p' \rightarrow jX}}{dp_T^j}(p_T^j) W_{AA}(x) D_{j \rightarrow h}(z) \delta(p_T^h - z(p_T^j - x \langle \Delta p_T^j \rangle))$$

$$\langle \Delta p_T^j \rangle = C_j \beta_g p_T^j \log(p_T) \quad W_{AA}(x) = \frac{\alpha^\alpha x^{\alpha-1} e^{-\alpha x}}{\Gamma(\alpha)}$$

Posterior distributions of parameters

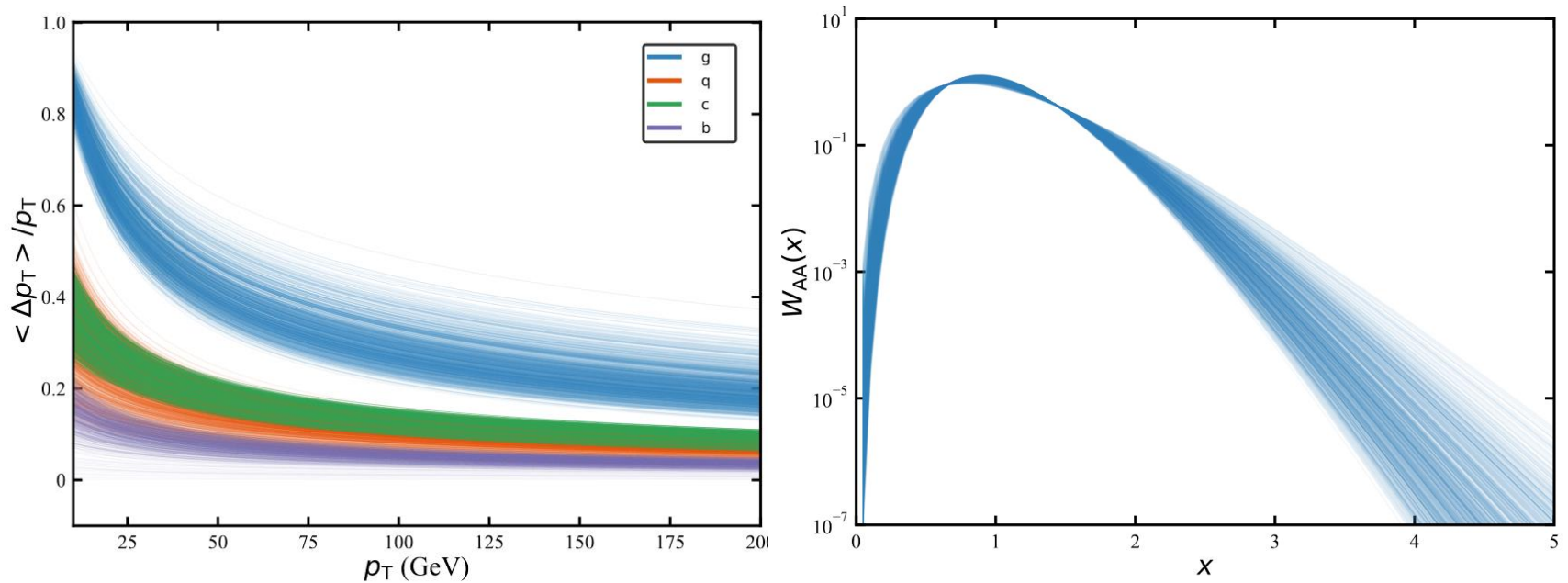


	with σ_{exp}	with $0.5\sigma_{exp}$
β_g	(1.646, 2.56)	(1.96, 2.39)
C_q	(0.129, 0.65)	(0.226, 0.454)
C_c	(0.3, 0.567)	(0.344, 0.459)
C_b	(0.065, 0.277)	(0.124, 0.207)
γ	(0.137, 0.378)	(0.184, 0.295)
α	(5.287, 9.061)	(6.266, 8.401)

The energy loss parameters for jet-medium interaction can be well constrained by the Bayesian analysis.

Reducing experimental data error bars can improve the precision of the extracted parameters.

Flavor hierarchy of parton energy loss

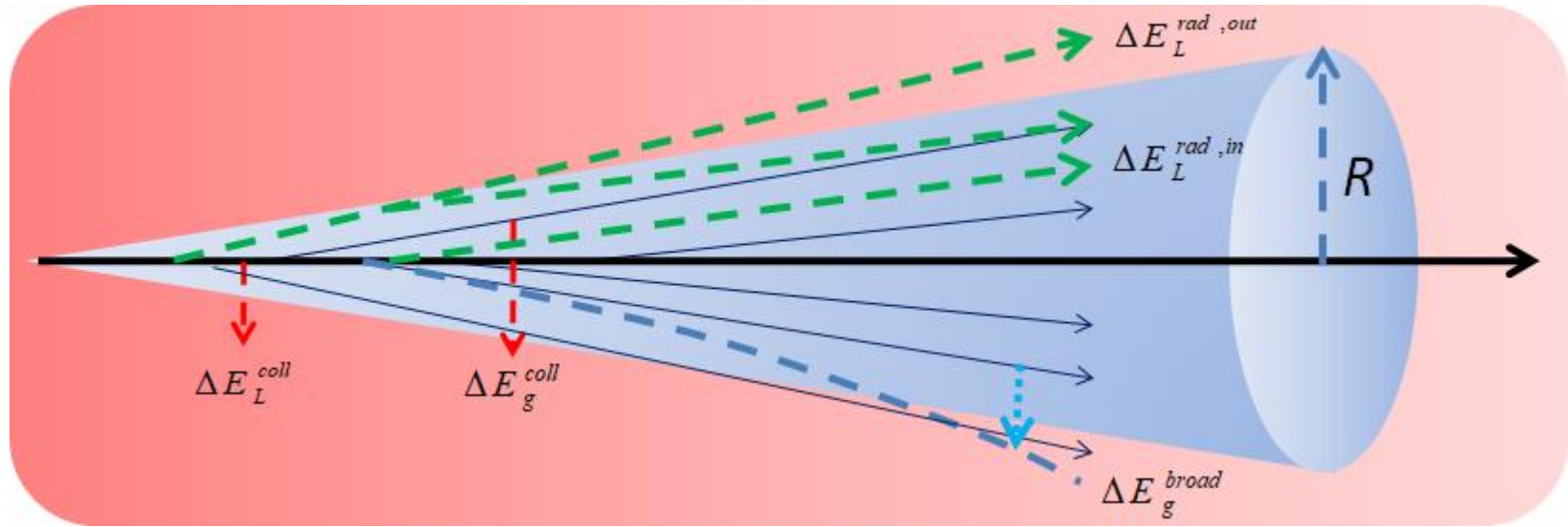


$$\frac{1}{\langle N_{\text{coll}} \rangle} \frac{d\sigma_{AA \rightarrow hX}}{dp_T^h} = \sum_j \int dp_T^j dx dz \frac{d\hat{\sigma}_{p'p' \rightarrow jX}}{dp_T^j}(p_T^j) W_{AA}(x) D_{j \rightarrow h}(z) \delta(p_T^h - z(p_T^j - x \langle \Delta p_T^j \rangle))$$

$$\langle \Delta E_g \rangle > \langle \Delta E_q \rangle \sim \langle \Delta E_c \rangle > \langle \Delta E_b \rangle$$

Direct extraction of the flavor dependence of parton energy loss in QGP from data.
Provides a stringent test of pQCD calculation of parton-medium interaction.

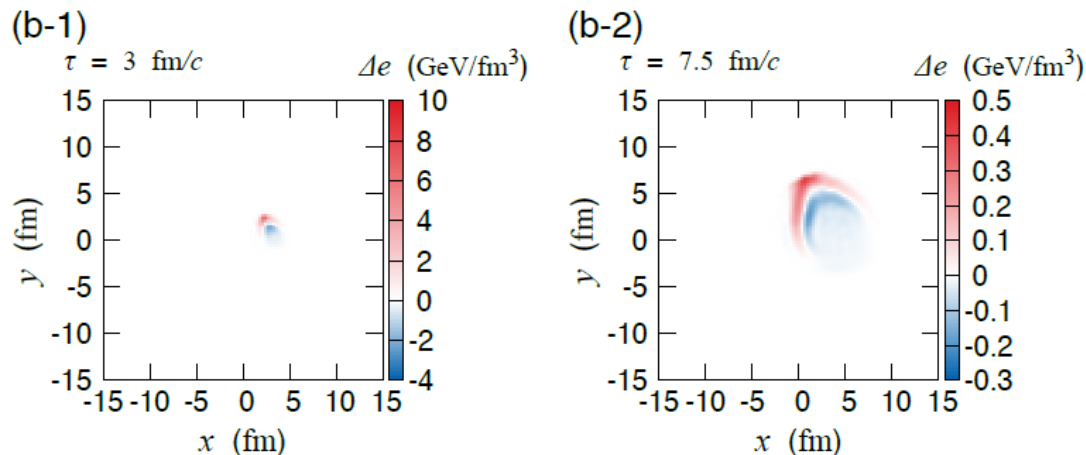
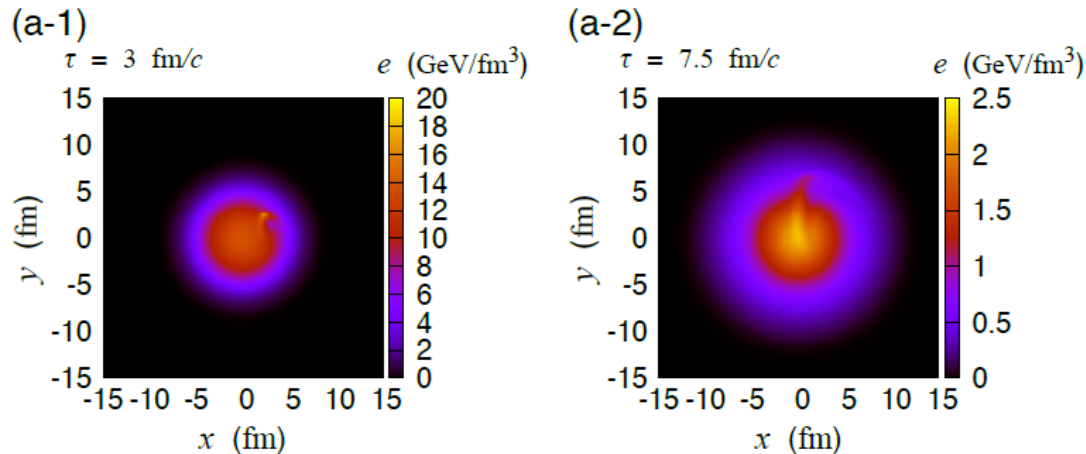
Full jet evolution & energy loss in QGP



$$E_{jet} = E_{in} + E_{lost} = E_{in} + E_{rad,out} + E_{kick,out} + (E_{th} - E_{th,in})$$

Vitev, Zhang, PRL 2010; GYQ, Muller, PRL, 2011; Casalderrey-Solana, Milhano, Wiedemann, JPG 2011; Young, Schenke, Jeon, Gale, PRC, 2011; Dai, Vitev, Zhang, PRL 2013; Wang, Zhu, PRL 2013; Blaizot, Iancu, Mehtar-Tani, PRL 2013; etc.

Jet evolution & medium response



Jet-fluid model:

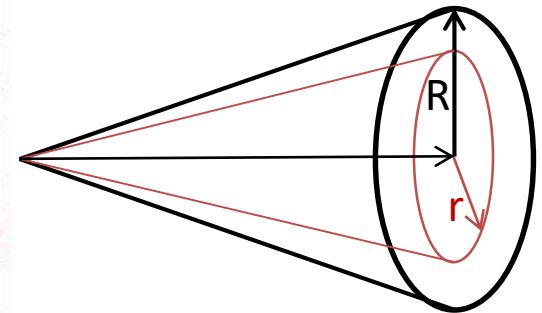
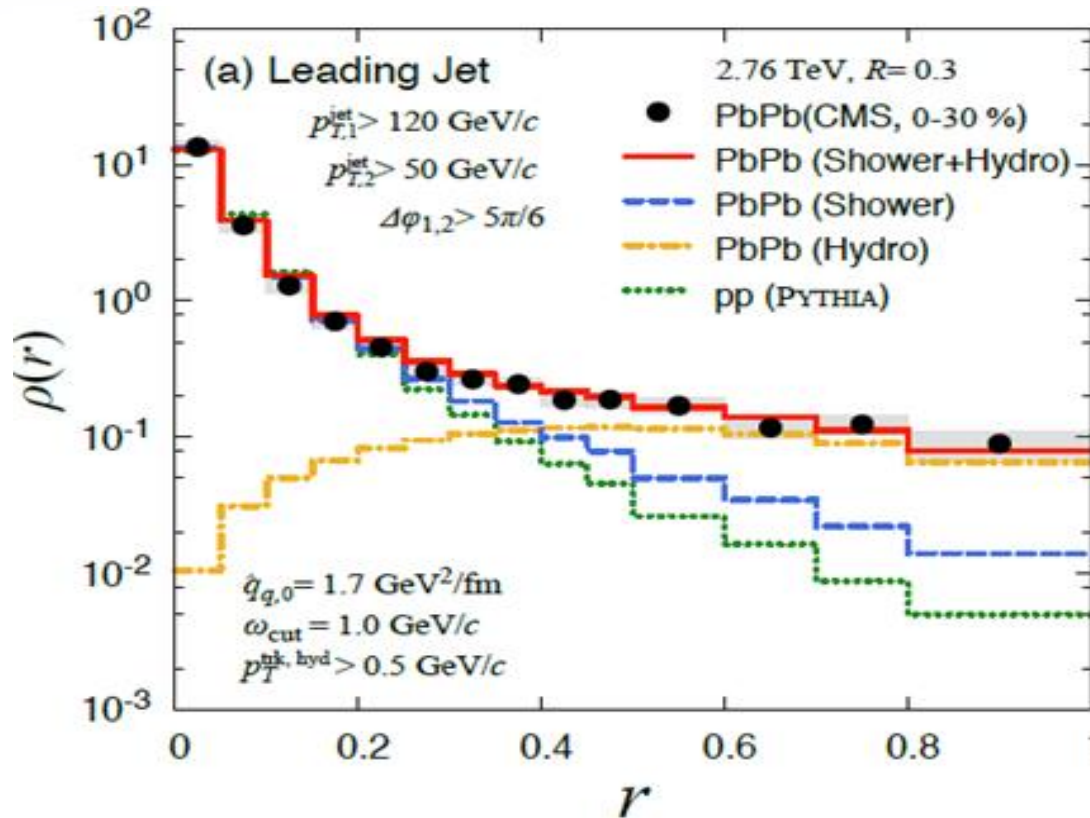
$$\frac{df}{dt} = C[f], \partial_\mu T^{\mu\nu} = J^\nu$$

Jet deposits energy and momentum into medium, and induces V-shaped wave fronts

The wave fronts carry energy and momentum, propagates forward and outward, and depletes the energy behind the jet (diffusion wake)

Jet-induced flow and the radial flow of medium are pushed and distorted by each other

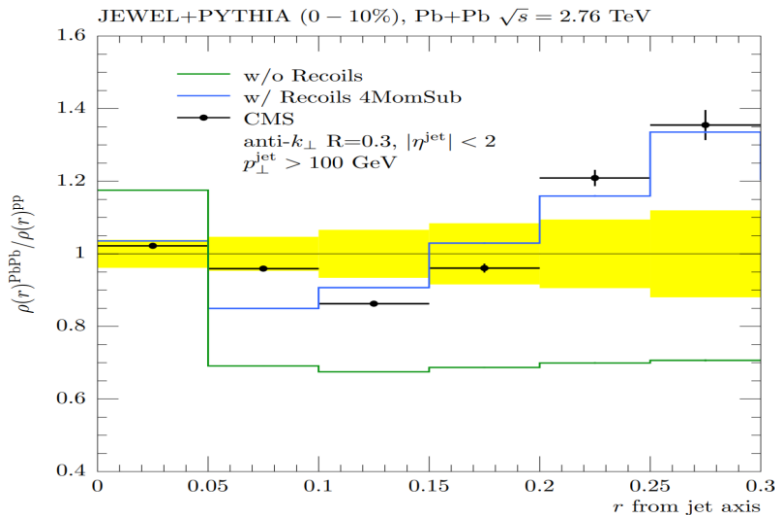
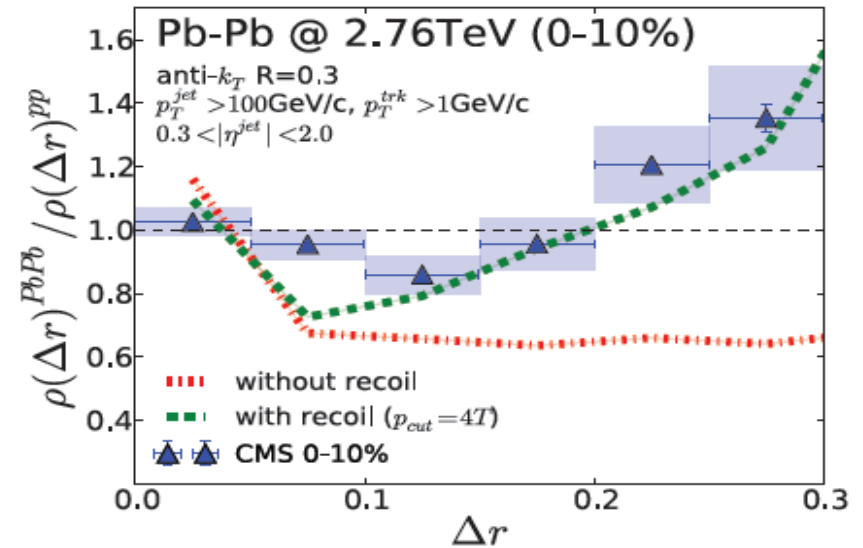
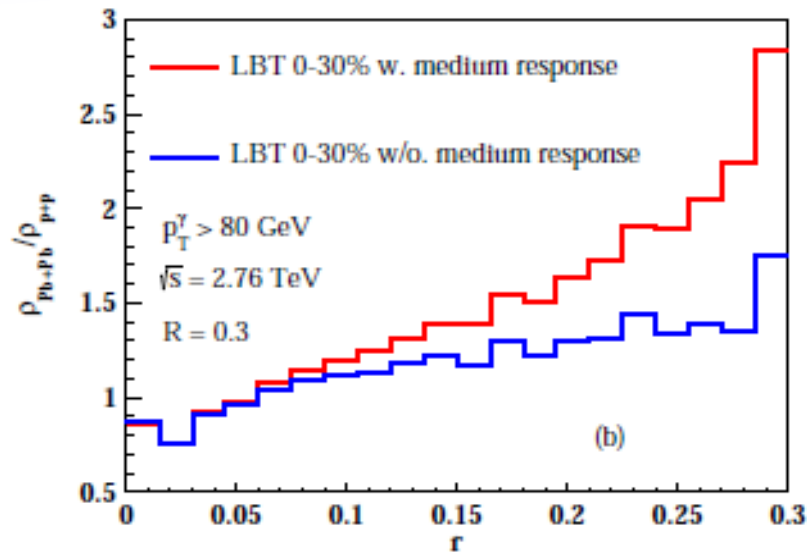
Signal of jet-induced flow in jet shape



The contribution from the hydro part is quite flat and finally dominates over the shower part in the region from $r = 0.4-0.5$.

Signal of medium response in full jet shape at large r .

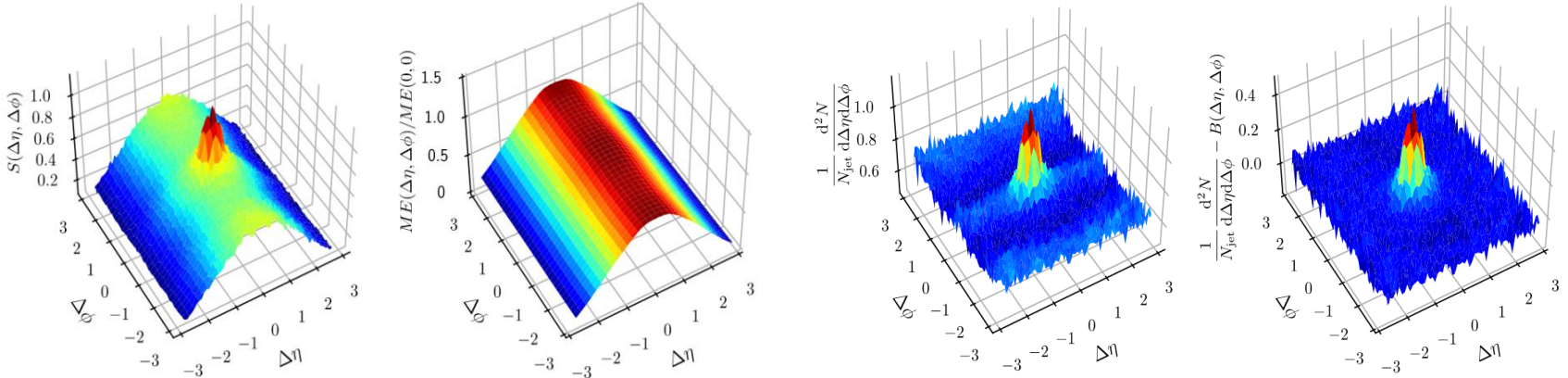
Effect of jet-induced flow on jet shape



Luo, Cao, He, Wang, PLB 2018;
 C. Park, S. Jeon, C. Gale, 2018;
 Elayavalli, Zapp, JHEP 2017;

The inclusion of medium response
 can naturally explain the
 enhancement of jet shape at larger r .

Hadron chemistry around quenched jets

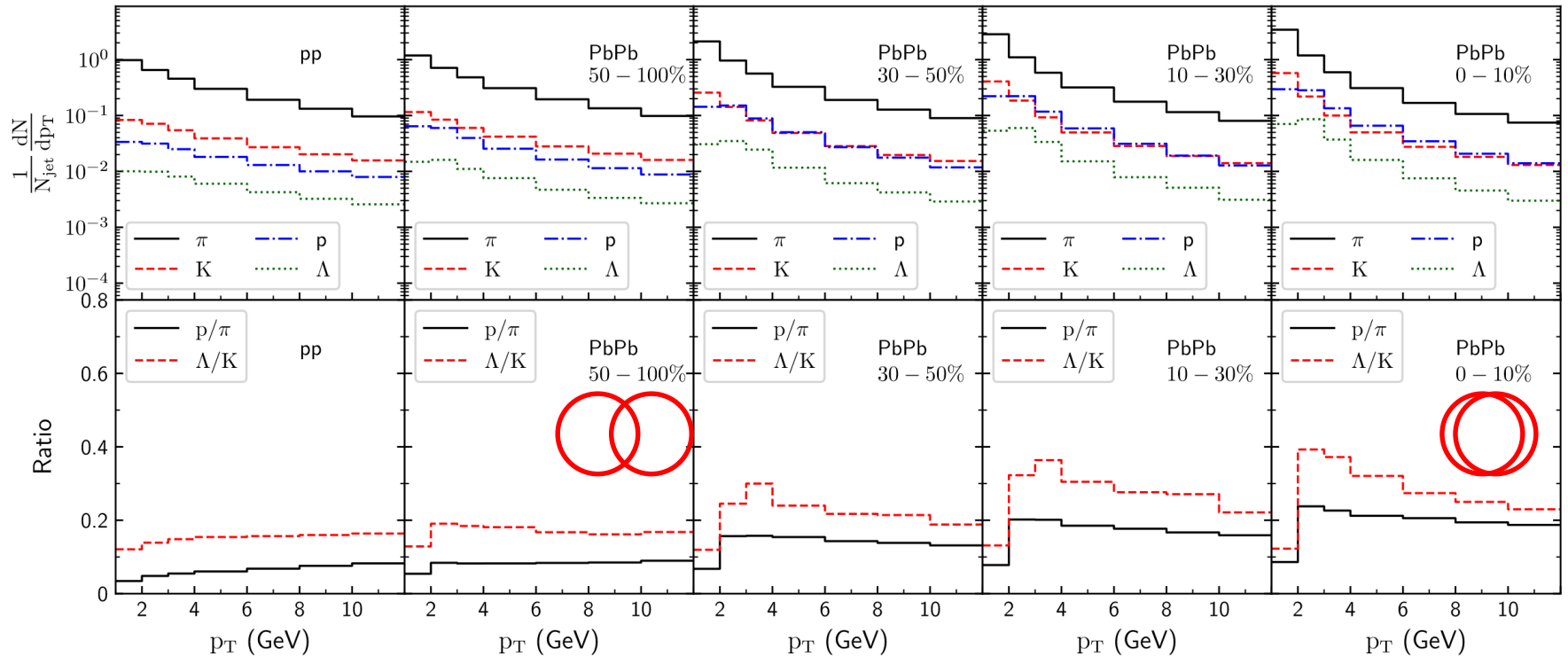


$$\frac{1}{N_{\text{jet}}} \frac{d^2N}{d\Delta\eta d\Delta\phi} = \frac{ME(0,0)}{ME(\Delta\eta, \Delta\phi)} S(\Delta\eta, \Delta\phi) \quad \longrightarrow \quad \frac{d^3N}{dp_T d\Delta\phi d\Delta\eta}$$

$$\frac{dN}{dp_T} = \int d\Delta\phi \int d\Delta\eta \left. \frac{d^3N}{dp_T d\Delta\phi d\Delta\eta} \right|_{\Delta r < 1}$$

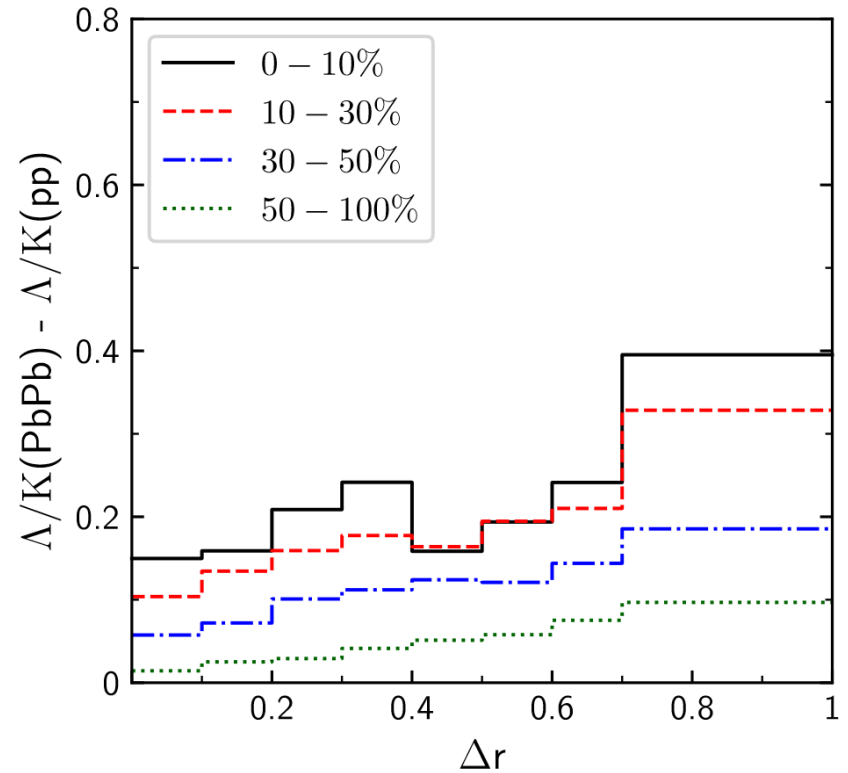
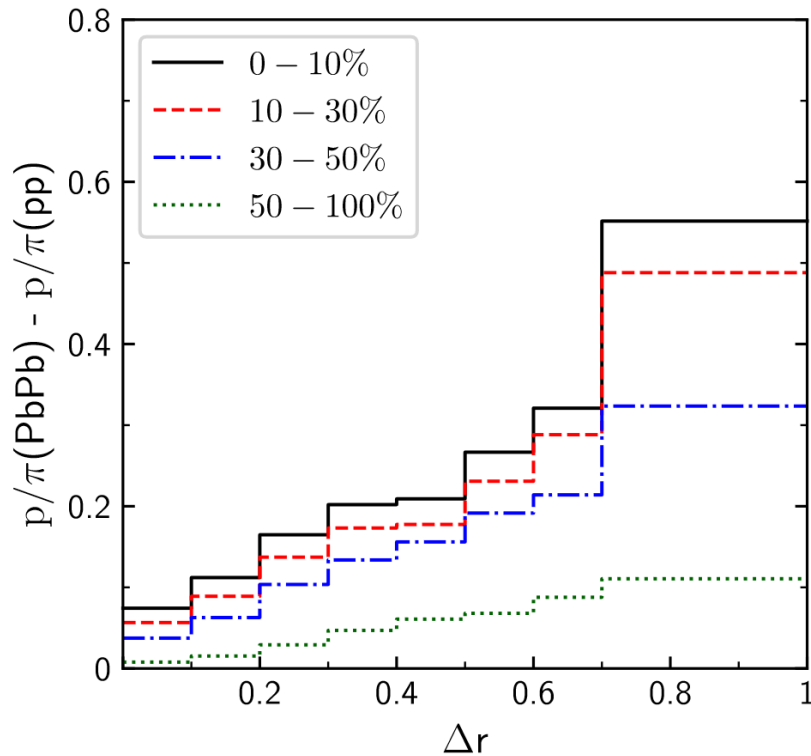
$$\frac{dN}{d\Delta r} = \int d\Delta\phi \int d\Delta\eta \int dp_T \frac{d^3N}{dp_T d\Delta\phi d\Delta\eta} \delta(\Delta r - \sqrt{(\Delta\phi)^2 + (\Delta\eta)^2})$$

B/M enhancement around jets: p_T dependence



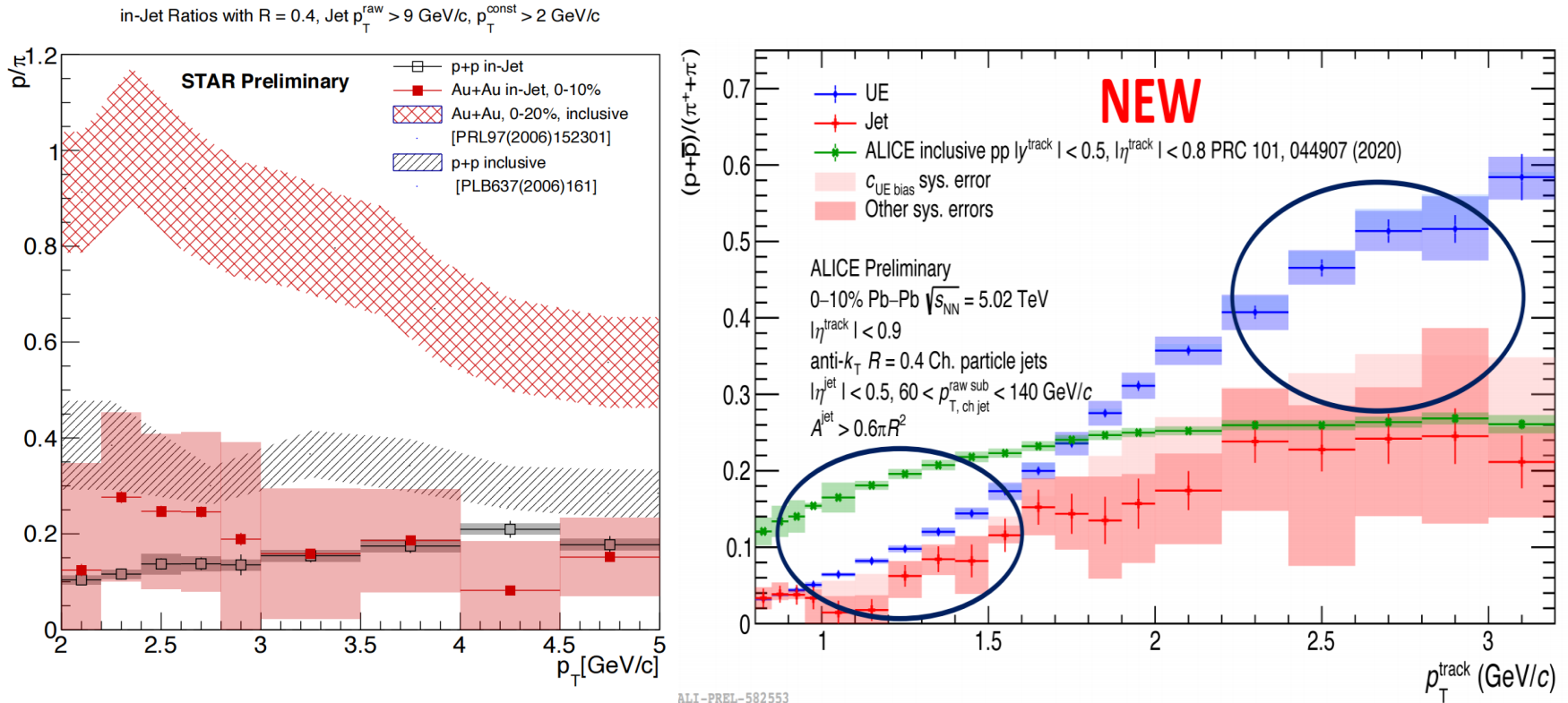
We find a strong enhancement of B/M ratios for associated particles at intermediate p_T around the quenched jets, due to the coalescence of jet-excited medium partons.

B/M enhancement around jets: radial dependence



For intermediate p_T (2-6GeV) regime, the enhancement of jet-induced B/M ratios is stronger for larger distance because the lost energy from quenched jets can diffuse to large angle.

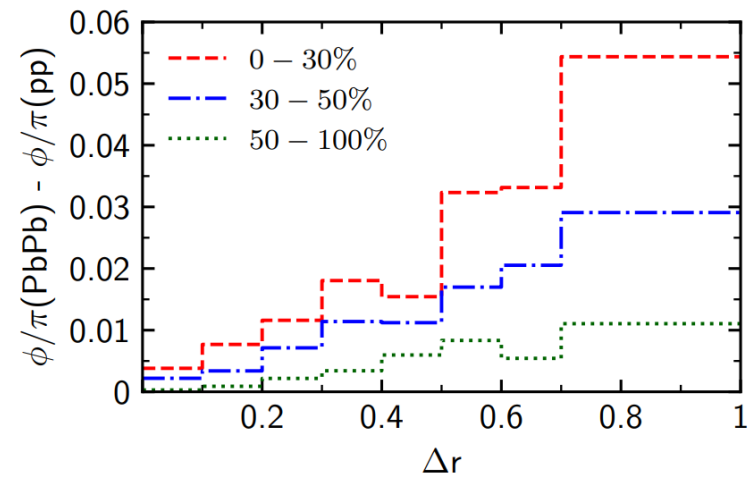
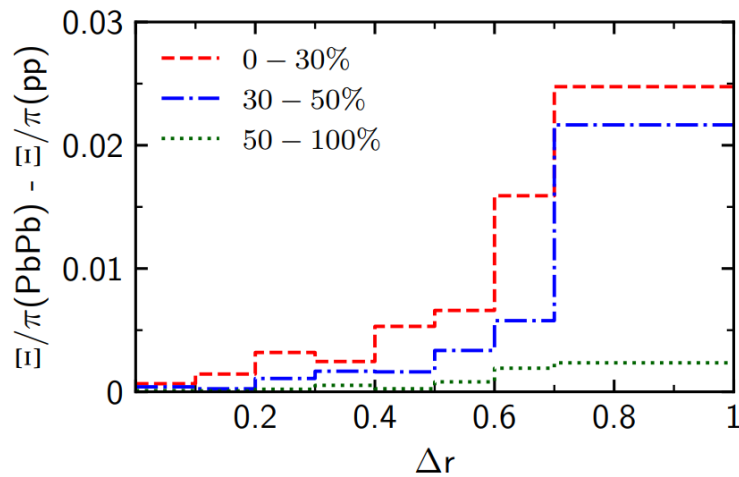
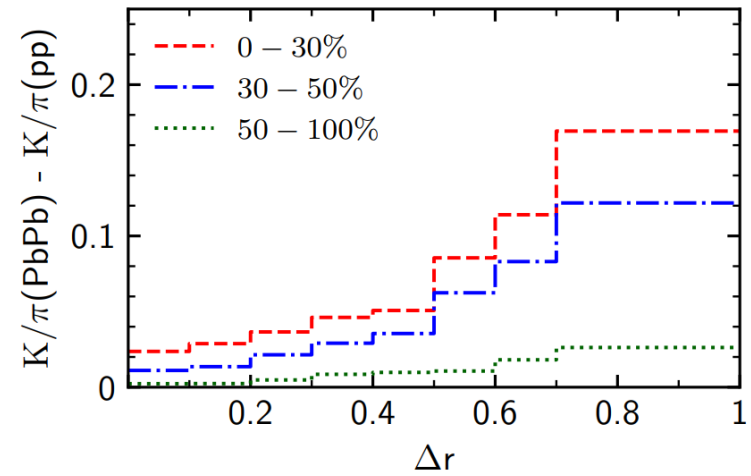
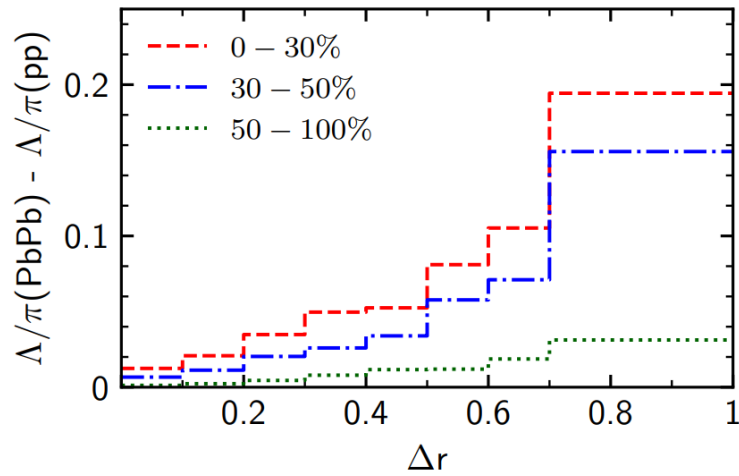
Experimental result on in-jet B/M



Can we measure hadron chemistry around (outside) the quenched jets?

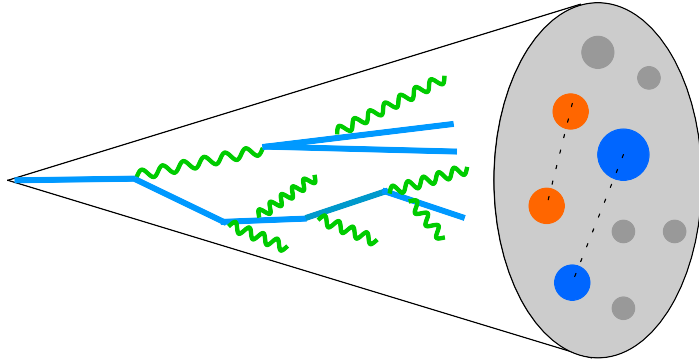
Gabriel Dale-Gau (for STAR) & Sierra Cantway (for ALICE), talks at Hard Probes 2024

Strangeness enhancement around jet: radial dependence



Luo, Cao, GYQ, in preparation

Jet energy-energy correlator (EEC)



$$\frac{d\sigma_{\text{EEC}}}{dR_L} = \int d\sigma(\Delta R_{ij}) \frac{p_{T,i} p_{T,j}}{p_{T,\text{jet}}^2} \delta(\Delta R_{ij} - R_L)$$

$$\Delta R_{ij} = \sqrt{\Delta\phi_{ij}^2 + \Delta\eta_{ij}^2}$$

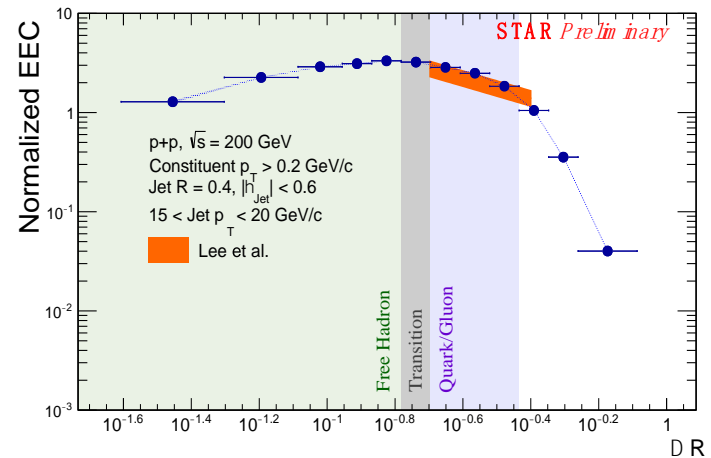
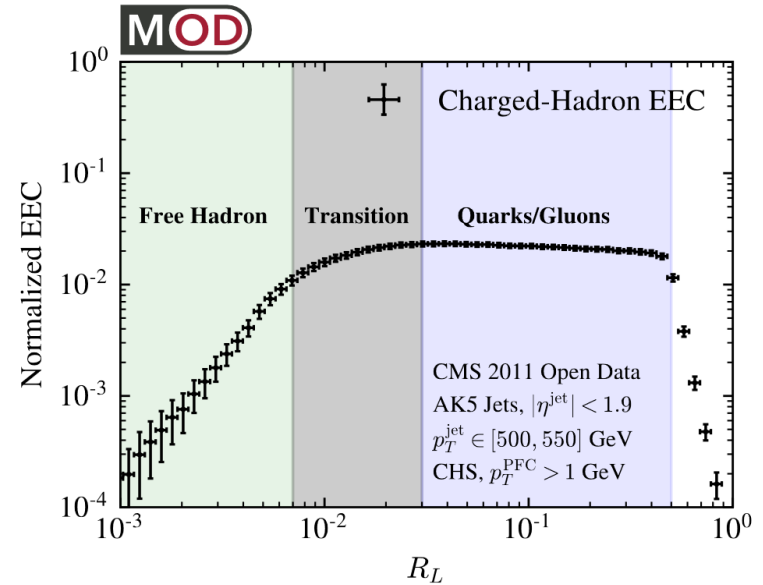
Jet energy correlators are sensitive to various intrinsic or emergent scales.

Jet EEC presents a clear transition between perturbative and non-perturbative regions.

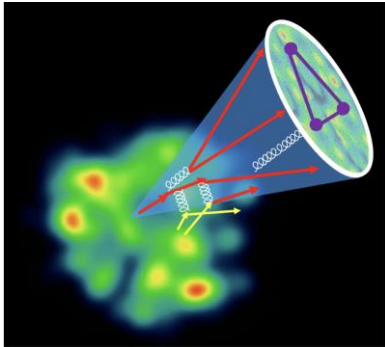
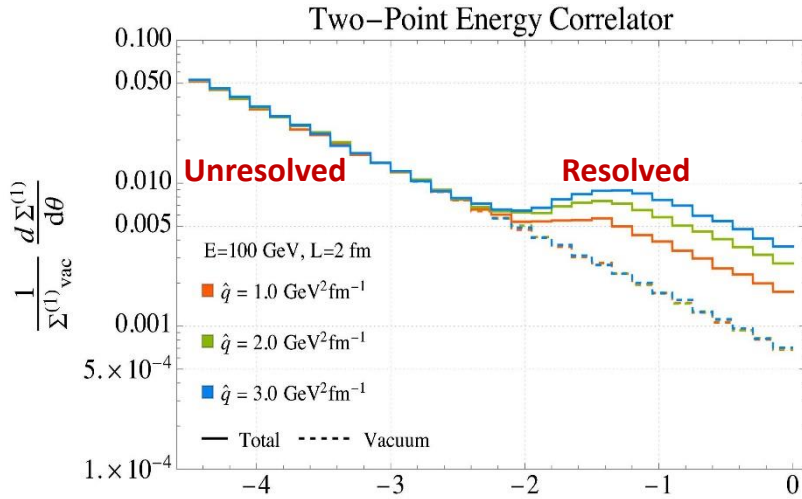
Komiske, IMoult, Thaler, Zhu, PRL 130, 051901 (2023)

Liu, Zhu, PRL 130, 091901 (2023)

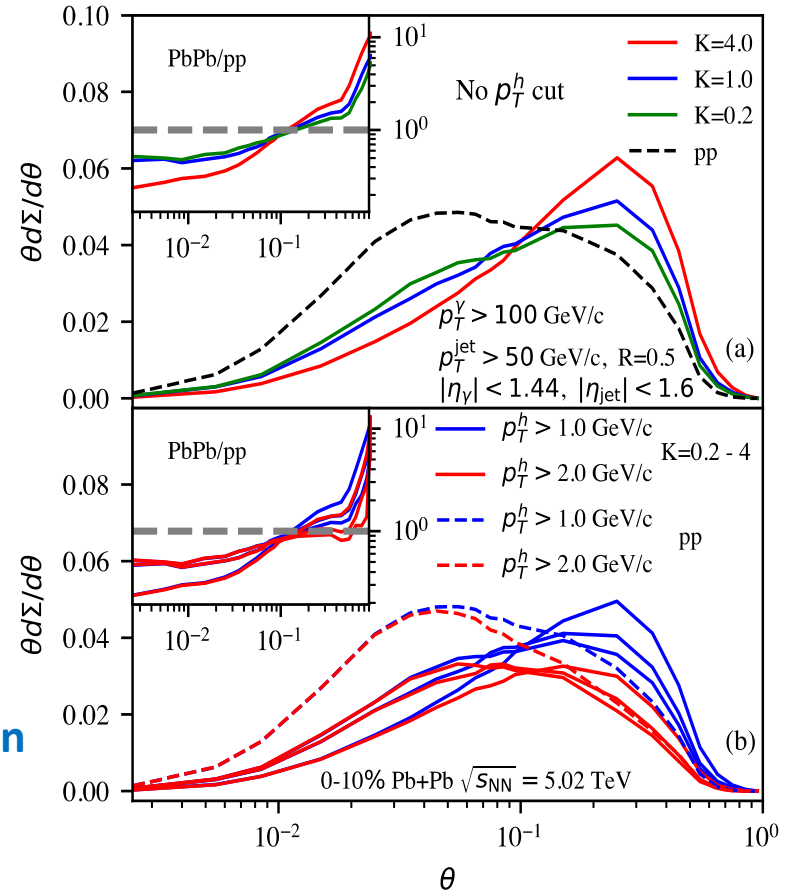
Liu, Liu, Pan, Yuan, Zhu, PRL 130, 181901 (2023)



Jet EEC in QGP

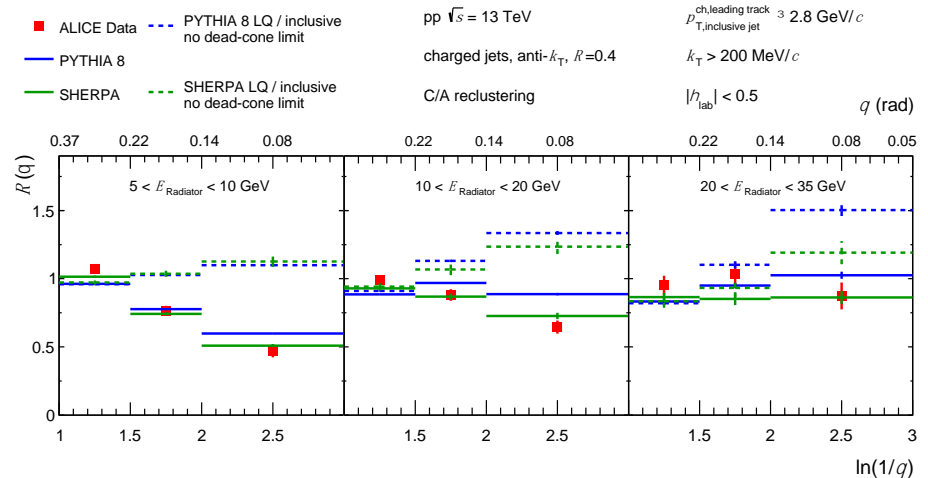
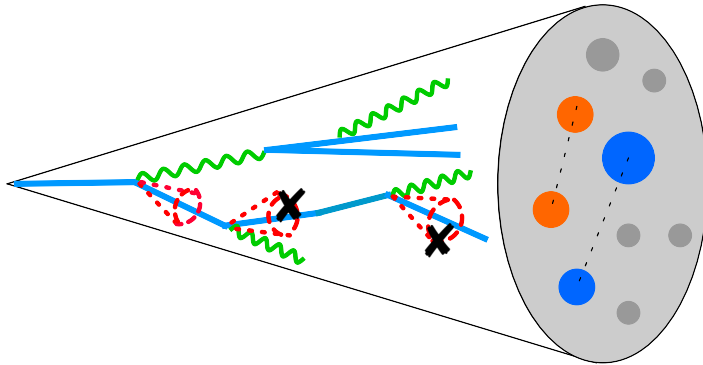


Medium-modified jet EEC provides unique opportunity to probe jet-medium interaction mechanisms and QGP properties.



Andres, Dominguez, Elayavalli, Holguin, Marquet, PRL 130 (2023) 26, 262301;
 Yang, He, Moul, Wang, PRL 132 (2024) 1, 1

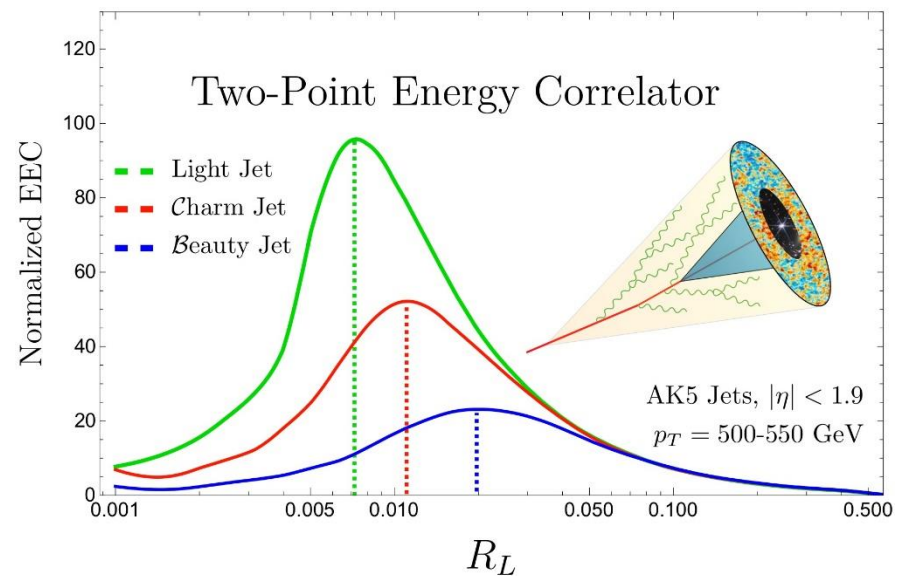
Heavy flavor jets in vacuum



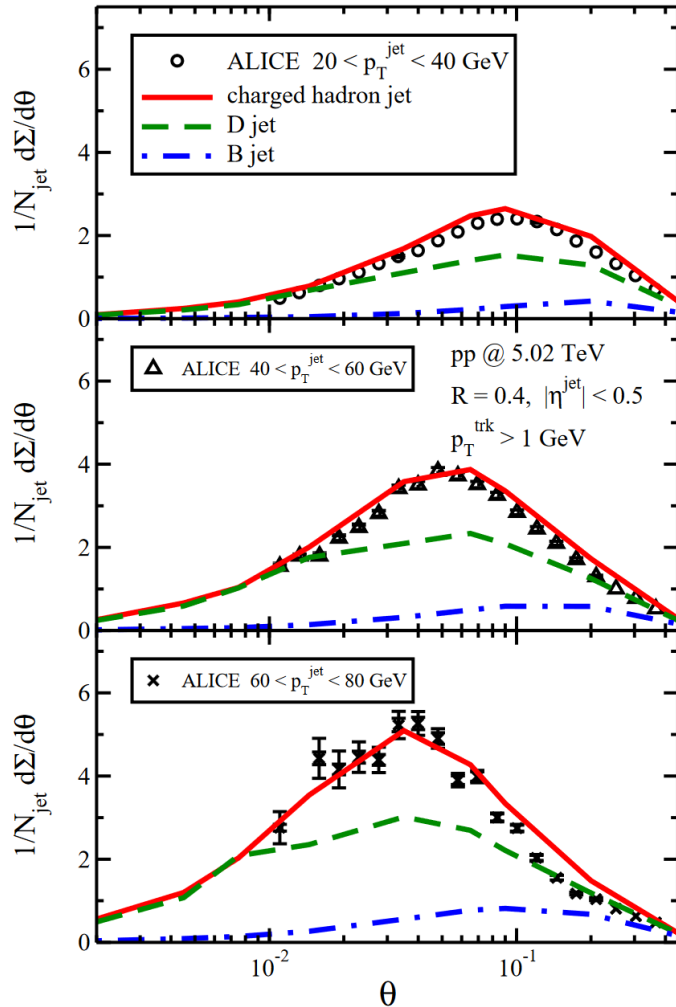
Heavy flavor jets provide a direct access to the mass effect on jet substructure.

Dead-cone effect in QCD: gluon emissions from massive quark are suppressed within a cone of $\theta_0 \sim m_Q/E$.

Heavy flavor jet EEC can probe the mass effect on parton splitting.



Flavor hierarchy of jet EEC in vacuum



$\langle \theta \rangle$	Charged jet	D jet	B jet
$20 < p_T^{\text{jet}} < 40$ GeV	0.207	0.214	0.263
$40 < p_T^{\text{jet}} < 60$ GeV	0.167	0.18	0.233
$60 < p_T^{\text{jet}} < 80$ GeV	0.144	0.162	0.214

Flavor (mass) dependence:

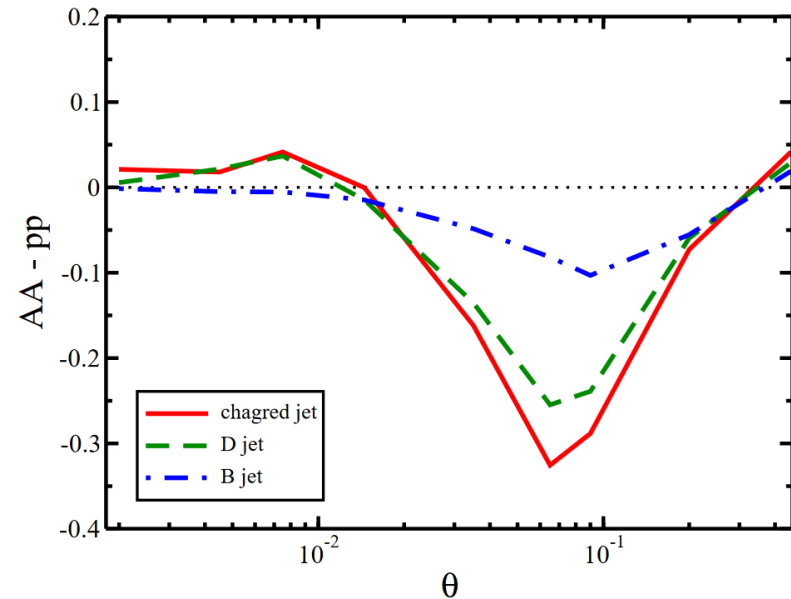
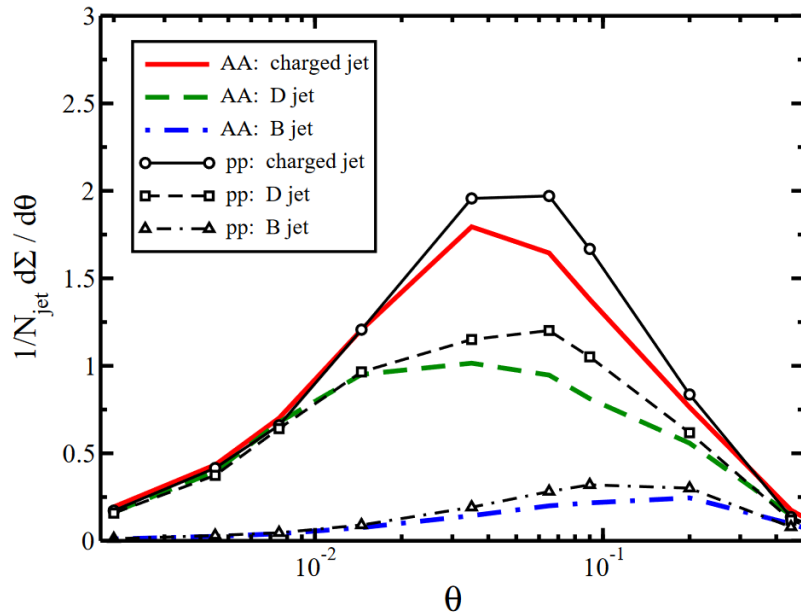
$\Sigma(\text{ch. jet}) > \Sigma(\text{D jet}) > \Sigma(\text{B jet})$

$\theta^{\text{peak}}(\text{ch. jet}) < \theta^{\text{peak}}(\text{D jet}) < \theta^{\text{peak}}(\text{B jet})$

Jet energy dependence:

Higher p_T jets peaks at smaller angles.

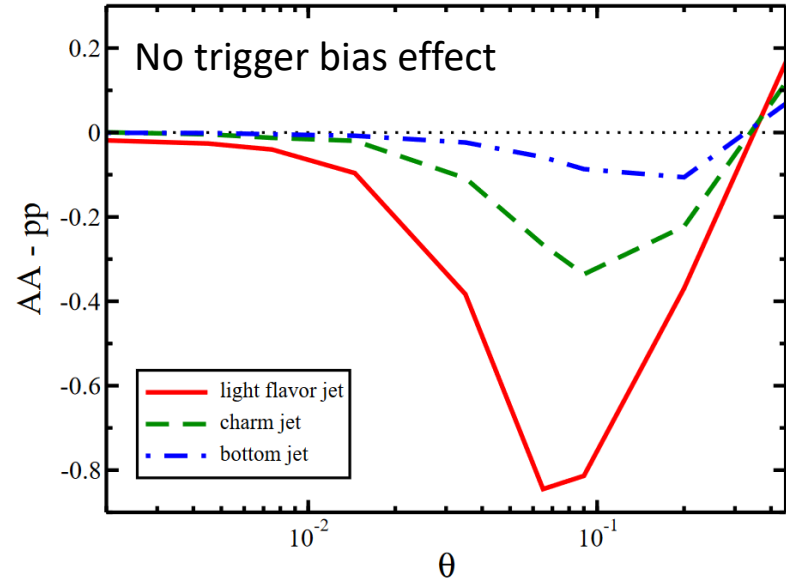
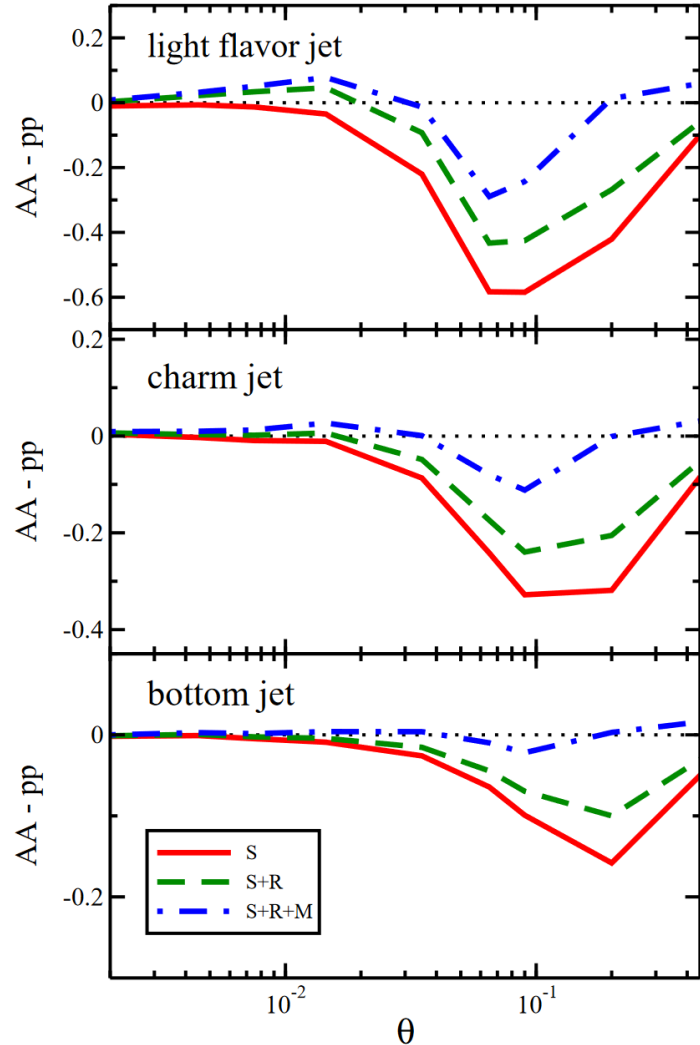
Flavor hierarchy of jet EEC in QGP



Flavor (mass) hierarchy in the nuclear modification of jet EEC:

- For charged jets, the EEC spectra gets a strong suppression at intermediate angle (due to energy loss), and gets enhanced at small and large angles.
- For heavy-meson-tagged jets, both suppression and enhancement become weaker.

Different medium effects on jet EEC



Jet energy loss is responsible for the suppression of jet EEC at intermediate angles.

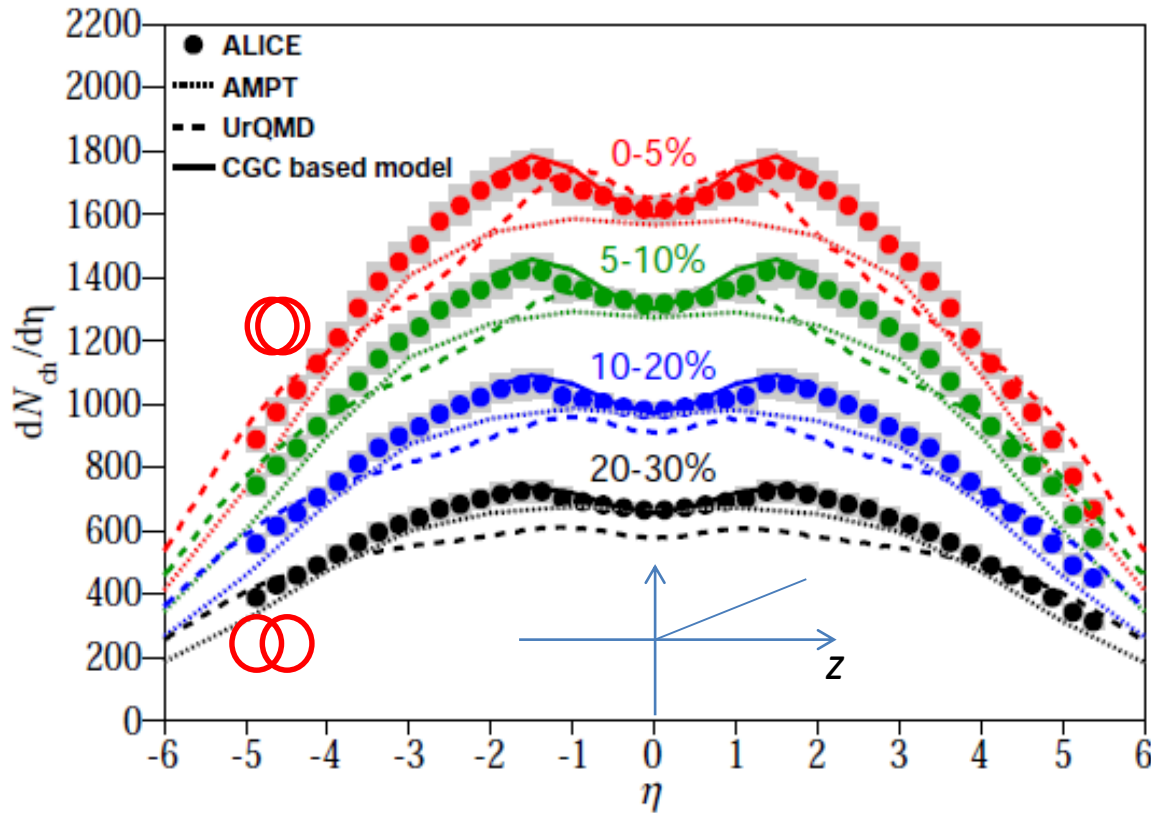
Medium response provides the most significant contribution to the enhancement of jet EEC at large angles.

Summary

- **Jets are versatile probes of quark-gluon plasma in heavy-ion collisions**
- **High p_T hadrons**
 - The NLO + LBT + Hydro framework can explain the flavor hierarchy of jet quenching
 - Gluons dominate high p_T J/ψ quenching
 - Extract flavor-dependent parton energy loss from Bayesian analysis
- **Full jets & medium response**
 - Interplay of various jet-medium interaction mechanisms and effects
 - Coupled Jet-fluid model shows medium response signal in jet shape at large r
 - Propose B/M & strangeness enhancement around quenched jets as a signature of medium response
 - Flavor dependent jet EEC can probe jet-medium interaction at different scales

Backup slides

Particle distribution in longitudinal direction



$$\eta = \frac{1}{2} \ln \left(\frac{p + p_z}{p - p_z} \right) = -\ln \left(\tanh \frac{\theta}{2} \right)$$

$$LHC : \frac{dN_{ch}}{d\eta} = 1600$$

$$RHIC : \frac{dN_{ch}}{d\eta} = 700$$

$$LHC : \varepsilon_0 = 16 \text{ GeV} / \text{fm}^3$$

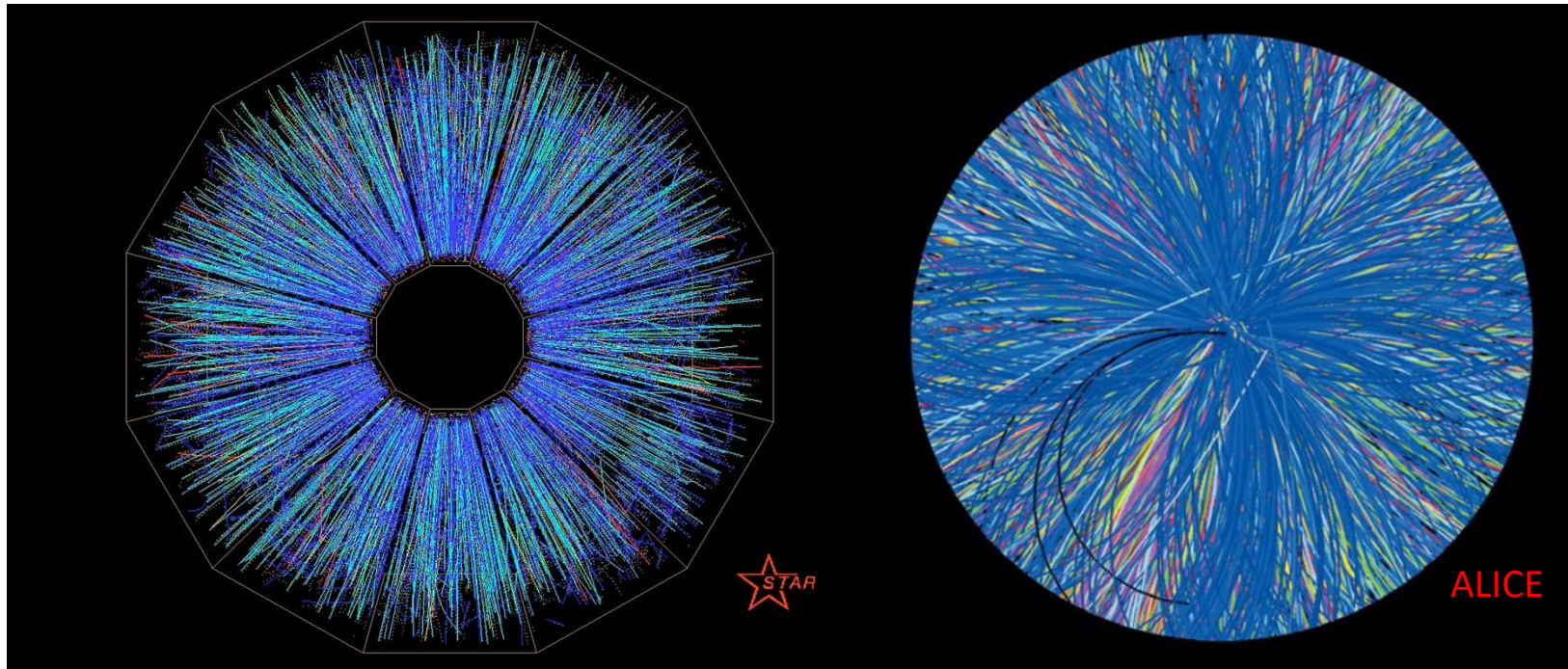
$$RHIC : \varepsilon_0 = 7 \text{ GeV} / \text{fm}^3$$

$$\varepsilon_0 = \frac{dE_T}{d\eta} \frac{1}{\tau_0 \pi R^2} = \frac{3}{2} \left\langle \frac{E_T}{N} \right\rangle \frac{dN_{ch}}{d\eta} \frac{1}{\tau_0 \pi R^2}$$

$$T_c = 155 \text{ MeV}$$

$$\varepsilon_c = 0.5 \text{ GeV} / \text{fm}^3$$

Particle distribution in transverse plane

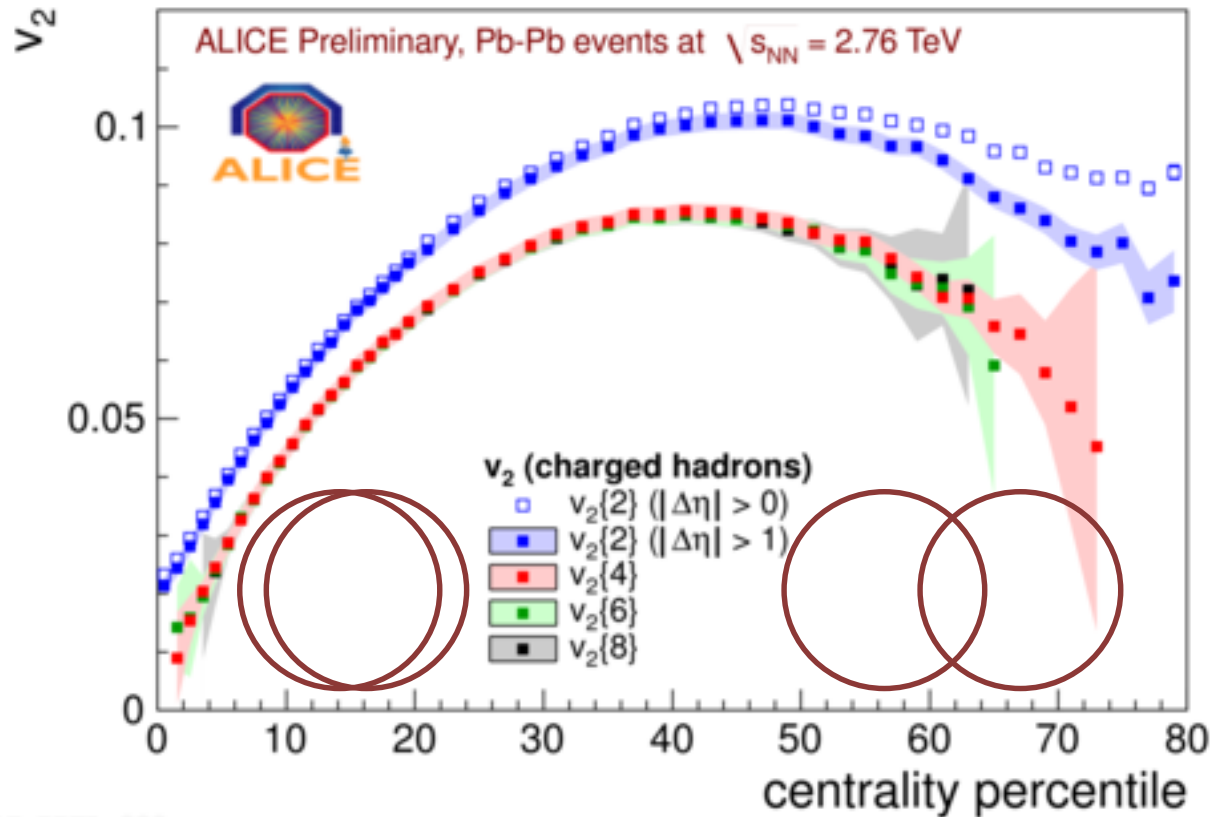


Particle production is not azimuthally symmetric.

The azimuthal anisotropy can be analyzed by Fourier decomposition:

$$\frac{dN}{d\varphi} \propto 1 + \sum_n 2v_n \cos[n(\varphi - \Psi_n)]$$

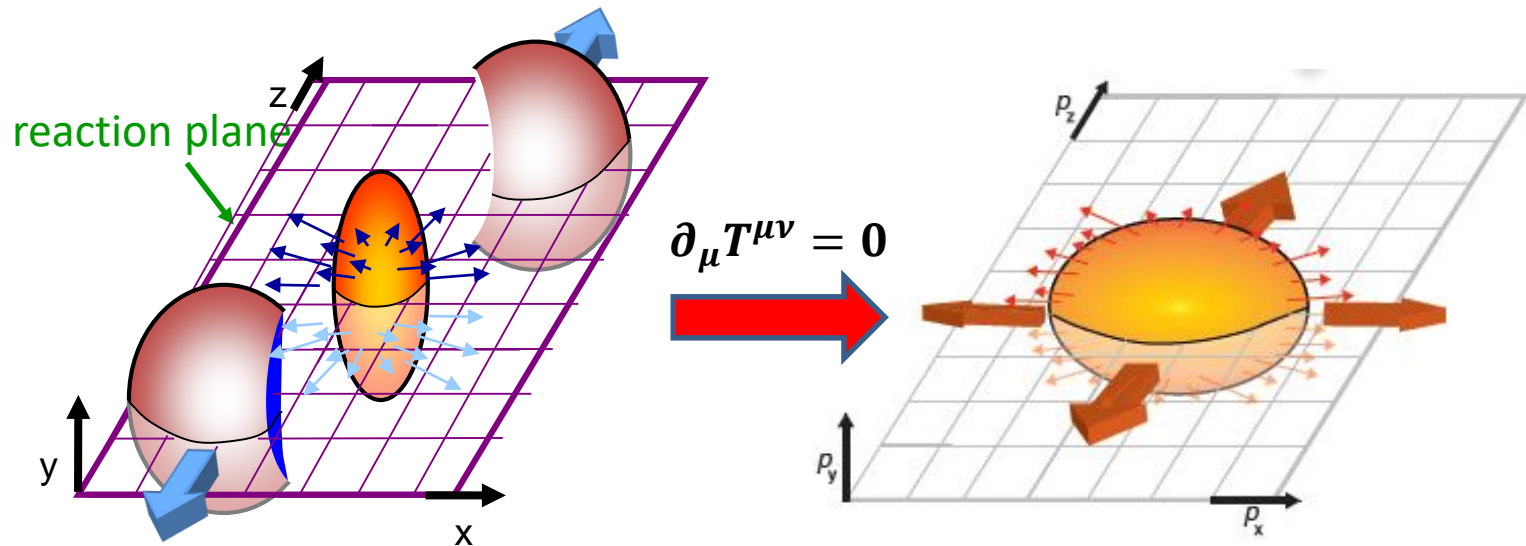
Elliptic flow depends on collision geometry



ALICE-900-980

Strong elliptic flow depends on collision centrality (system size & geometry)

The origin of elliptic flow

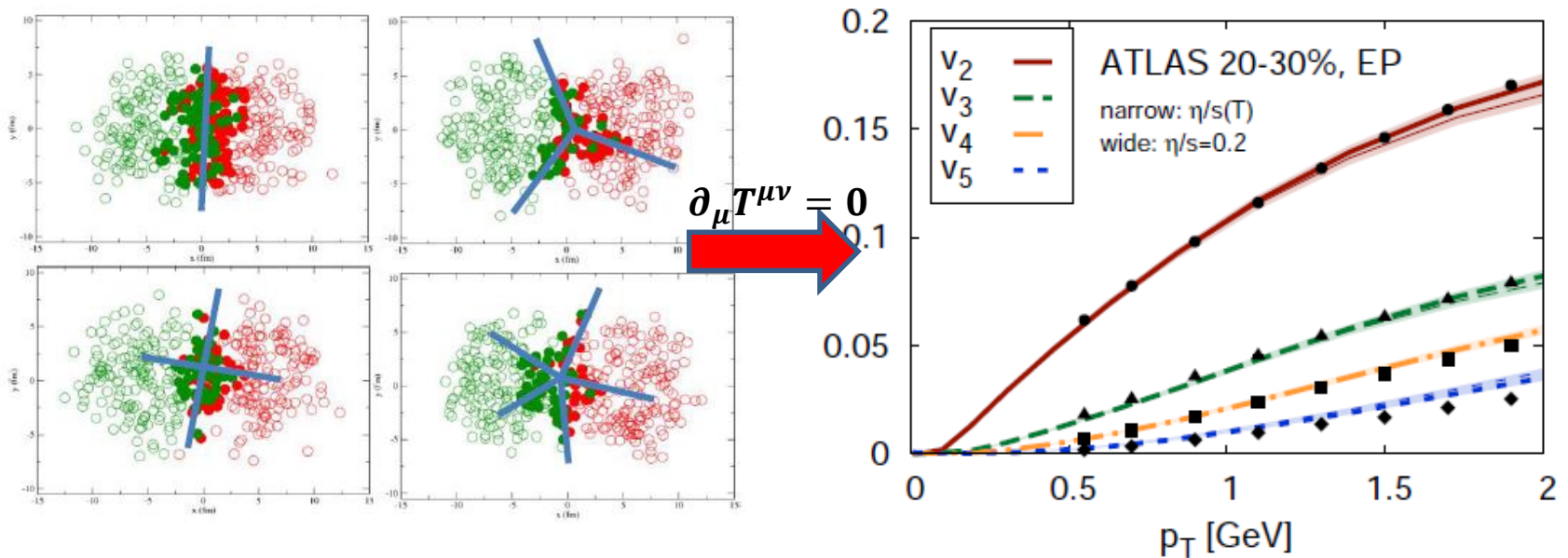


$$\text{eccentricity } \varepsilon_2 = \frac{\langle y^2 - x^2 \rangle}{\langle y^2 + x^2 \rangle}$$

$$\text{elliptic flow } V_2 = \left\langle \frac{p_x^2 - p_y^2}{p_x^2 + p_y^2} \right\rangle$$

Relativistic hydrodynamics: the interaction among QGP constituents translates initial geometric anisotropy into final state momentum anisotropy.
 => QGP is a strongly-coupled fluid

Initial-state fluctuations and final-state flows

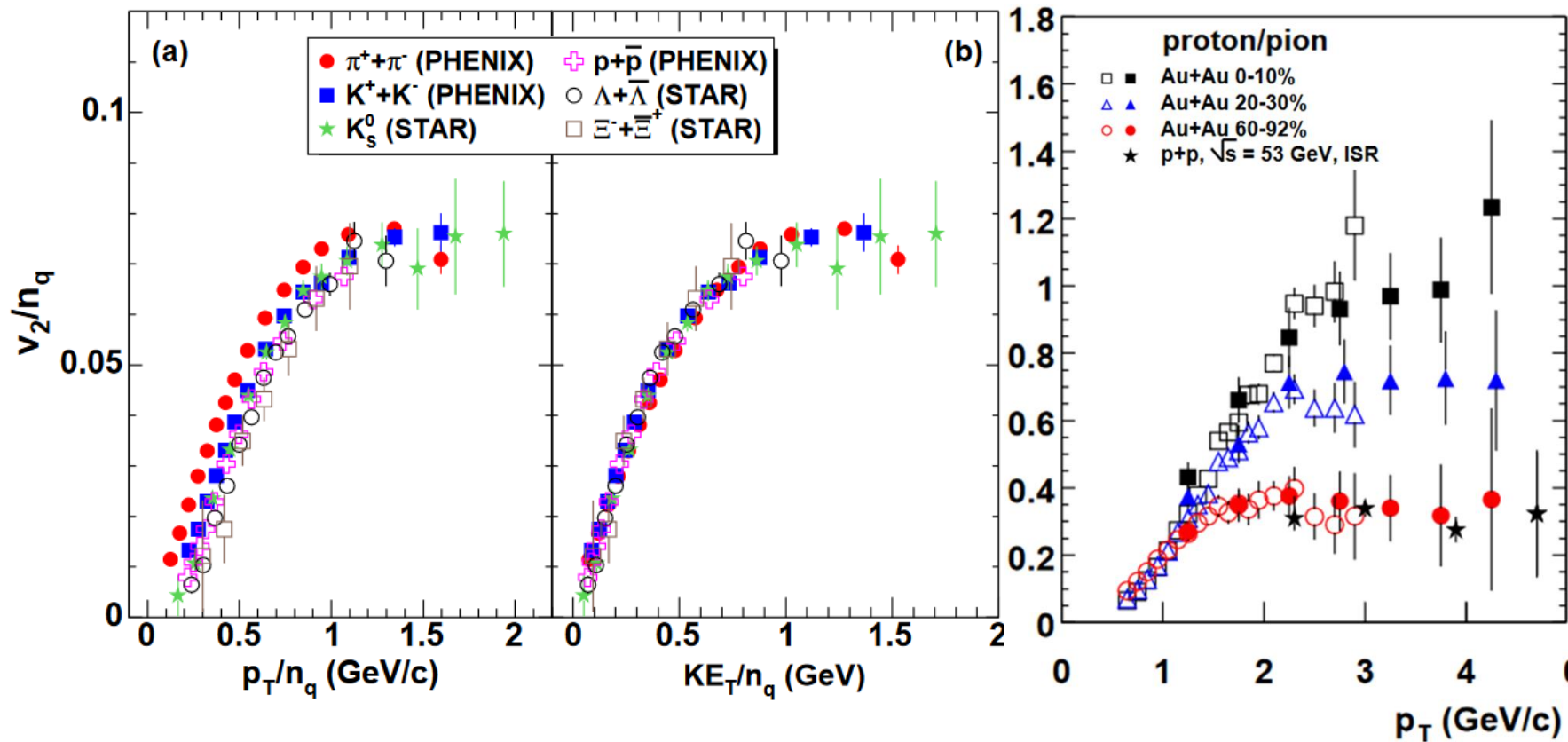


Event-by-event initial state density and geometry fluctuations are translated into final state anisotropic flows via hydrodynamic evolution.

$$\frac{dN}{p_T dp_T dy d\phi} = \frac{dN}{2\pi p_T dp_T dy} \left(1 + \sum_n 2v_n(p_T, y) \cos\{n[\phi - \Psi_n(p_T, y)]\} \right)$$

Alver and Roland, PRC 2010; GYQ, Petersen, Bass, Muller, PRC 2010; Staig, Shuryak, PRC 2011; Teaney, Yan, PRC 2011; Gale, Jeon, Schenke, Tribedy, Venugopalan, PRL 2012; etc.

Number of constituent quark (NCQ) scaling



Coalescence of thermal partons from QGP can naturally explain the NCQ scaling of v_2 and the enhancement of baryon/meson ratio at intermediate p_T .

Relativistic hydrodynamics

- **Energy-momentum conservation:**

$$\partial_\mu T^{\mu\nu} = 0$$

$$T^{\mu\nu} = \varepsilon U^\mu U^\nu - (P + \Pi)\Delta^{\mu\nu} + \pi^{\mu\nu}$$

- **Equations of motion (Israel-Stewart viscous hydrodynamics):**

$$\dot{\varepsilon} = -(\varepsilon + P + \Pi)\theta + \pi^{\mu\nu}\sigma_{\mu\nu}$$

$$(\varepsilon + P + \Pi)\dot{U}^\alpha = \nabla^\alpha(P + \Pi) + \dot{U}_\mu\pi^{\mu\nu} - \Delta_\nu^\alpha\nabla_\mu\pi^{\mu\nu}$$

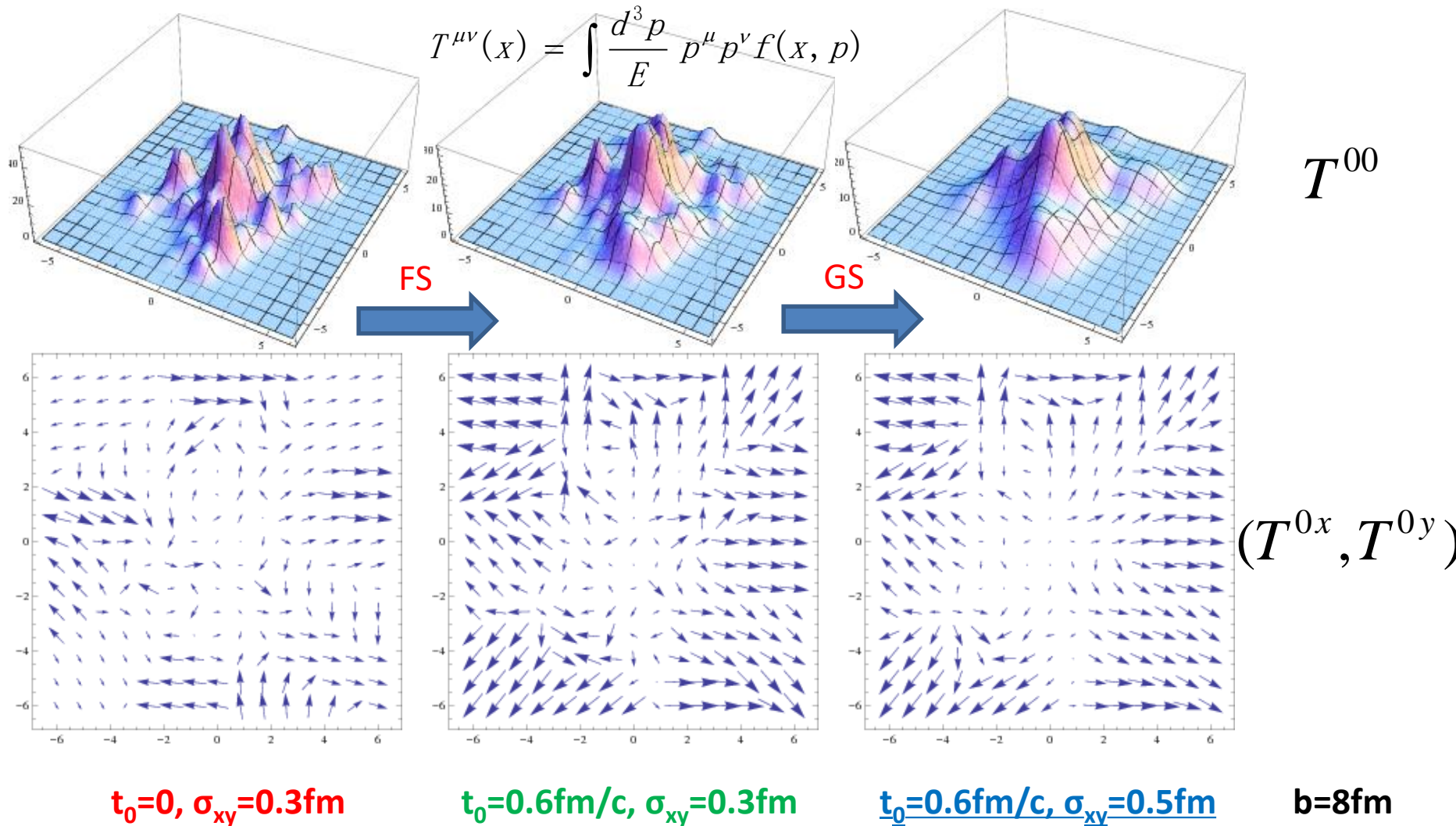
$$\dot{\Pi} = -\frac{1}{\tau_\Pi}\left[\Pi + \zeta\theta + \Pi\zeta T\partial_\alpha\left(\frac{\tau_\Pi}{2\zeta T}U^\alpha\right)\right]$$

$$\Delta_{\alpha\beta}^{\mu\nu}\dot{\pi}^{\alpha\beta} = -\frac{1}{\tau_\pi}\left[\pi^{\mu\nu} - 2\eta\sigma^{\mu\nu} + \pi^{\mu\nu}\eta T\partial_\alpha\left(\frac{\tau_\pi}{2\eta T}U^\alpha\right)\right]$$

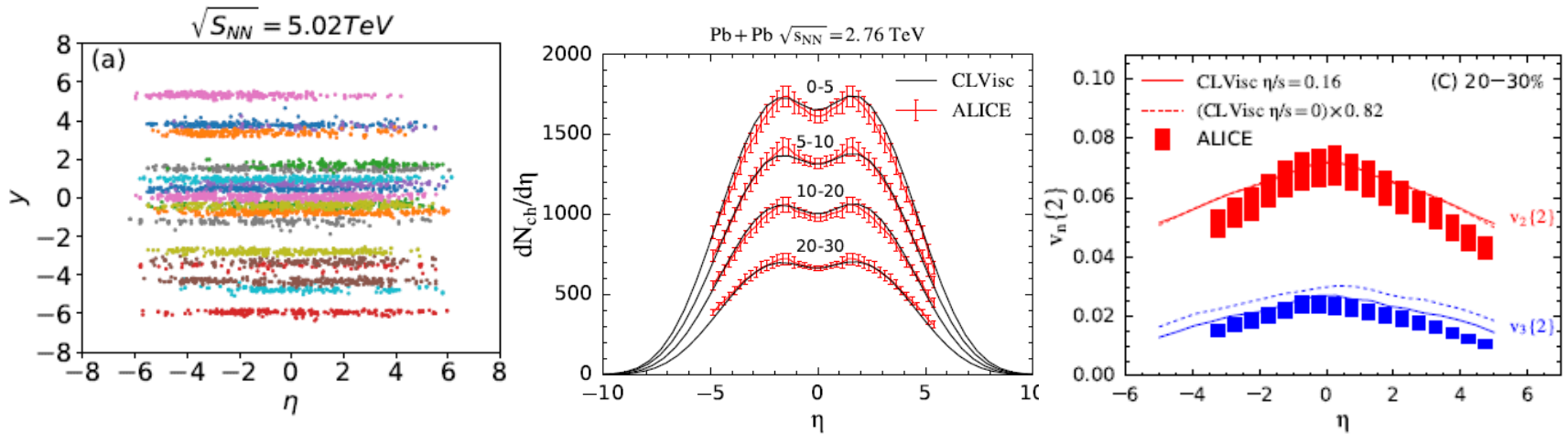
- **Equation of state:** $P = P(\varepsilon)$

arXiv:0902.3663; arXiv:1301.2826; arXiv:1301.5893; arXiv:1311.1849; arXiv:1401.0079...

Initial conditions before hydro



Longitudinal fluctuations



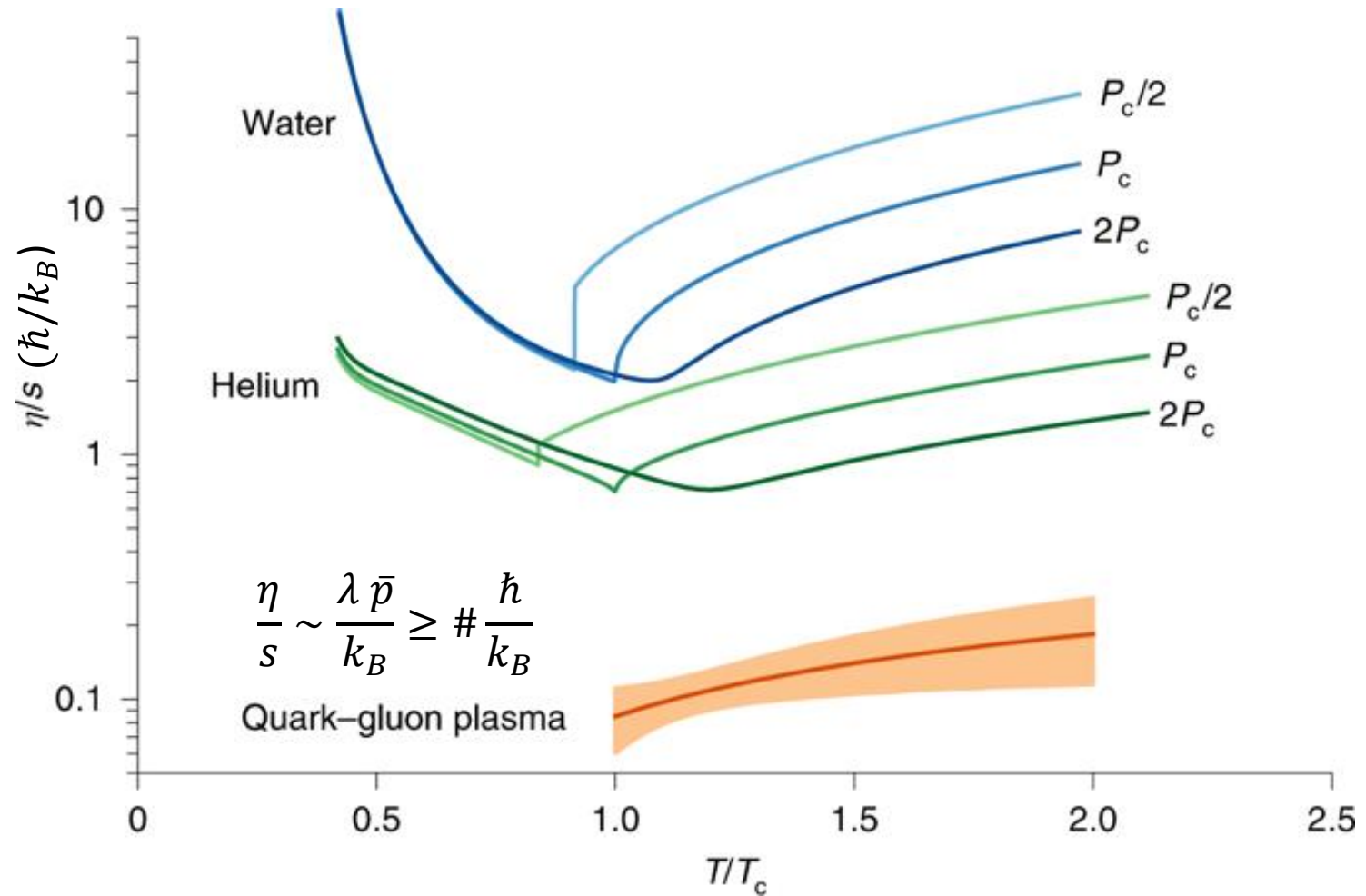
The initial states are fluctuating also in longitudinal (rapidity) directions

Longitudinal fluctuations can lead to rapidity-dependent particle yield and v_n

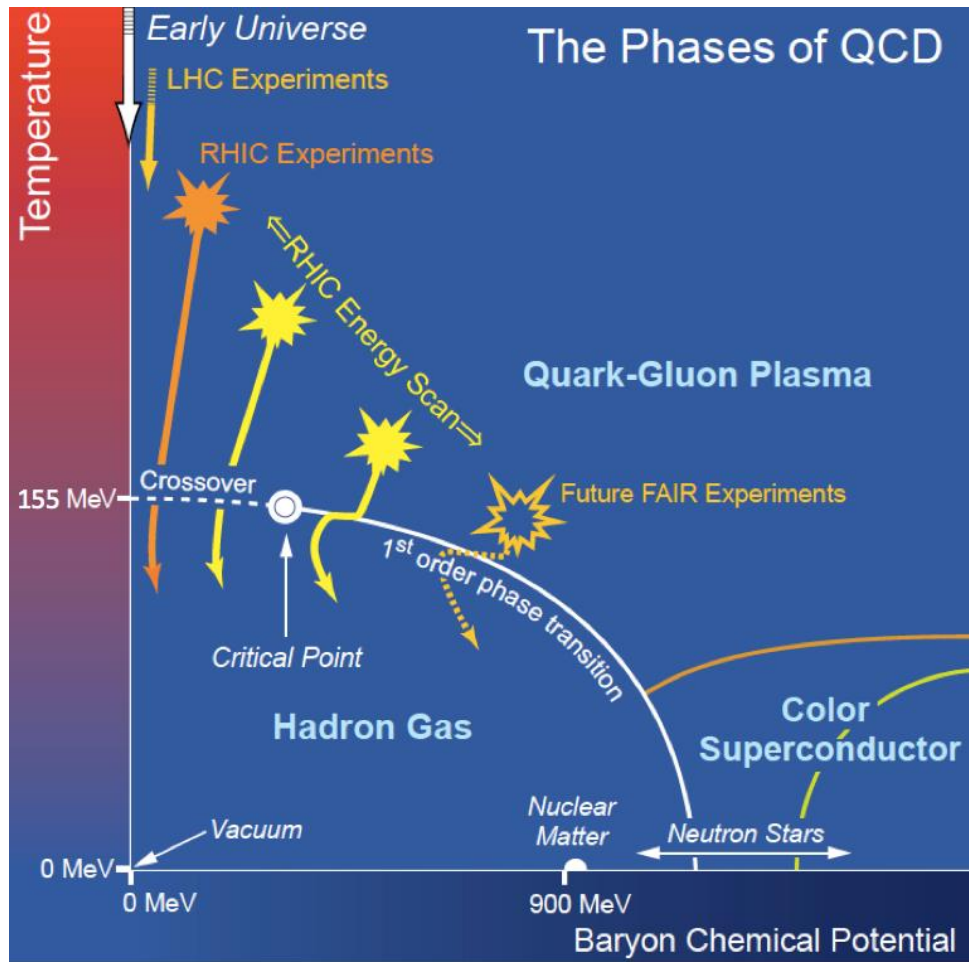
The rapidity dependence (decorrelation) of v_n provide another tool to probe the QGP properties

Gabriel et al. PRL 2016; Pang, Petersen, Wang PRC 2018; Wu, Pang, GYQ, Wang, PRC 2018

Most perfect liquid



Phases of strong-interaction matter



Low T & $\mu_B \Rightarrow$ hadrons
(hadron matter)

$T_c = 155 \text{ MeV} \Rightarrow$ hadron
matter melts into quark-
gluon plasma (QGP)

Very high $T \Rightarrow$ early Universe.

QGP can be produced by
colliding two nuclei at
extremely high energies

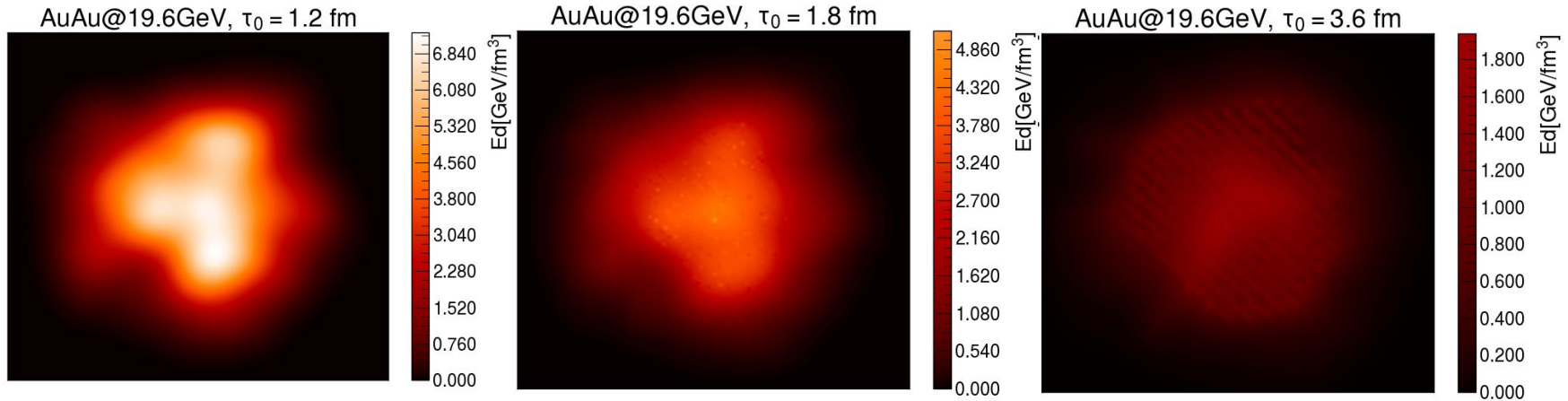
As E_{cm} increases, S increases,
 N_B is unchanged, S/N_B , s/n_B
and T/μ_B increase

CLvisc (3+1)-D hydrodynamics for BES energies

$$\nabla_{\mu} T^{\mu\nu} = \nabla_{\mu} (eU^{\mu}U^{\nu} - P\Delta^{\mu\nu} + \pi^{\mu\nu}) = 0; \quad \nabla_{\mu} J^{\mu} = \nabla_{\mu} (nU^{\mu} + V^{\mu}) = 0$$

$$\Delta_{\alpha\beta}^{\mu\nu} D\pi^{\alpha\beta} = -\frac{1}{\tau_{\pi}}(\pi^{\mu\nu} - \eta_{\nu}\sigma^{\mu\nu}) - \frac{4}{3}\pi^{\mu\nu}\theta - \frac{5}{7}\pi^{\alpha<\mu}\sigma_{\alpha}^{\nu>} + \frac{9}{70e+P}\pi^{\alpha<\mu}\pi_{\alpha}^{\nu>};$$

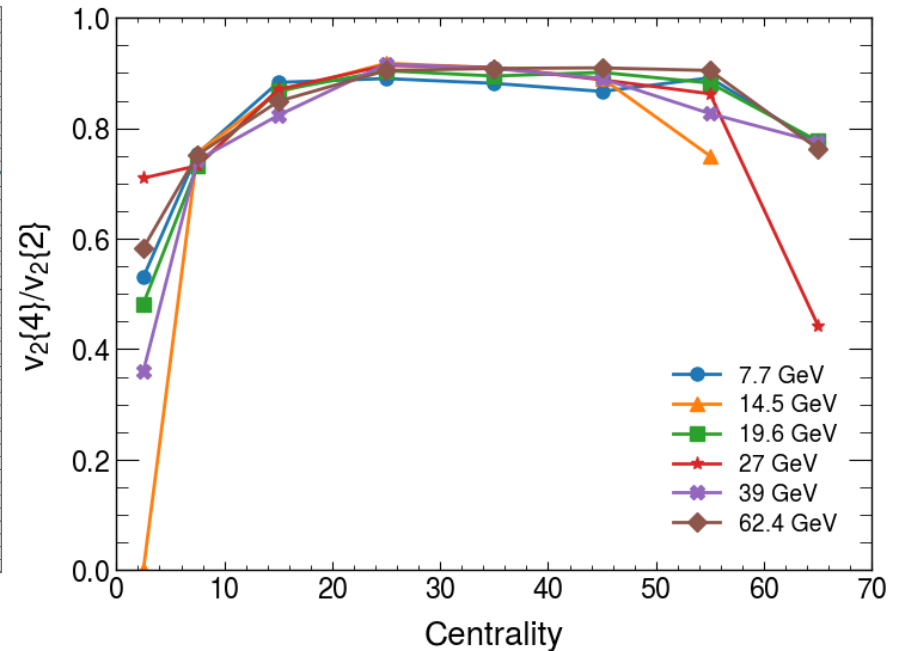
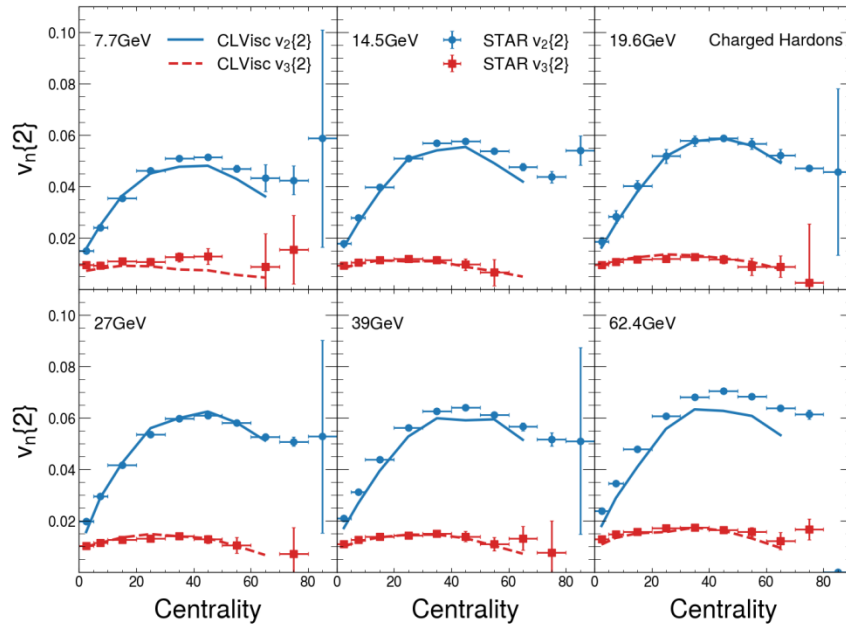
$$\Delta^{\mu\nu} DV_{\nu} = -\frac{1}{\tau_V}(V^{\mu} - \kappa_B \nabla^{\mu} \frac{\mu}{T}) - V^{\mu}\theta - \frac{3}{10}V_{\nu}\sigma^{\mu\nu}$$



(3+1)-dimensional relativistic viscous hydrodynamics model CLVisc2.0 includes baryon conservation and Israel-Stewart-like diffusion, NEOS-BQS equation of state, EbE initial conditions, SMASH hadron cascade.

Wu, GYQ, Pang, Wang, 2107.04949

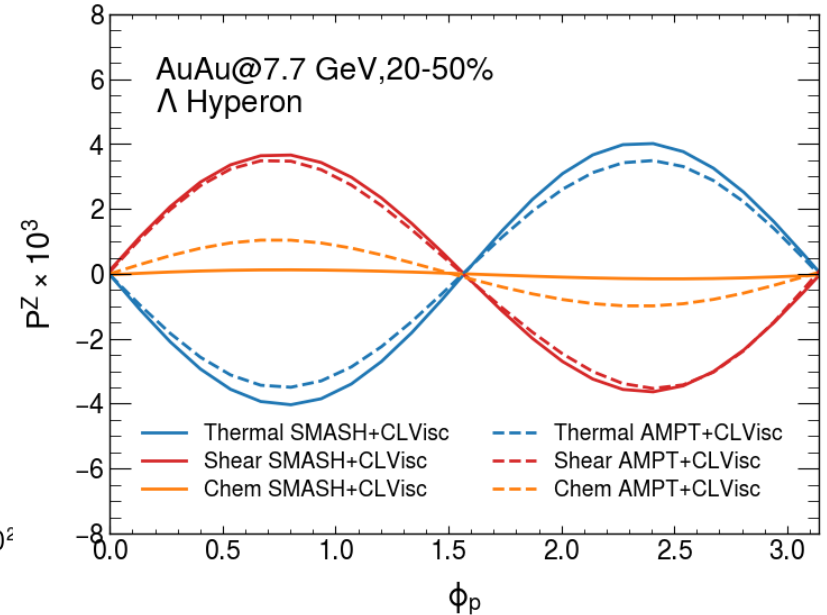
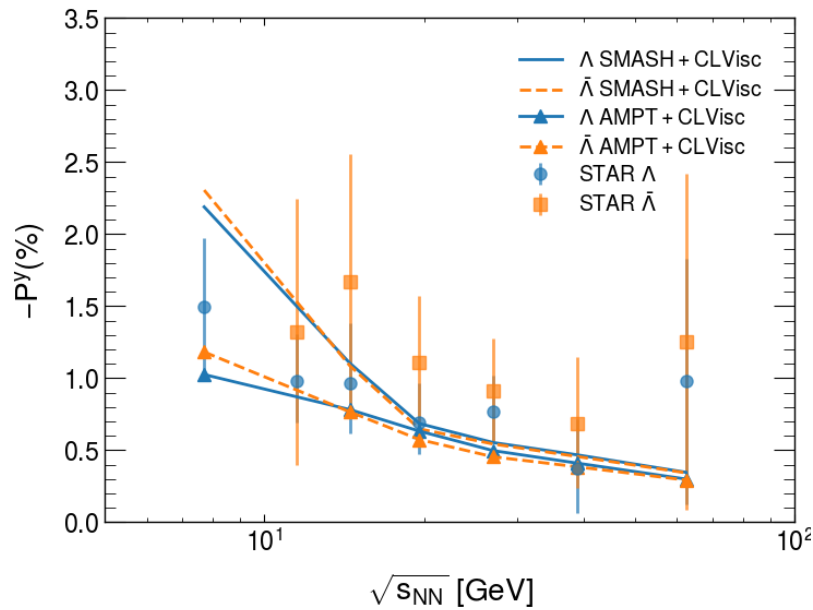
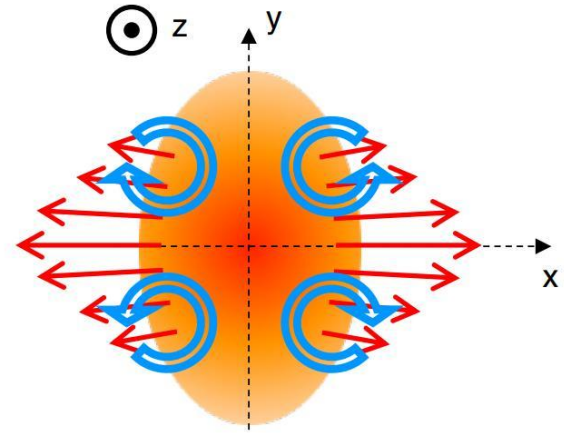
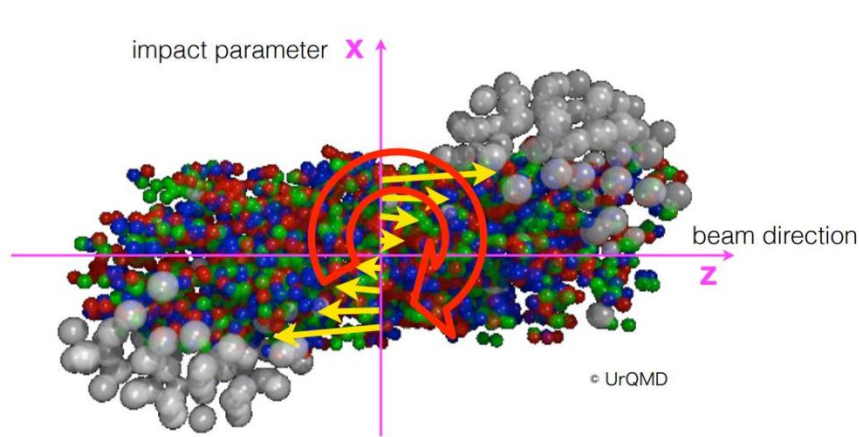
CLvisc (3+1)-D hydrodynamics for BES energies



CLVisc2.0 can provide a good description of identified particle spectra, mean transverse momenta and anisotropic flows for different centralities and over a wide range of collision energies (7.7-62.4 GeV).

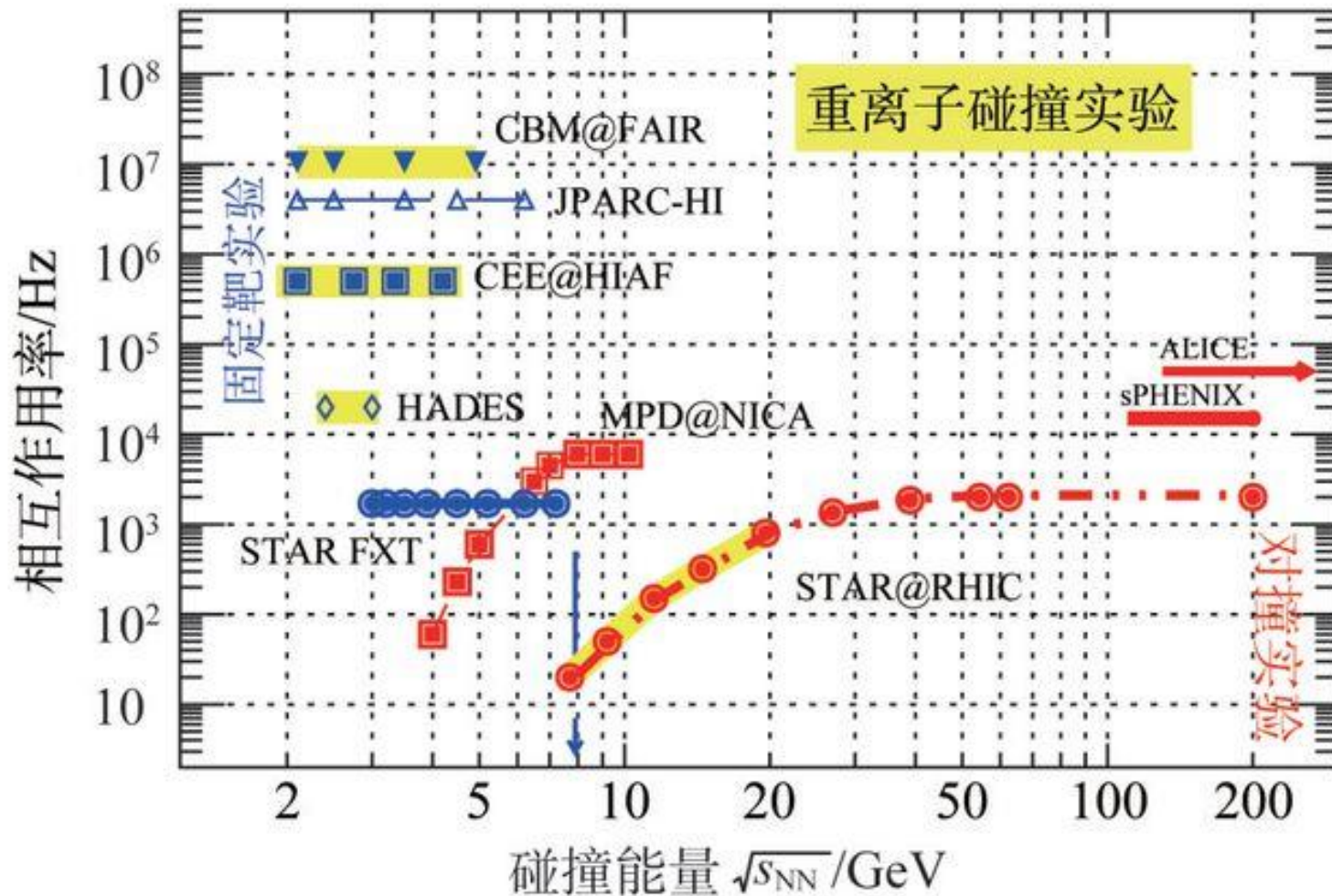
The relative fluctuations of v_2 are not sensitive to collision energies, which indicates that the flow fluctuations are mainly driven by initial states

Global and local Λ polarization at BES energies

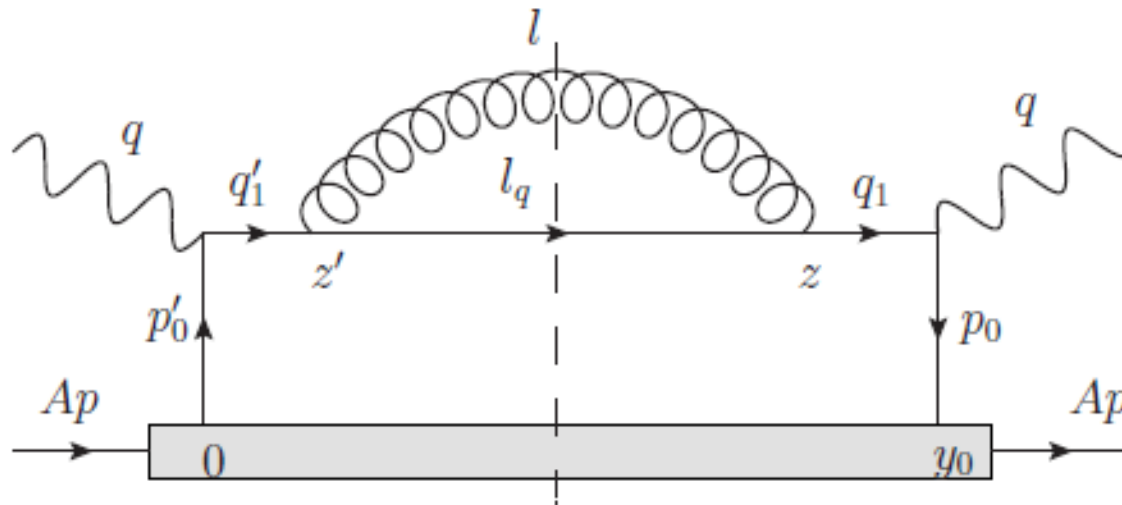


Wu, GYQ et al, in preparation

相对论重离子碰撞实验



Gluon emission in vacuum



$$\frac{dN_g^{\text{vac}}}{dy d^2l_{\perp}} = C_F \frac{\alpha_s}{2\pi^2} P(y) \frac{l_{\perp}^2 + \frac{y^4}{1+(1-y)^2} M^2}{(l_{\perp}^2 + y^2 M^2)^2}.$$

Only transverse scatterings

- Modeling the traversed nuclear medium by heavy static scattering centers (only transverse scatterings)

$$\begin{aligned}
 \frac{dN_g^{\text{med}}}{dyd^2l_{\perp}} &= \frac{\alpha_s}{2\pi^2} P(y) \int dZ_1^- \int d^2\mathbf{k}_{1\perp} \frac{dP_{\text{el}}}{d^2\mathbf{k}_{1\perp} dZ_1^-} \\
 &\times \left\{ C_A \left[2 - 2 \cos \left(\frac{(\mathbf{l}_{\perp} - \mathbf{k}_{1\perp})^2 + y^2 M^2}{l_{\perp}^2 + y^2 M^2} \frac{Z_1^-}{\tilde{\tau}_{\text{form}}^-} \right) \right] \times \left[\frac{(\mathbf{l}_{\perp} - \mathbf{k}_{1\perp})^2 + \frac{y^4}{1+(1-y)^2} M^2}{\left[(\mathbf{l}_{\perp} - \mathbf{k}_{1\perp})^2 + y^2 M^2 \right]^2} \right. \right. \\
 &\left. \left. - \frac{1}{2} \frac{\mathbf{l}_{\perp} \cdot (\mathbf{l}_{\perp} - \mathbf{k}_{1\perp}) + \frac{y^4}{1+(1-y)^2} M^2}{[l_{\perp}^2 + y^2 M^2] \left[(\mathbf{l}_{\perp} - \mathbf{k}_{1\perp})^2 + y^2 M^2 \right]} - \frac{1}{2} \frac{(\mathbf{l}_{\perp} - \mathbf{k}_{1\perp}) \cdot (\mathbf{l}_{\perp} - y\mathbf{k}_{1\perp}) + \frac{y^4}{1+(1-y)^2} M^2}{\left[(\mathbf{l}_{\perp} - y\mathbf{k}_{1\perp})^2 + y^2 M^2 \right] \left[(\mathbf{l}_{\perp} - \mathbf{k}_{1\perp})^2 + y^2 M^2 \right]} \right] \right. \\
 &\left. + \left(\frac{C_A}{2} - C_F \right) \left[2 - 2 \cos \left(\frac{Z_1^-}{\tilde{\tau}_{\text{form}}^-} \right) \right] \left[\frac{\mathbf{l}_{\perp} \cdot (\mathbf{l}_{\perp} - y\mathbf{k}_{1\perp}) + \frac{y^4}{1+(1-y)^2} M^2}{[l_{\perp}^2 + y^2 M^2] \left[(\mathbf{l}_{\perp} - y\mathbf{k}_{1\perp})^2 + y^2 M^2 \right]} - \frac{l_{\perp}^2 + \frac{y^4}{1+(1-y)^2} M^2}{[l_{\perp}^2 + y^2 M^2]^2} \right] \right. \\
 &\left. + C_F \left[\frac{(\mathbf{l}_{\perp} - y\mathbf{k}_{1\perp})^2 + \frac{y^4}{1+(1-y)^2} M^2}{\left[(\mathbf{l}_{\perp} - y\mathbf{k}_{1\perp})^2 + y^2 M^2 \right]^2} - \frac{l_{\perp}^2 + \frac{y^4}{1+(1-y)^2} M^2}{[l_{\perp}^2 + y^2 M^2]^2} \right] \right\}.
 \end{aligned}$$

Soft gluon emission approximation

- Further taking soft gluon emission approximation: $y^2 M \ll yM \sim l_\perp \sim k_{1\perp}$

$$\frac{dN_g^{\text{med}}}{dy d^2 l_\perp} = \frac{\alpha_s}{2\pi^2} P(y) \int dZ_1^- \int d^2 k_{1\perp} \frac{dP_{\text{el}}}{d^2 k_{1\perp} dZ_1^-} \times C_A \left[2 - 2 \cos \left(\frac{(l_\perp - k_{1\perp})^2 + y^2 M^2}{l_\perp^2 + y^2 M^2} \frac{Z_1^-}{\tilde{\tau}_{\text{form}}^-} \right) \right] \\ \times \left[\frac{(l_\perp - k_{1\perp})^2}{\left[(l_\perp - k_{1\perp})^2 + y^2 M^2 \right]^2} - \frac{l_\perp \cdot (l_\perp - k_{1\perp})}{[l_\perp^2 + y^2 M^2] \left[(l_\perp - k_{1\perp})^2 + y^2 M^2 \right]} \right].$$

- This agrees with the DGLV first-order-in-opacity formula.
- Jet transport parameter is related to the differential elastic scattering rate as follows:

$$\hat{q}_{lc} = \frac{d\langle k_{1\perp}^2 \rangle}{dL^-} = \int \frac{dk_1^- d^2 k_{1\perp}}{(2\pi)^3} k_{1\perp}^2 \mathcal{D}(k_1^-, k_{1\perp}) = \int \frac{d^2 k_{1\perp}}{(2\pi)^2} k_{1\perp}^2 \mathcal{D}_\perp(k_{1\perp}) = \int d^2 k_{1\perp} k_{1\perp}^2 \rho^- \frac{d\sigma_{\text{el}}}{d^2 k_{1\perp}}.$$

Implementation of inelastic radiation in LBT

- **Average number of radiated gluons in Δt :**

$$\langle N_g \rangle(E, T, t, \Delta t) = \Gamma_g \Delta t = \Delta t \int dx dk_{\perp}^2 \frac{dN_g}{dx dk_{\perp}^2 dt}$$

- **Poisson distribution for the number n of radiated gluons during Δt :**

$$P(n) = \frac{\langle N_g \rangle^n}{n!} e^{-\langle N_g \rangle}$$

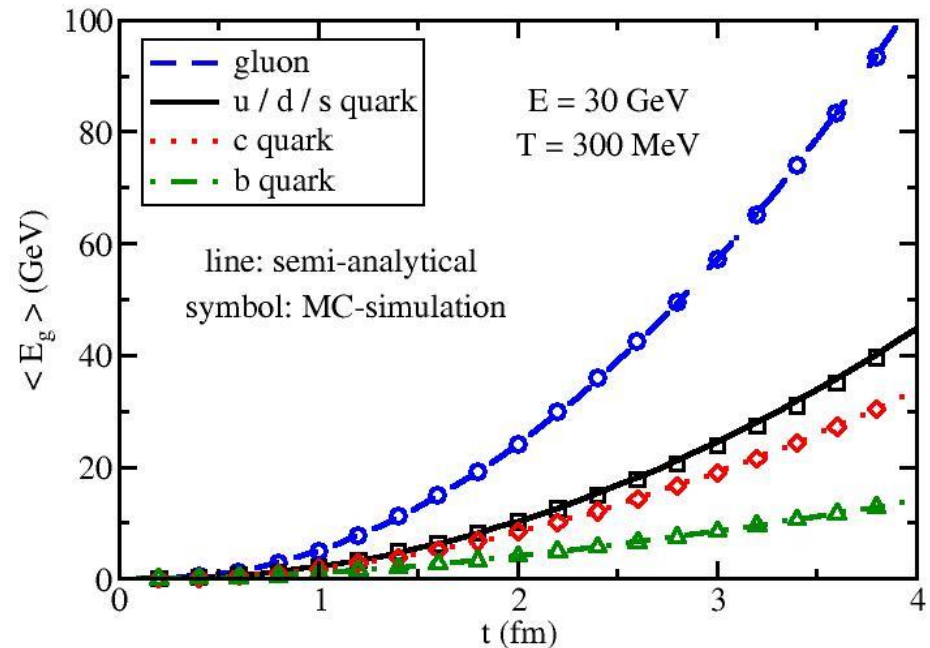
- **Probability of inelastic interaction during Δt :**

$$P_{inel} = 1 - e^{-\langle N_g \rangle}$$

- Zhu, Wang, PRL 2013; He, Luo, Wang, Zhu, PRC 2015; Cao, Tan, GYQ, Wang, Phys.Rev.C 94 (2016) 1, 014909; Phys.Lett.B 777 (2018) 255-259

Model implementation of inelastic radiation

- Calculate $\langle N_g \rangle$ and P_{inel}
- If gluon radiation happens, sample n gluons from Poisson distribution
- Sample E & p of radiated gluons using the differential radiation spectrum
- First do $2 \rightarrow 2$ process, then adjust E & p of $2 + n$ final partons to guarantee E & p conservation for $2 \rightarrow 2 + n$ process



$\langle E_g \rangle$ from our MC simulation agrees with the semi-analytical result.

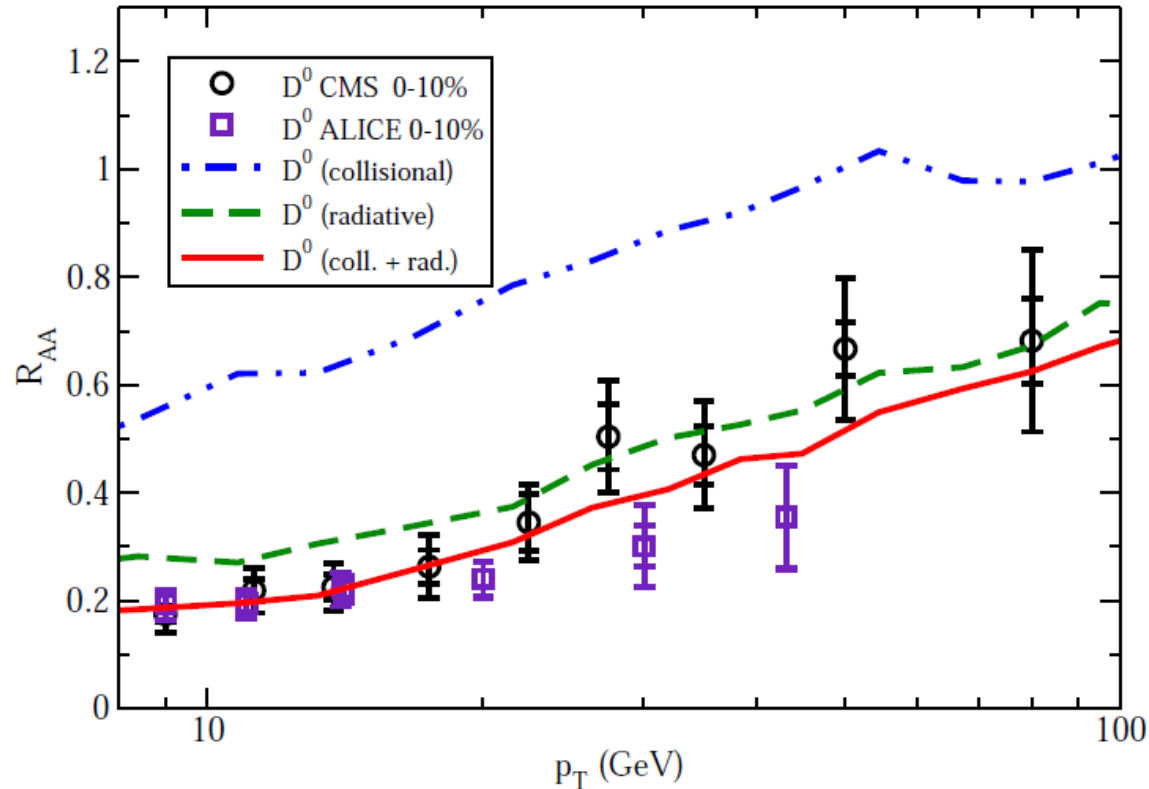
Combine elastic & inelastic

- **Total probability:**

$$P_{tot} = 1 - e^{-\Gamma_{tot}\Delta t} = P_{el} + P_{inel} - P_{el}P_{inel}$$

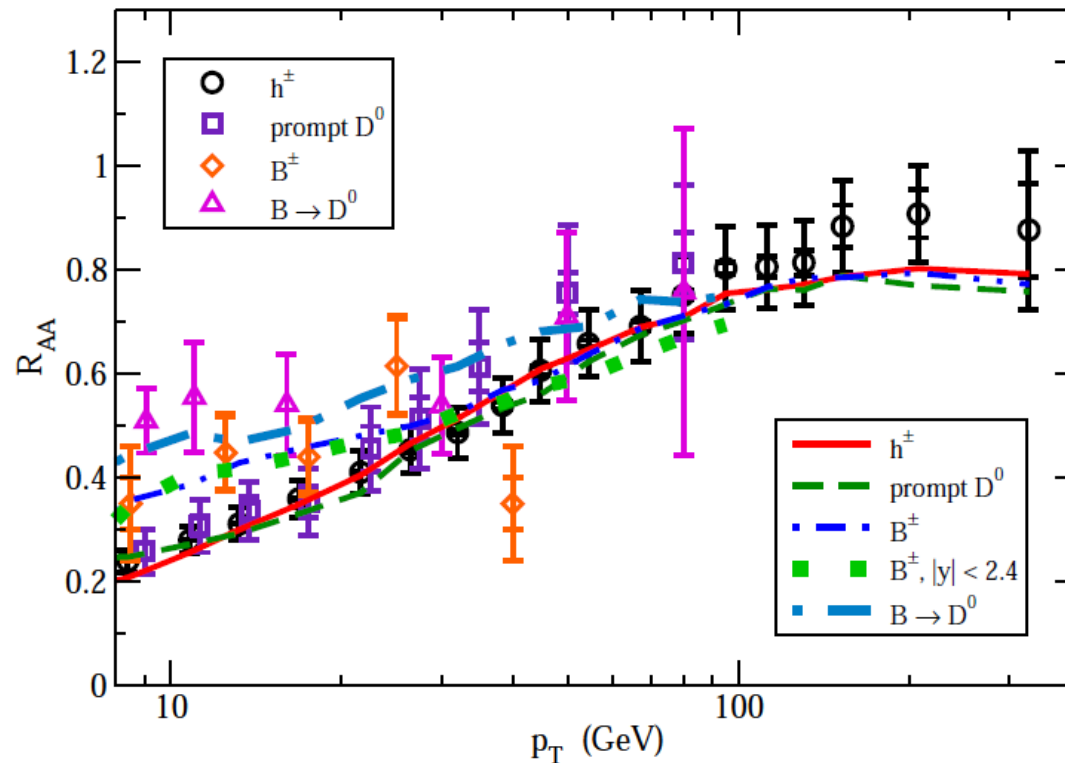
- **Pure elastic scattering without gluon radiation: $P_{el}(1 - P_{inel})$**
 - **Inelastic scattering: P_{inel}**
- **Use P_{tot} to determine whether jet parton interact with thermal medium**
 - **If jet-medium interaction happens, then determine whether it is pure elastic or inelastic**
 - **Then simulate $2 \rightarrow 2$ or $2 \rightarrow 2 + n$ process**

Radiative and collisional contributions



Radiative E loss provides more dominant contributions to R_{AA} , collisional E loss also has sizable contributions to R_{AA} at not-very-high p_T regime and diminishes with increasing p_T .

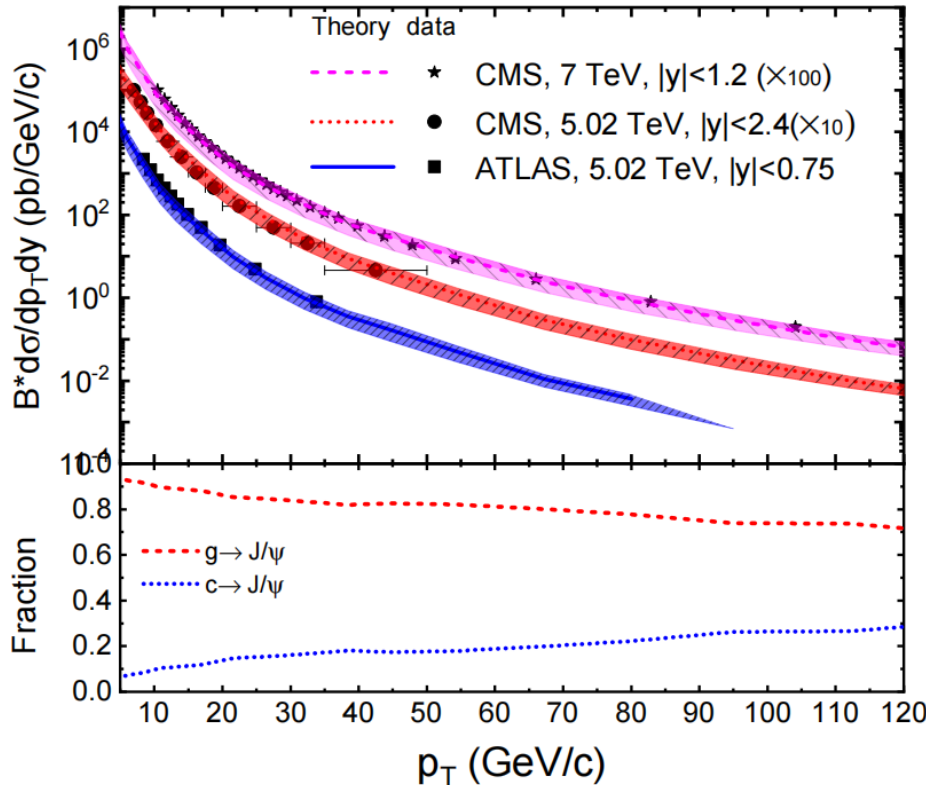
Flavor hierarchy of jet quenching



A state-of-art jet quenching framework (NLO-pQCD + LBT + Hydrodynamics)
At $p_T > 30\text{-}40$ GeV, B mesons will also exhibit similar suppression effects to charged hadrons and D mesons, which can be tested by future measurements.

Xing, Cao, GYQ, Xing, PLB 2020

Gluons dominate high p_T J/Ψ production



Leading power (p_T^2/m_c^2) NRQCD:

$$d\sigma[AB \rightarrow J/\psi + X] = \sum_i d\hat{\sigma}_{AB \rightarrow i+X} \otimes D_{i \rightarrow J/\psi}$$

$$D_{i \rightarrow J/\psi}(z, \mu) = \sum_n \hat{d}_{i \rightarrow [Q\bar{Q}(n)]}(z, \mu) \langle \mathcal{O}_{[Q\bar{Q}(n)]}^{J/\psi} \rangle$$

Gluon fragmentation-improved PYTHIA (GFIP)

MadGraph for hard parton creation

PYTHIA8 for parton shower

Short-distance coefficients from 1311.7078, 1208.5301

Long-distance matrix element from 1403.3612.

Within the framework of leading power NRQCD, gluons dominate high p_T J/Ψ production.

S.-L. Zhang, J. Liao, GYQ, E. Wang, H. Xing, 2208.08323

Ma, Qiu, Zhang, PRD, 2014; Bodwin, Kim, Lee, JHEP 2012; Bodwin, Chung, Kim, Lee, PRL 2014

Details about the analysis

- **The formula for hadron production in AA collisions:**

$$\frac{1}{\langle N_{\text{coll}} \rangle} \frac{d\sigma_{AA \rightarrow hX}}{dp_T^h} = \sum_j \int dp_T^j dx dz \frac{d\hat{\sigma}_{p'p' \rightarrow jX}}{dp_T^j}(p_T^j) W_{AA}(x) D_{j \rightarrow h}(z) \delta(p_T^h - z(p_T^j - x \langle \Delta p_T^j \rangle))$$

- **Parameterize p_T -dependence of $\langle \Delta p_T \rangle$ for gluons (g), light quarks (q), charm quarks (c) and bottom quarks (b) as:**

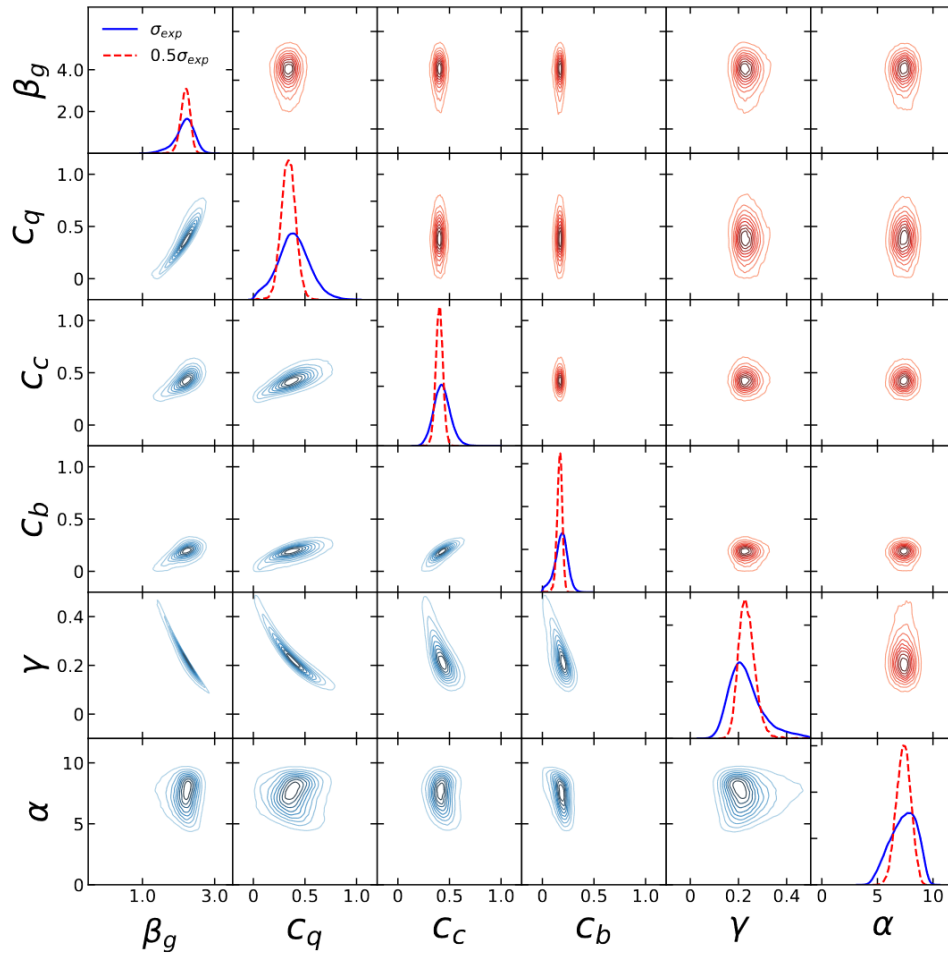
$$\langle \Delta p_T^j \rangle = C_j \beta_g p_T^\gamma \log(p_T)$$

- $C_g = 1$ and C_q, C_c, C_b represents the $\langle \Delta p_T \rangle$ ratio relative to gluon's.
- **The parton energy loss distribution $W_{AA}(x)$ is taken as:**

$$W_{AA}(x) = \frac{\alpha^\alpha x^{\alpha-1} e^{-\alpha x}}{\Gamma(\alpha)}$$

- **The parameter set $\theta = (\beta_g, C_q, C_c, C_b, \gamma, \alpha)$ is to be calibrated.**

Posterior distributions of parameters

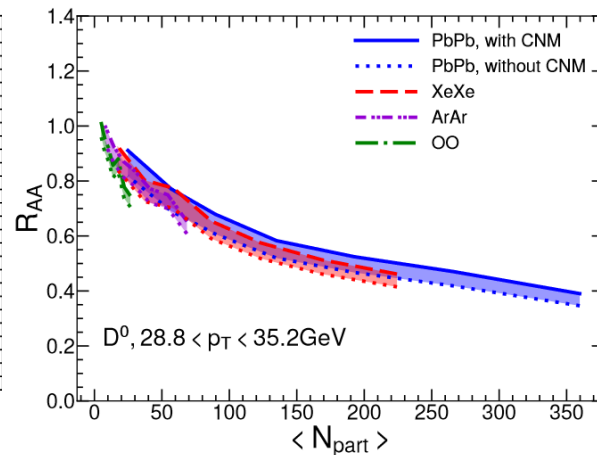
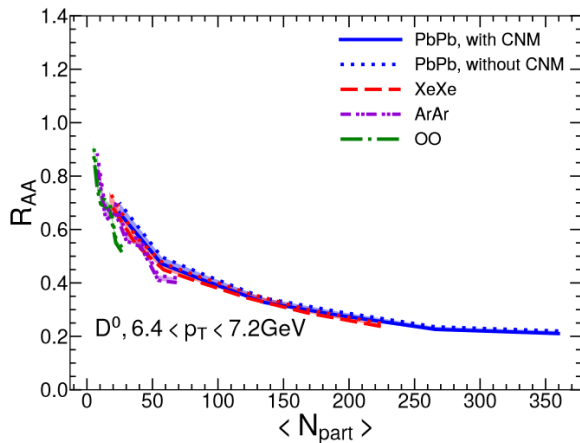
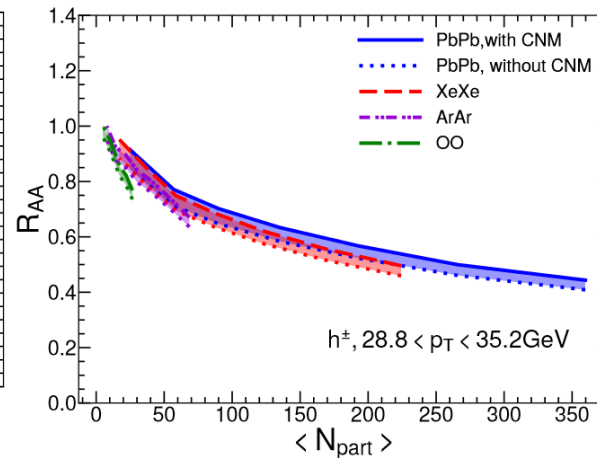
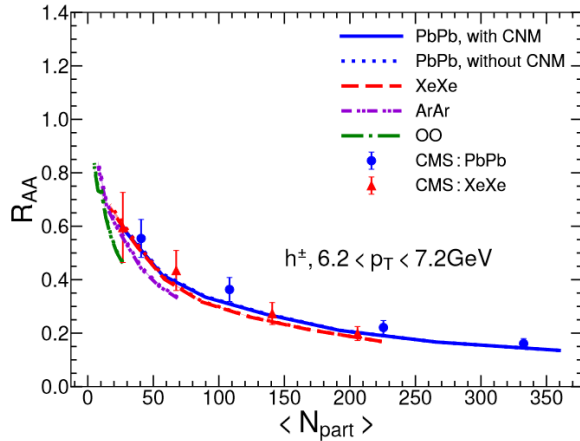


	with σ_{exp}	with $0.5\sigma_{exp}$
β_g	(1.646, 2.56)	(1.96, 2.39)
C_q	(0.129, 0.65)	(0.226, 0.454)
C_c	(0.3, 0.567)	(0.344, 0.459)
C_b	(0.065, 0.277)	(0.124, 0.207)
γ	(0.137, 0.378)	(0.184, 0.295)
α	(5.287, 9.061)	(6.266, 8.401)

The energy loss parameters for jet-medium interaction can be well constrained by the Bayesian analysis.

Reducing experimental data error bars can improve the precision of the extracted parameters.

When does jet quenching disappear?



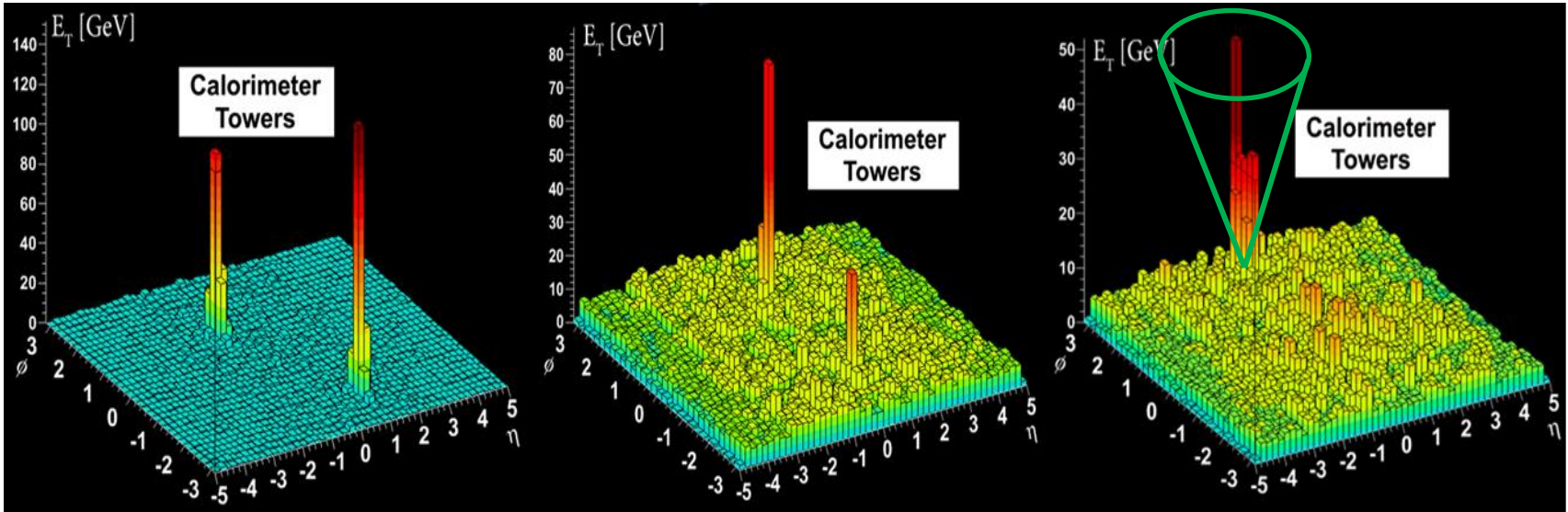
R_{AA} have good scaling behaviors with respect to systems size.

Prediction of sizable jet quenching in OO collisions.

$R_{pA} \sim 1$ in pA is mainly due to small system size

Xing, Cao, GYQ, Xing, PLB 2020; Liu, Xing, Wu, GYQ, Cao, Xing, PRC 2022

Full jets in heavy-ion collisions



How much energy is lost from the jet?

Where does the lost energy go?

How does the medium respond to the lost energy?

How does the lost energy redistribute and manifest in final state?

Where to search for the signal of medium response?

How to use medium response to probe the medium properties?

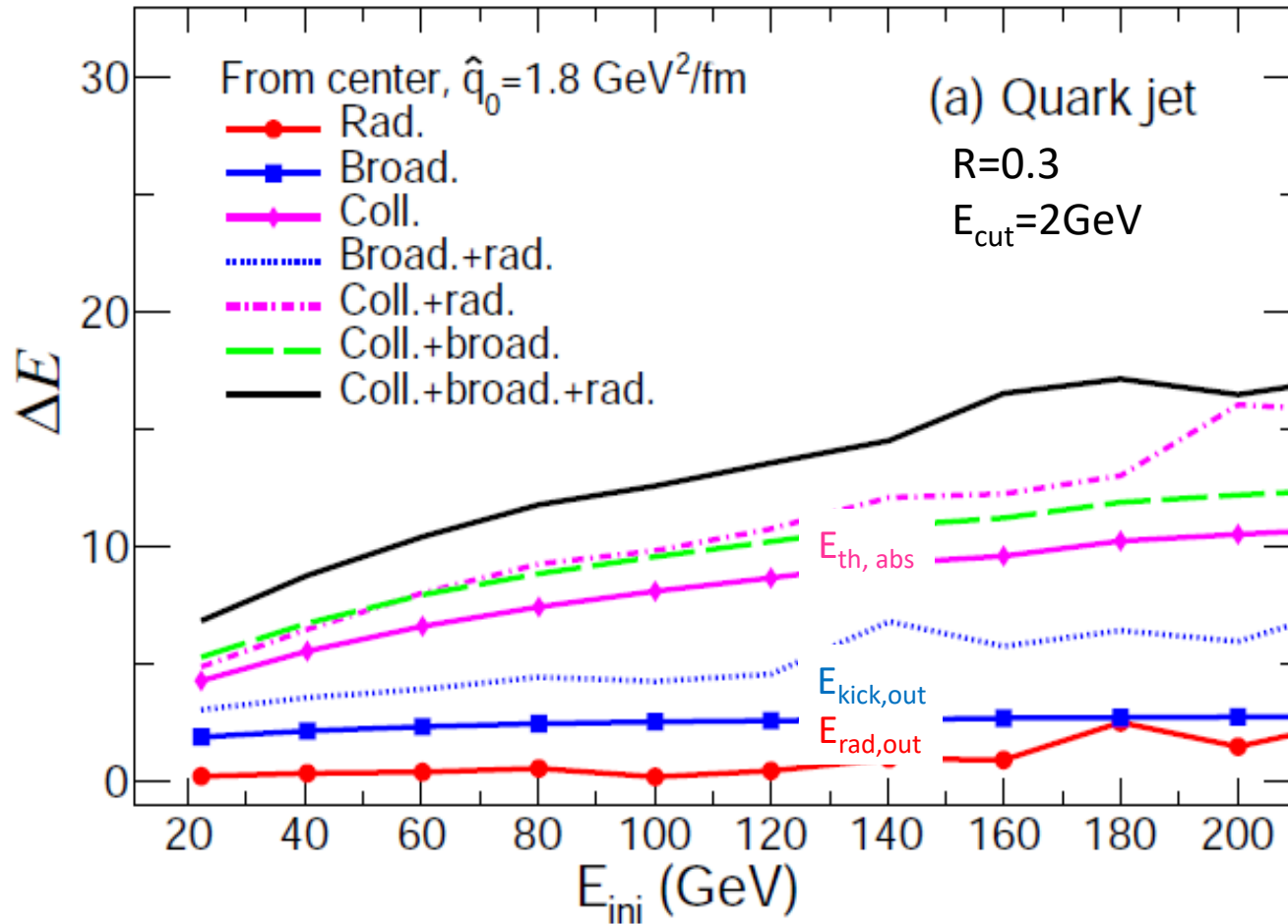
Full jet evolution in medium

- Solve the 3D (energy & transverse momentum) evolution for shower partons inside the full jet
- Include both collisional (the longitudinal drag and transverse diffusion) and all radiative/splitting processes

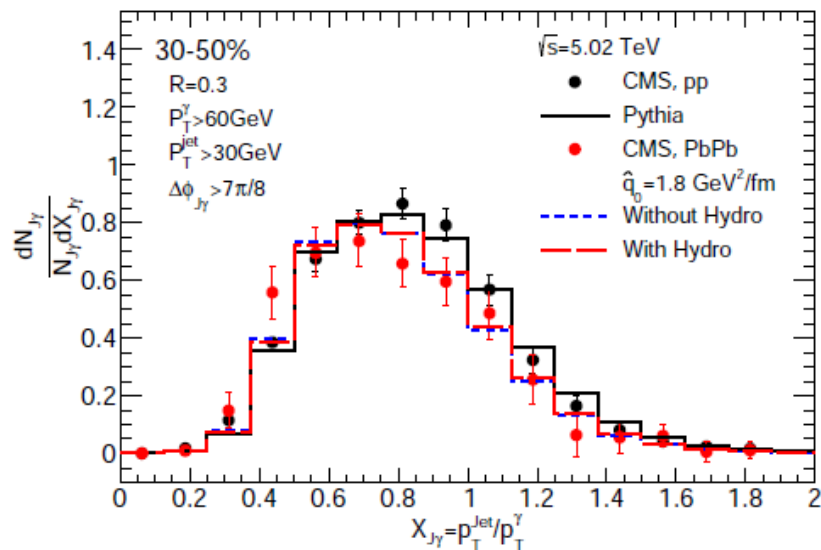
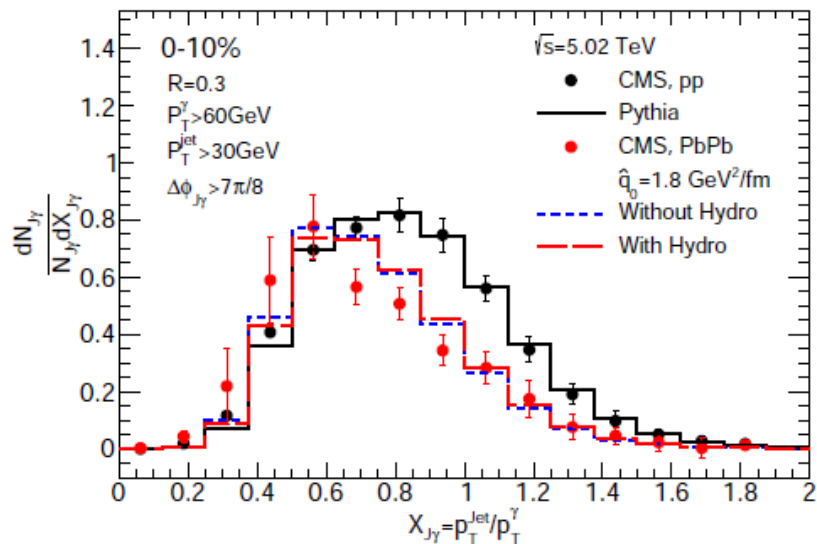
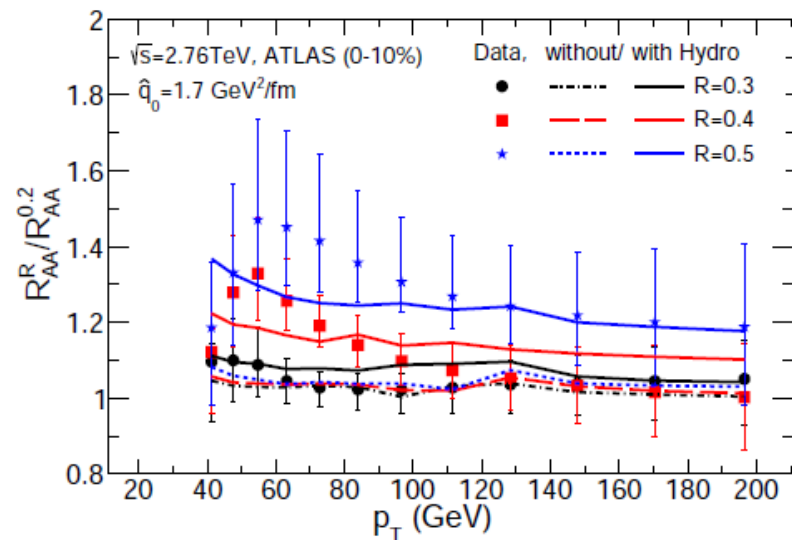
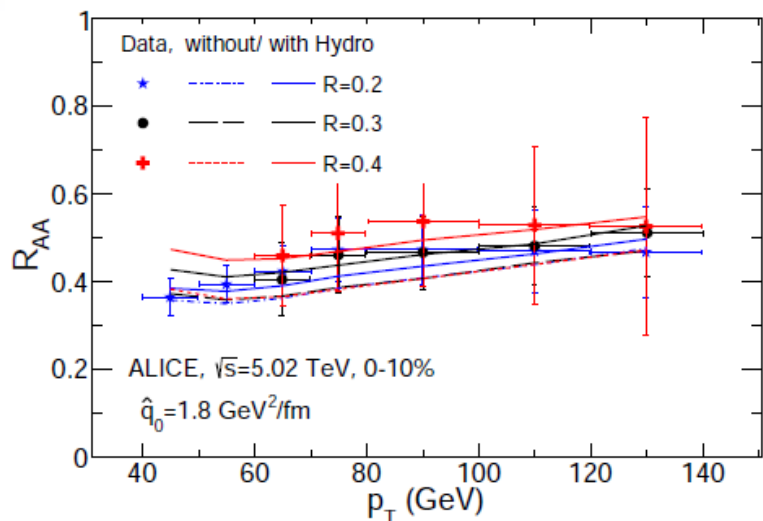
$$\begin{aligned} \frac{d}{dt} f_j(\omega_j, k_{j\perp}^2, t) &= \left(\hat{e}_j \frac{\partial}{\partial \omega_j} + \frac{1}{4} \hat{q}_j \nabla_{k_\perp}^2 \right) f_j(\omega_j, k_{j\perp}^2, t) && \text{Drag \& transverse broadening} \\ + \sum_i \int d\omega_i dk_{i\perp}^2 \frac{d\tilde{\Gamma}_{i \rightarrow j}(\omega_j, k_{j\perp}^2 | \omega_i, k_{i\perp}^2)}{d\omega_j d^2 k_{j\perp} dt} f_i(\omega_i, k_{i\perp}^2, t) &&& \text{Gain terms} \\ - \sum_i \int d\omega_i dk_{i\perp}^2 \frac{d\tilde{\Gamma}_{j \rightarrow i}(\omega_i, k_{i\perp}^2 | \omega_j, k_{j\perp}^2)}{d\omega_i d^2 k_{i\perp} dt} f_j(\omega_j, k_{j\perp}^2, t) &&& \text{Loss terms} \end{aligned}$$

$$E_{jet}(R) = \sum_i \int_R \omega_i f_i(\omega_i, k_{i\perp}^2) d\omega_i dk_{i\perp}^2$$

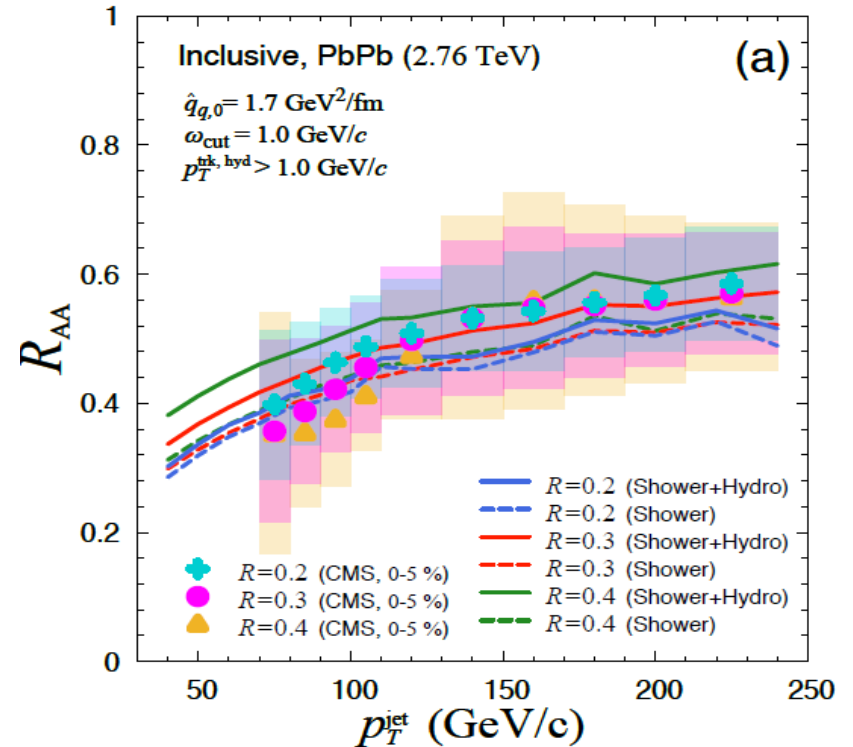
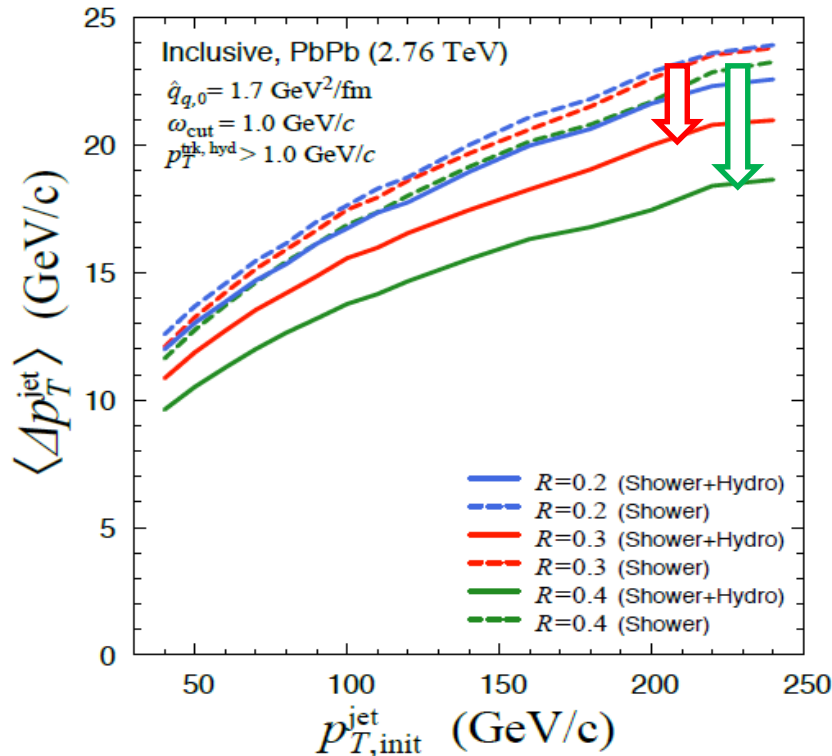
Full jet energy loss (radiative, collisional, broadening)



R_{AA} and photon-jet asymmetry



Effect of jet-induced flow on R_{AA}



Hydro part partially compensates the energy loss experienced by jet shower part. Jet-induced flow evolves with medium, diffuses, and spreads widely around jet axis, leading to stronger jet cone size dependence.

Generalized k_T family of jet reconstruction algorithms

- (1) Consider all particles in the list, and compute all distances d_{iB} and d_{ij}
- (2) For particle i , find $\min(d_{ij}, d_{iB})$
- (3) If $\min(d_{iB}, d_{ij}) = d_{iB}$, declare particle i to be a jet, and remove it from the list of particles. Then return to (1)
- (4) If $\min(d_{iB}, d_{ij}) = d_{ij}$, recombine i & j into a single new particle. Then return to (1)
- (5) Stop when no particles are left

$$d_{iB} = p_{T,i}^{2p}$$

$$d_{ij} = \min(p_{T,i}^{2p}, p_{T,j}^{2p}) \frac{\Delta R_{ij}^2}{R^2}$$

$$\Delta R_{ij}^2 = (\phi_i - \phi_j)^2 + (\eta_i - \eta_j)^2$$

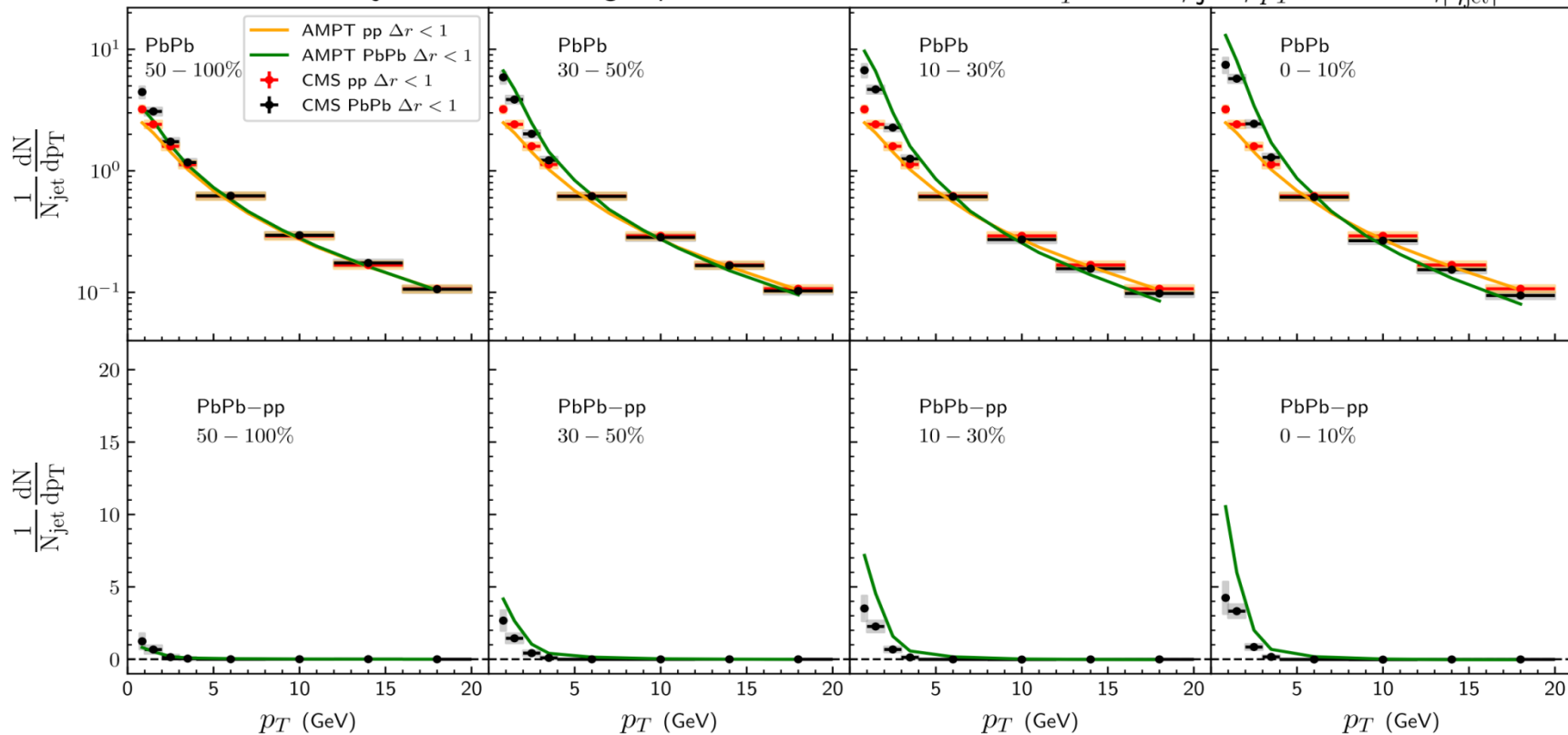
$p=1$: k_T algorithm

$p=0$: Cambridge/Aachen algorithm

$p=-1$: anti- k_T algorithm

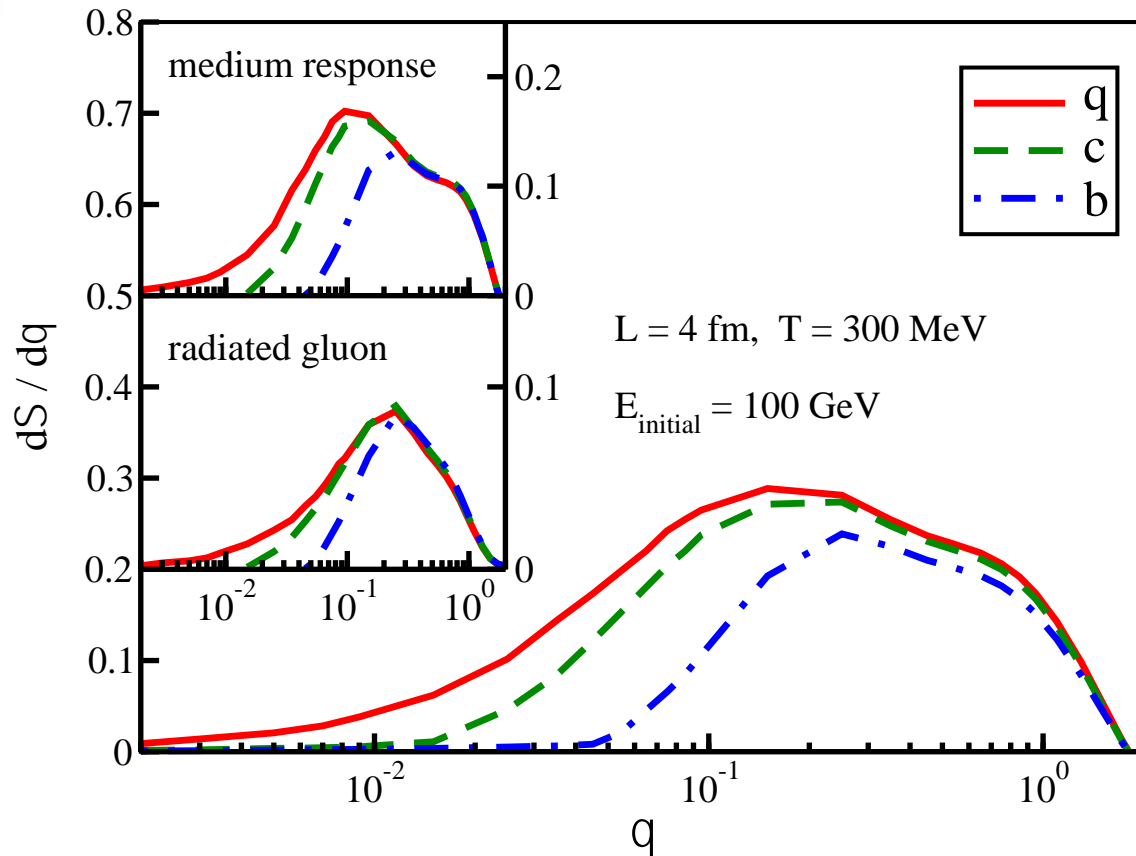
Jet-induced particle yield around jets

The distribution of jet-correlated charged-particles with $\Delta r < 1$ anti- $k_T R = 0.4$, jets, $p_T > 120 \text{ GeV}$, $|\eta_{\text{jet}}| < 1.6$



Jet quenching leads to the enhancement of soft particles and the suppression of hard particles around the jets. Such effect is more pronounced for more central collisions.

Medium effect on jet EEC

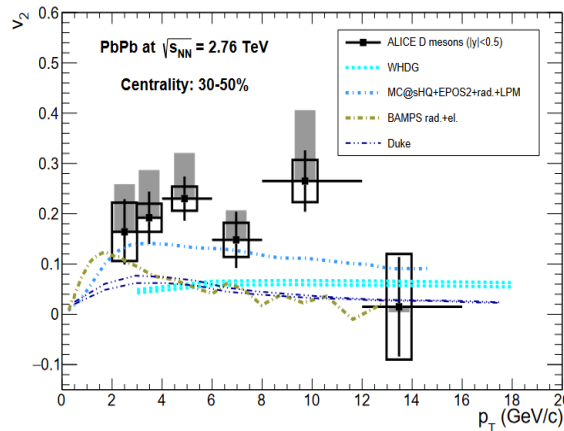
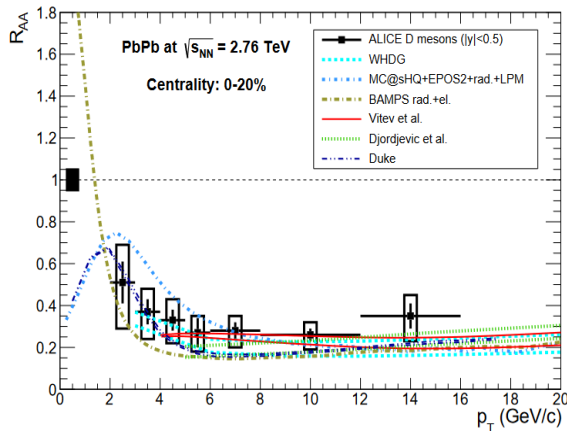
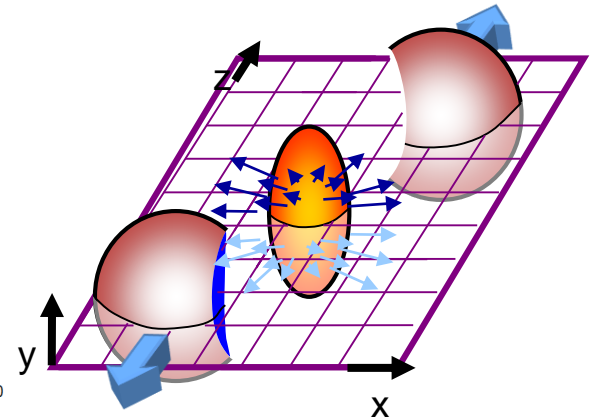
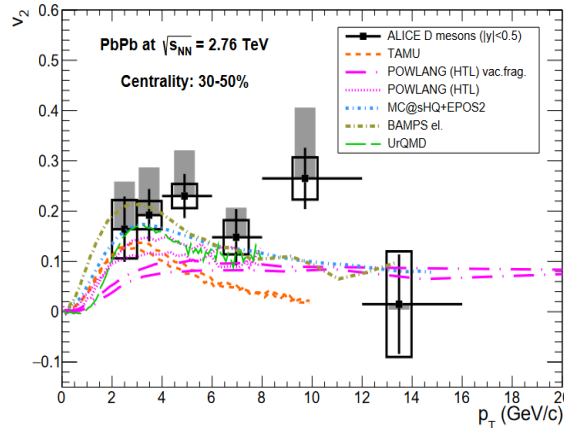
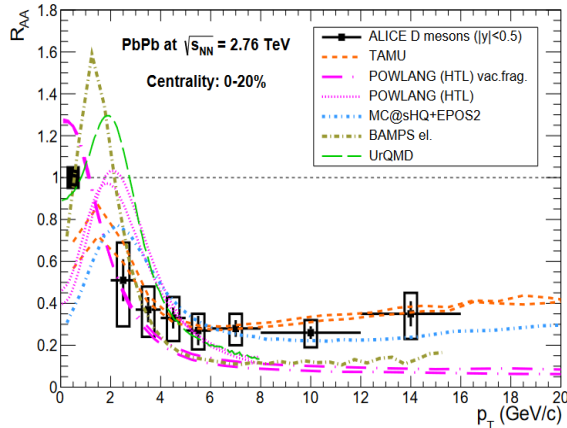


Flavor (mass) hierarchy in quark-jet EEC:

$\Sigma(\text{light jet}) > \Sigma(\text{charm jet}) > \Sigma(\text{bottom jet})$, this hierarchy maintains in the contribution from medium response and medium-induced radiation.

Xing , Cao, GYQ, 2409.12843 [hep-ph]

Heavy flavor R_{AA} and v_2 puzzle



Eur.Phys.J.C 76 (2016) 3, 107

It is difficult for models to simultaneously describe R_{AA} and v_2 for D mesons

Different HQ models vary in a few aspects: radiative & collisional energy loss, Boltzmann & Langevin/Fokker-Planck, fragmentation & recombination, partonic & hadronic interactions, shadowing, Cronin, ...

LBT-PNP: pert. & non-pert. int. btw HQ & QGP

$$V(r) = V_Y(r) + V_S(r) = -\frac{4}{3}\alpha_s \frac{e^{-m_d r}}{r} - \frac{\sigma e^{-m_s r}}{m_s} \quad \begin{array}{l} \alpha_s = 0.27, \sigma = 0.45 \text{ GeV}^2 \\ m_d = 2T + 0.2 \text{ GeV} \\ m_s = \sqrt{0.1 \text{ GeV} \times T} \end{array}$$

$$V(\vec{q}) = -\frac{4\pi\alpha_s C_F}{m_d^2 + |\vec{q}|^2} - \frac{8\pi\sigma}{(m_s^2 + |\vec{q}|^2)^2}$$

$$\begin{aligned} i\mathcal{M} &= \mathcal{M}_Y + \mathcal{M}_S \\ &= \bar{u}(p')\gamma^\mu u(p)V_Y(\vec{q})\bar{u}(k')\gamma^\nu u(k) \\ &\quad + \bar{u}(p')u(p)V_S(\vec{q})\bar{u}(k')u(k), \end{aligned}$$

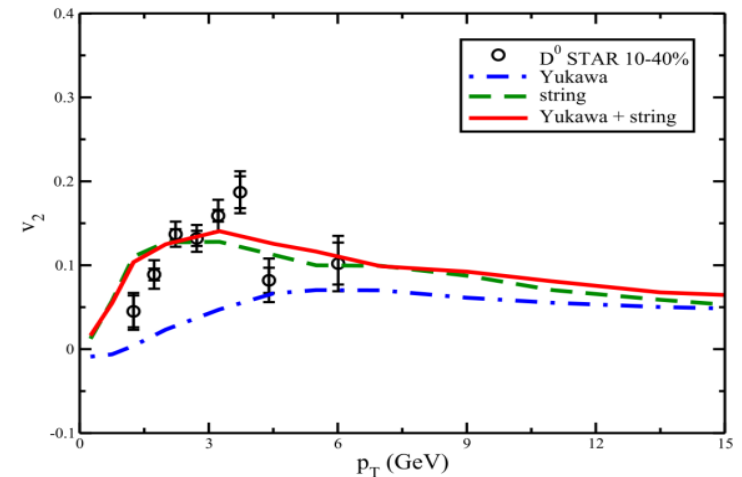
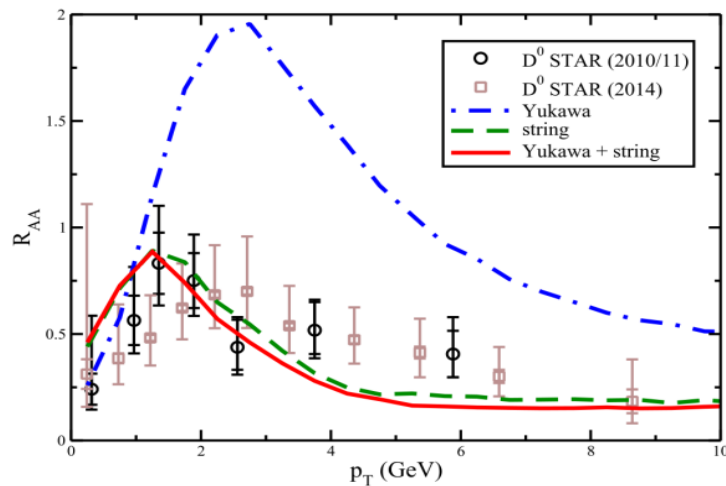
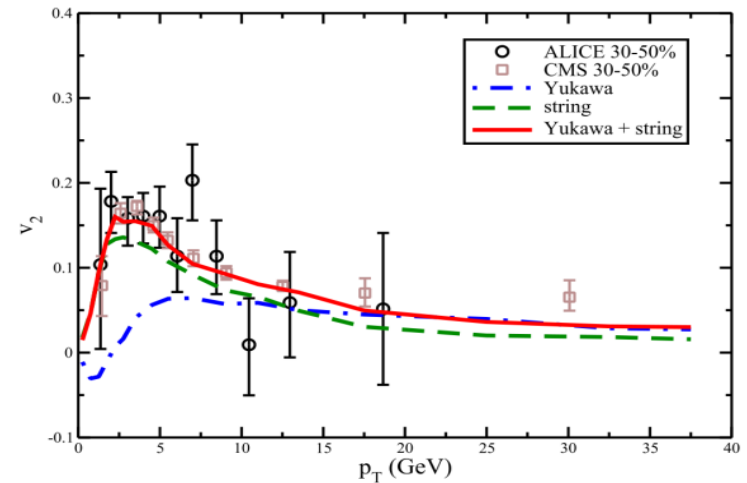
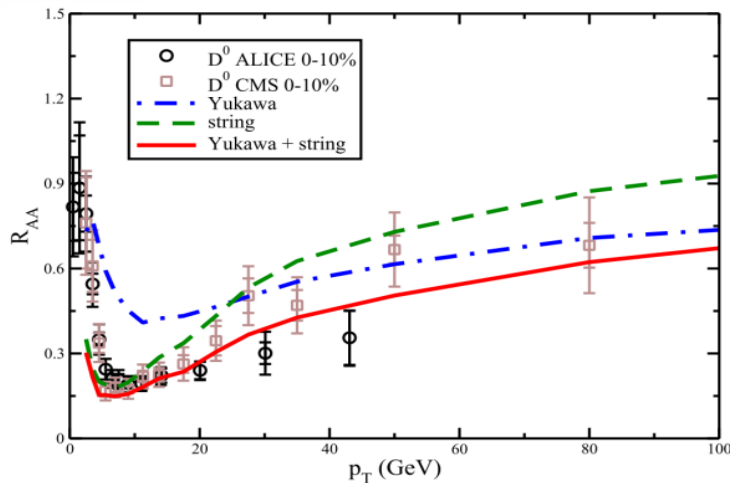
$$\begin{aligned} |\mathcal{M}_{Qq}|^2 &= \frac{64\pi^2\alpha_s^2}{9} \frac{(s - m_Q^2)^2 + (m_Q^2 - u)^2 + 2m_Q^2 t}{(t - m_d^2)^2} \\ &\quad + \frac{(8\pi\sigma)^2}{N_c^2 - 1} \frac{t^2 - 4m_Q^2 t}{(t - m_s^2)^4}, \end{aligned}$$

$$\begin{aligned} |\mathcal{M}_{Qg}|^2 &= \\ &\frac{64\pi^2\alpha_s^2}{9} \frac{(s - m_Q^2)(m_Q^2 - u) + 2m_Q^2(s + m_Q^2)}{(s - m_Q^2)^2} \\ &+ \frac{64\pi^2\alpha_s^2}{9} \frac{(s - m_Q^2)(m_Q^2 - u) + 2m_Q^2(u + m_Q^2)}{(u - m_Q^2)^2} \\ &+ 8\pi^2\alpha_s^2 \frac{5m_Q^4 + 3m_Q^2 t - 10m_Q^2 u + 4t^2 + 5tu + 5u^2}{(t - m_d^2)^2} \\ &+ 8\pi^2\alpha_s^2 \frac{(m_Q^2 - s)(m_Q^2 - u)}{(t - m_d^2)^2} \\ &+ 16\pi^2\alpha_s^2 \frac{3m_Q^4 - 3m_Q^2 s - m_Q^2 u + s^2}{(s - m_Q^2)(t - m_d^2)} \\ &+ \frac{16\pi^2\alpha_s^2}{9} \frac{m_Q^2(4m_Q^2 - t)}{(s - m_Q^2)(m_Q^2 - u)} \\ &+ 16\pi^2\alpha_s^2 \frac{3m_Q^4 - m_Q^2 s - 3m_Q^2 u + u^2}{(t - m_d^2)(u - m_Q^2)} + \frac{C_A}{C_F} \frac{(8\pi\sigma)^2}{N_c^2 - 1} \frac{t^2 - 4m_Q^2 t}{(t - m_s^2)^4}. \end{aligned}$$

HQ dynamics at low energy & close to T_c is highly non-perturbative.

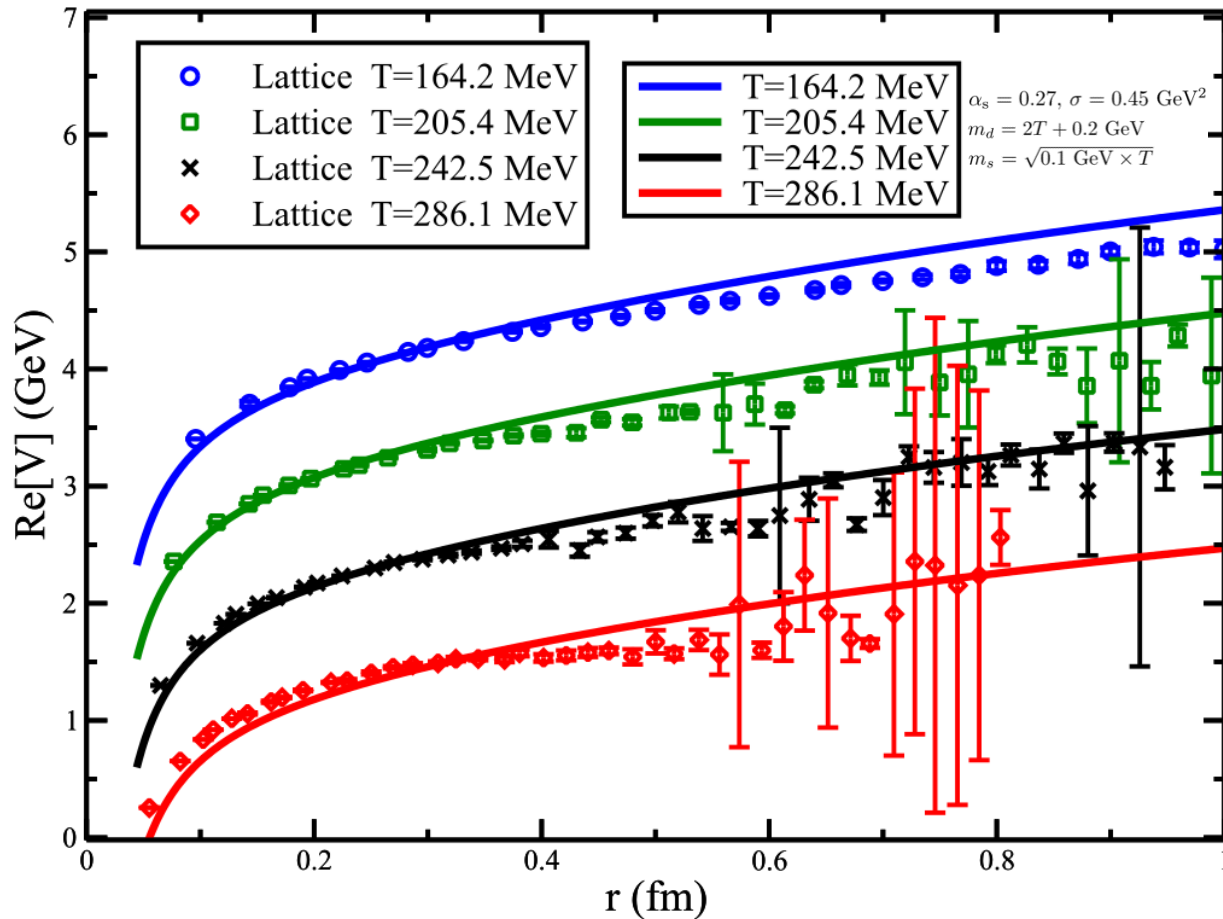
Include the contributions from long-range confining term & short-range Yukawa term.

D meson R_{AA} & v_2 from low to high p_T



Perturbative interaction dominates R_{AA} and v_2 at high p_T , non-perturbative interaction dominates at low p_T .

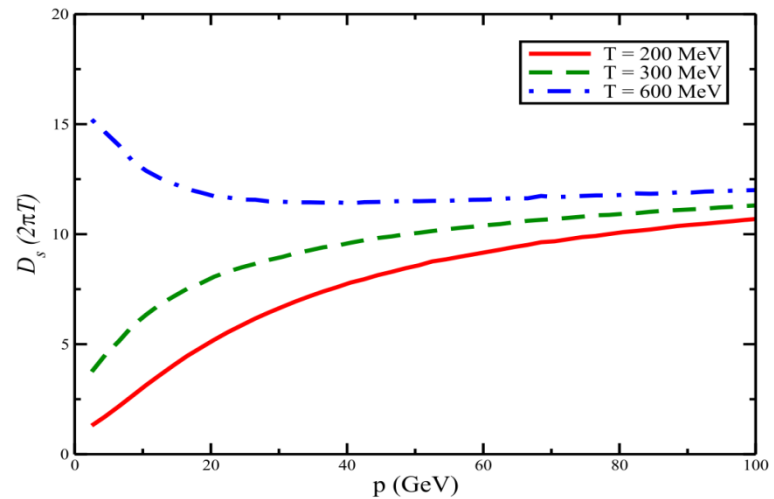
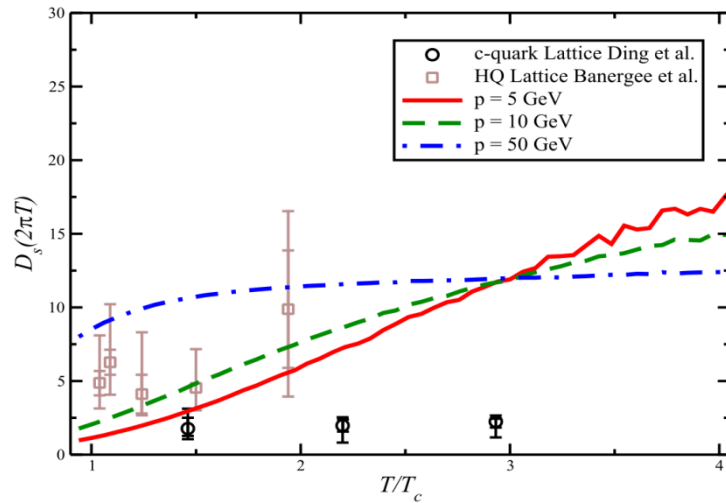
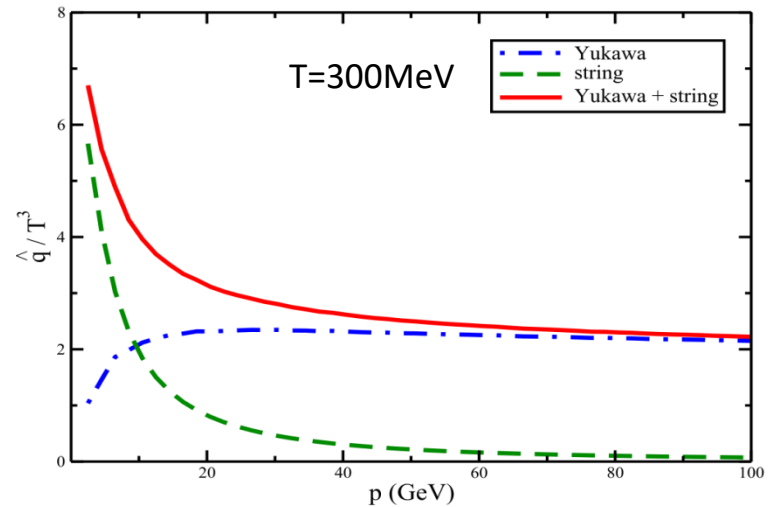
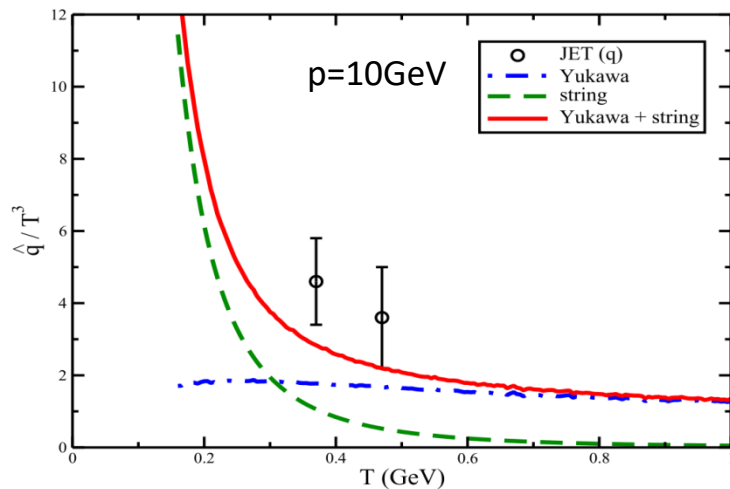
Heavy quark potential from open HF R_{AA} & v_2



First extraction of heavy quark potential from open HF observables.

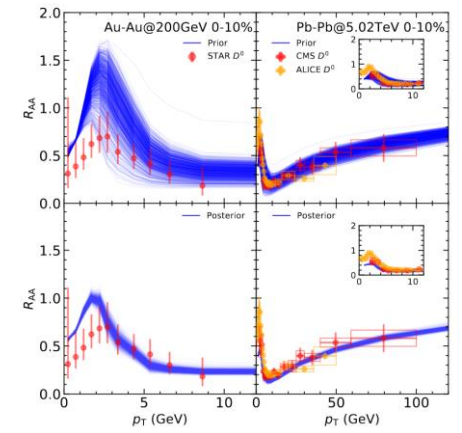
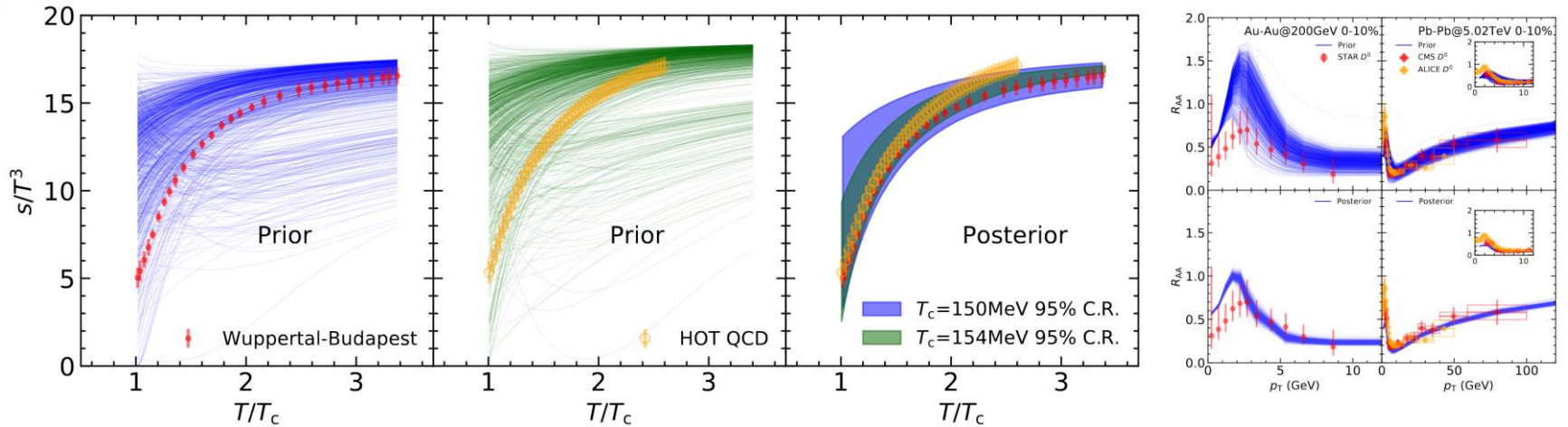
Xing, GYQ, Cao, Phys.Lett.B 838 (2023) 137733

Transport coefficients



Perturbative & non-perturbative interactions dominate high & low $T(p_T)$ respectively.

Probe EoS and η/s with heavy quarks



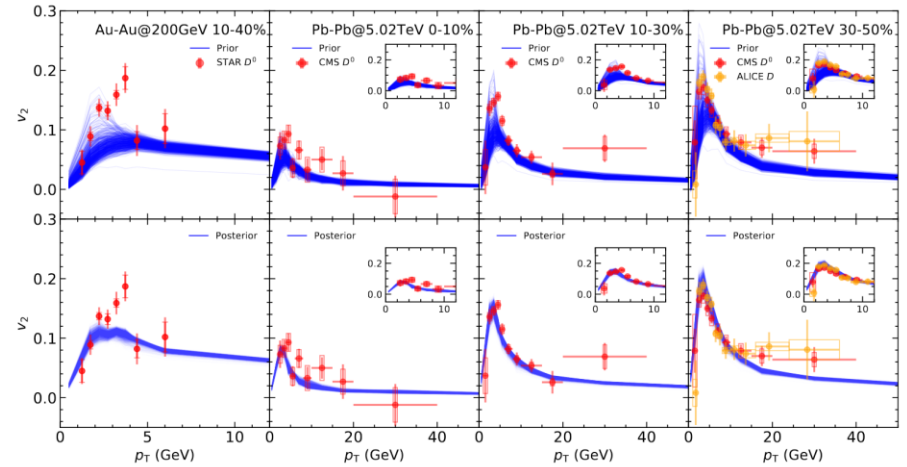
$$m_q^2(T) = \frac{N_c^2 - 1}{8N_c} g^2(T) T^2,$$

$$m_g^2(T) = \frac{1}{6} \left(N_c + \frac{1}{2} N_f \right) g^2(T) T^2,$$

$$g^2(T) = \frac{48\pi^2}{(11N_c - 2N_f) \ln \left[\frac{(aT/T_c + b)^2}{1 + ce^{-d(T/T_c)^2}} \right]},$$

$$P(T) = \sum_i \gamma_i \int \frac{d^3p}{(2\pi)^3} \frac{p^2}{3E_i(p, T)} f_i(p, T) - B(T),$$

$$\epsilon(T) = \sum_i \gamma_i \int \frac{d^3p}{(2\pi)^3} E_i(p, T) f_i(p, T) + B(T).$$



$$g^2(E) = \frac{48\pi^2}{(11N_c - 2N_f) \ln \left[(AE/T_c + B)^2 \right]},$$

Probe EoS and η/s with heavy quarks

